Spray–turbulence–chemistry interactions under engine-like conditions

Lei Zhou[1,#], Wanhui Zhao[1,#], Kai Hong Luo[2,*], Ming jia[3], Haiqiao Wei[1], Maozhao Xie[3,*]

1, State Key Laboratory of Engines, Tianjin University, Tianjin 300072, China

2, Department of Mechanical Engineering, University College London, Torrington Place, London WC1E 7JE, UK

3, School of Energy and Power Engineering, Dalian University of Technology, Dalian, Liaoning 116024, PR China

*Corresponding authors

[#] These authors contributed equally to this work and should be considered co-first authors.

Abstract

Turbulent multiphase combustion plays an important role in both nature (e.g., volcanos and pool fires) and industry (e.g., industrial furnaces, aeroengines, and internal combustion engines). It is a highly complex multiscale and multi-physicochemical process in which interactions between the dispersed and continuous phases, phase change, droplet collisions, evaporation, mixing, heat transfer, and chemical reactions occur simultaneously. In recent years, significant progress has been made in understanding the mechanisms of spray flames and their behaviors in combustion engines. This paper covers key and representative developments in the area of turbulent spray combustion with a focus on spray–chemistry–turbulence interactions. The effects of turbulence–chemistry, spray–turbulence, and spray–chemistry interactions on the spray process, ignition, flame stabilization and emission are comprehensively discussed under engine-like conditions. Furthermore, spray–radiation and spray flame–wall interactions, which are important to engine performance and emission characteristics, are scrutinized. Supercritical spray flames and turbulent spray flames in dual-fuel engines are also discussed. Finally, outlooks and further challenges for the research field are outlined.

Key Words: Turbulent spray flame; Spray flame–wall interaction; Spray–radiation interaction; Diesel engine; Dual fuel

Content

1. Introduction

Turbulent multiphase combustion plays a critical role in both nature (e.g., volcanos and pool fires) and industry (e.g., industrial furnaces, gas turbine engines, and internal combustion engines). In particular, the combustion of liquid fuels is the main process of generating energy for land, air, and sea transportation and industries [1]. The engine performance and emission characteristics of both continuous-combustion systems and reciprocating internal combustion engines are strongly influenced by the characteristics of the turbulent spray combustion involved. Turbulent spray combustion is a complicated multiscale and multi-physicochemical process, which involves atomization, droplet collision, evaporation, mixing, heat transfer, and chemical reactions simultaneously. In addition, turbulence significantly influences each of the above phenomena. Understanding the complex interactions in turbulent spray combustion is essential to developing advanced combustion strategies for improved fuel and energy efficiencies as well as reduced emissions.

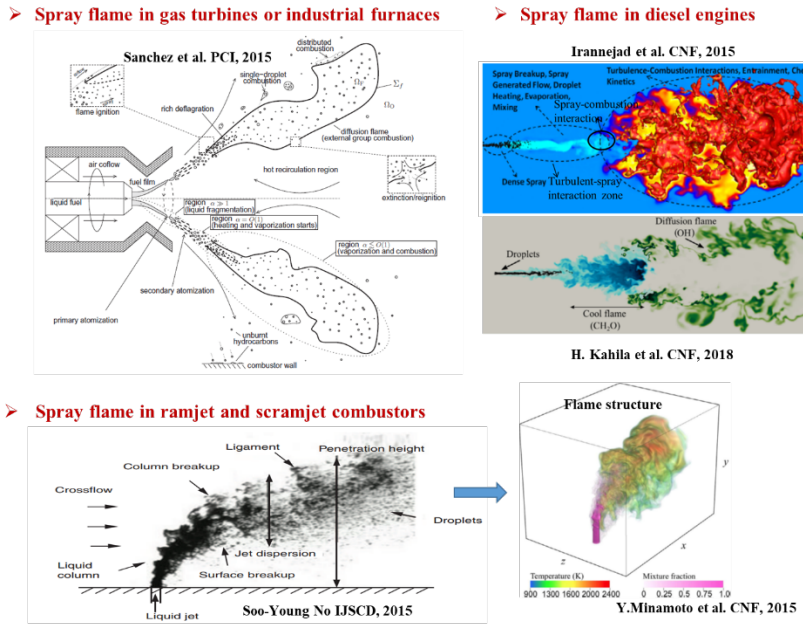

Fig. 1 Turbulent spray flames in different engines. Reprinted from Ref. [2-6] with permission of Elsevier and SAGE publications.

Figure 1 illustrates the spray flame structures in different combustion devices, including gas turbines, ramjets, scramjet engines, and reciprocating internal combustion engines. For the spray flame in gas turbines, liquid fuel is injected from a pressure-swirl atomizer, generating a high-velocity jet. Then, primary atomization and secondary atomization follow. Droplet heating and vaporization in the dilute downstream region occur because of the heat exchange between the cold fuel droplets and surrounding hot gas, including hot combustion products. Finally, ignition is triggered when the suitable temperature and equivalence ratio are attained. Ignition involves single droplet combustion, distributed combustion, and diffusion flame with an extinction/re-ignition process. A cool flame may exist in the upstream of the nonpremixed flame, which is distinguished by the formaldehyde (CH_2O) mass fraction,

while the high-temperature diffusion flame can be identified by the OH field. Overall, spray flames in these devices are characterized by the phenomena of spray–turbulence–chemistry interactions, although the macro-features of these flames have some differences.

A prime example of liquid fuel spray combustion is found in diesel engines, which have been widely utilized in the transport industry, stationary applications (e.g., construction and small power generation), and agriculture. The spray flames in diesel engines occur under high-temperature and high-pressure conditions. However, to meet the increasingly stringent legislation on engine efficiency and pollutant emissions, especially NO_x and particulate matter, a new low-temperature combustion (LTC) concept has been proposed in recent decades, which has led to several advanced technologies such as homogeneous charge compression ignition, premixed charge compression ignition (PCCI), and reactivity controlled compression ignition [7]. Unlike traditional diesel combustion, LTC employs a long ignition delay (ID) to provide sufficient time for fuel–air mixing to achieve high efficiency and low emissions by utilizing high compression ratios and exhaust-gas recirculation (EGR) strategies. Recent studies have shown that the combustion and pollutant formation processes using the LTC strategy are significantly different from those in the conventional combustion mode [7, 8]. The LTC strategy involves a two-stage ignition process, which includes cool flames in a prolonged first-stage ignition and high-temperature combustion (HTC) in the second stage. It should be noted that turbulence–spray–chemistry interactions are more important for LTC, as a slow combustion process is more susceptible to the influence of turbulence, and the separation of chemistry and turbulence scales is no longer justified. For example, in predicting the autoignition process in LTC diesel combustion, considering the effect of the turbulence–chemistry interaction results in better agreement with experimental data, especially under low temperature and/or low oxygen concentrations [9-11].

1.1 Features of turbulent spray flame

Spray–turbulence–chemistry interactions determine the performance of combustion devices with respect to flame stabilization and pollutant emissions [12, 13]. The typical characteristics of turbulent spray flames are displayed in **Fig. 2** [5, 14, 15], which involve the following:

(1) Spray structures: Turbulent spray characteristics, such as liquid and vapor penetrations and spray morphology, are determined by the liquid fuel properties, injection parameters, and ambient conditions.

(2) Ignition or low-temperature reactions: Ignition in a cool flame stage with LTC can be observed; the fuel–air mixture starts to react and long-chain hydrocarbon radicals, as well as smaller radicals, such as H_2O_2, HO_2, and CH_2O, are formed in the rich-mixture region of the spray tip.

(3) HTC: The low-temperature reactions precede the second-stage ignition, during which high-temperature reactions and diffusion flames lead to the formation of ignition kernels with key oxidation products, such as OH, CO, and H_2O.

(4) The spray flame achieves a quasi-steady state: the cool flame located upstream of the diffusion

flame is distinguished by the CH_2O mass fraction and the HTC region of the diffusion flame is represented by the high-concentration OH field.

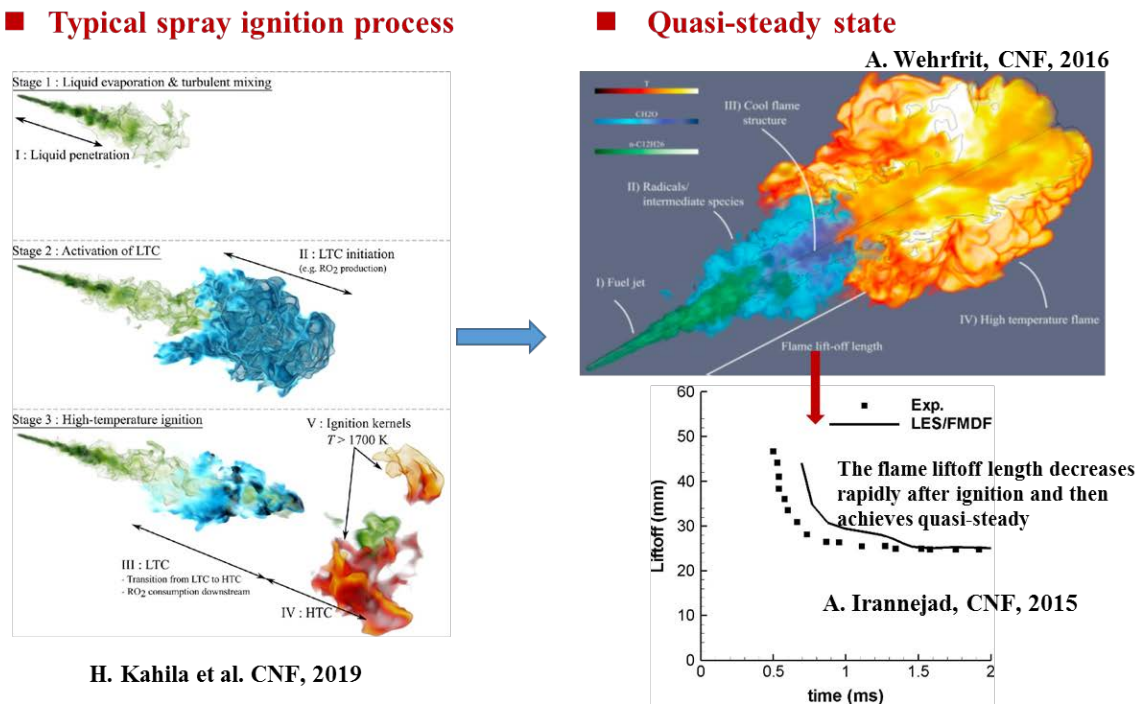

Fig. 2 Structure of spray flames under diesel engine-like conditions. Reprinted from Ref. [5, 15, 16] with permission of Elsevier.

Spray structures

Using liquid sprays is very effective in controlling the combustion process to improve engine performance and reduce emissions. Spray injection can be divided into a series of sub-processes, involving cavitation within the injector, the primary and secondary breakup of a liquid jet into small droplets, droplet collision, and coalescence, evaporation, turbulent mixing or micromixing, spray impingement, etc. as shown in **Fig. 3**. The mechanisms of spray breakup are important because the breakup processes determine the spray structure, initial droplet size and distribution, and control the initial conditions for vaporization and subsequent processes. In addition, aerodynamic, turbulence, and cavitation-induced breakup can affect the breakup process in diesel sprays. However, understanding the spray formation process using either computational or experimental methodologies is challenging because of the multi-scale, multi-dimensional, and multi-physics nature of the problem. Currently, numerical research on the liquid fuel jet atomization process can be classified into two principal categories [17, 18]: (1) using a Eulerian approach to simulate primary breakup in the dense spray regime region and (2) using a Lagrangian approach to simulate turbulence–combustion–droplet interaction in the dilute spray region. However, to systematically investigate fuel spray atomization and combustion of liquid fuel cannot be achieved by either approach. Tracking a large number of atomized droplets using the Lagrangian approach is difficult while the reliability of the Eulerian approach is fully established. Therefore, many researchers have studied the liquid jet process using

multi-scale methods combining Eulerian and Lagrangian methods. Recently, Luo et al. [19] reviewed the application of the level set method in the study of the spray atomization process, including the primary breakup and secondary atomization.

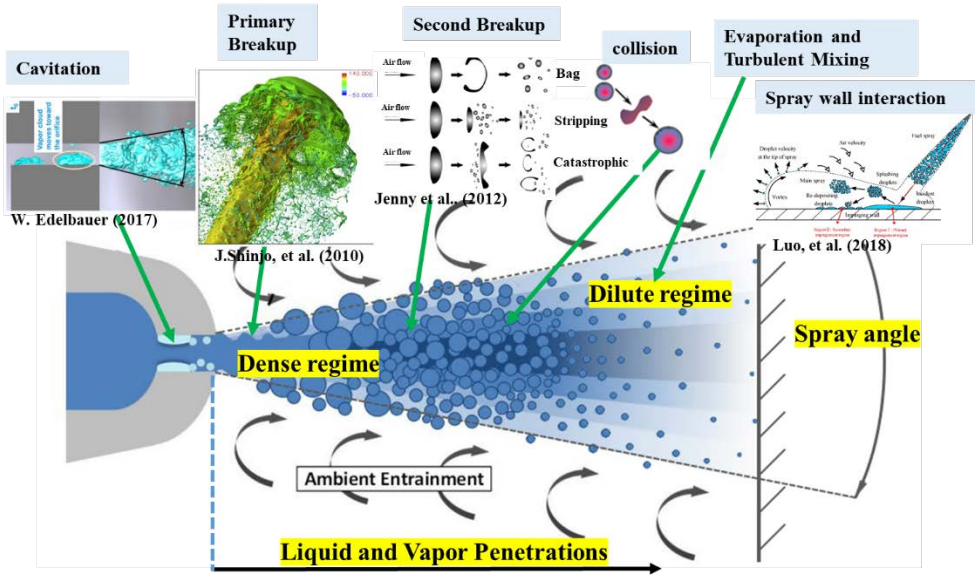

Fig. 3 A schematic of diesel spray process. Reprinted from Ref. [1, 20-22] with permission of Elsevier.

Ignition or low-temperature reaction

The ID time is the time interval between the start of the injection and the appearance of high-temperature reactions. It is affected by both physical and chemical delays in the spray flame [15]. Liquid fuel injection, atomization, evaporation, and mixing contribute to the physical effect. The formation of the key intermediate species and heat release from the early reactions cause the chemical effect. Many studies [23-25] have been devoted to understanding the mechanisms of multi-stage ignition from fundamental chemical aspects.

Three modes of ignition are distinguished based on the relative timescales of evaporation, convection, and diffusion in the surrounding gas for liquid fuel combustion [26]: (1) individual droplet ignition, (2) group ignition around droplets, and (3) spray ignition or global ignition. Turbulent sprays exhibit a multistage and multimode ignition process. During the first-stage ignition (also known as the LTC stage), different products, such as ketohydroperoxide (KET) and CH_2O are formed, leading to a slow increase in the gas temperature. Therefore, the mass formation of these species can be used to identify the first-stage ignition, which can cause a ‘softening’ effect of the characteristic refractive index gradients before the high-temperature ignition (HTI) event [27]. Once high-temperature reactions occur in spray flames, the schlieren images become dark again. During the second stage of ignition, CH_2O is quickly consumed, and H_2O_2 rapidly decomposes to OH radicals, leading to a rapid increase in temperature.

The second-stage ignition is expected to occur away from the stoichiometry and at the most

reactive mixture fraction location [28]. Evaporation of droplets requires the absorption of heat from the environment, causing a drop in the gas temperature. Thus, high-temperature reactions must occur at a location with a suitable temperature and equivalence ratio. The ignition location can also be influenced by the initial conditions, such as gas temperature, oxygen concentration, and gas density [29]. For a highly reactive mixture, HTI tends to initialize at fuel-rich locations behind the spray tip with low mixture gradients [30]. At lower gas temperatures, the reactivity of the mixture is reduced. The already formed heat and intermediate radicals can be transported outside owing to the gradients. Therefore, the first ignition location is away from the spray tip. Overall, during the mutlistage ignition process of spray flames, the first-stage ignition dominates because the heat release and key intermediate species formed during the stage determine the second-stage ignition [23, 24].

Flame lift-off length (LOL) and flame stabilization process:

The LOL represents the most upstream location of the combustion region, where the flame is stabilized and becomes quasi-steady, as depicted in **Fig. 2**. In experiments, the LOL can be measured by OH* chemiluminescence with a pre-selected percentage of the local peak, for example, 50% in one study [31]. The LOL influences the entrainment of fresh gas and eventually the formation of pollutant emissions, such as soot. The LOL itself is the result of the complex processes of fuel breakup, atomization, vaporization, mixing, and fresh air entrainment. Therefore, it is influenced by many parameters, such as ambient gas temperature, oxygen concentration, ambient density, turbulence, and injection pressure variation. A higher mixture reactivity, for example, results in a shorter flame LOL, indicating that the interaction between the flame and the fuel droplets as well as the evaporation at the tip of injection, is enhanced, which in turn causes faster combustion [5].

1.2 Motivation

Recent reviews on the turbulent spray flame or two-phase flow can be found in [1, 8, 32], where new experimental and modeling developments in spray combustion are summarized. For instance, Jenny et al. [1] outlined the main interactions among turbulence, spray and combustion, and focused their review on spray models in the dilute spray regime. However, spray breakup in the dilute regime as well as atomization and droplet collisions in the dense regime are not included. Jiang et al. [33] focused on the physical models and numerical techniques for DNS and LES of gas–liquid two-phase jet flow atomization and spray processes in internal combustion engines and gas turbine combustors, but combustion mechanisms were not considered. Subsequently, Masri [32] covered both dilute and dense sprays, providing detailed discussions on current experimental and numerical capabilities for understanding spray flame structures. Moreover, Sánchez et al. [2] presented the progress made in the mathematical description of spray vaporization and spray flame for interacting multiscale processes and attempted to make use of the disparities between lengths and timescales in spray combustion. So far, there has been a lack of a comprehensive review focussing on the three-way turbulence–spray–

combustion interactions under diesel engine-like conditions. In particular, discussion has been limited on turbulent spray flames in supercritical environments and in methane–air mixtures, which are of importance to marine diesel engines and dual-fuel engines. Additional complexities, such as the presence of walls and radiation effects, have not been given sufficient attention in previous review articles. As pointed out by Sánchez et al. [2], understanding of the complex phenomena in turbulent spray combustion is far from complete.

Within the above context, this review covers key and representative developments in the area of turbulent spray combustion in terms of the spray–chemistry–turbulence interactions under engine-like conditions, as shown in **Fig. 4**. Valuable insights into the turbulence–chemistry, spray–turbulence, and spray-chemistry interactions under engine-like conditions are discussed. Furthermore, the spray–radiation interaction and spray flame-wall interaction (FWI), which usually occur in engines, are discussed. Finally, future research directions and further challenges involving supercritical spray flames, turbulent spray flames in dual fuel engines, and spray flames of real diesel fuels are also discussed briefly.

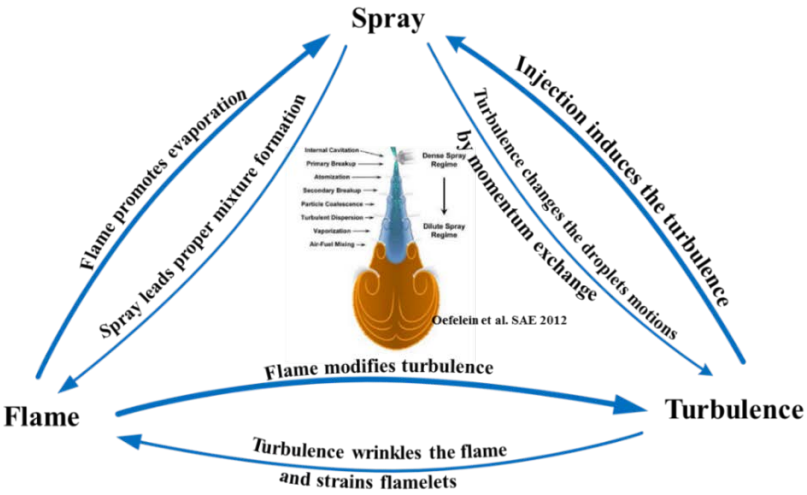

Fig. 4 Illustration of mutual interactions between spray, flame, and turbulence. The image of spray is reproduced from Ref. [34] with permission of SAE International.

2. Turbulent spray combustion

Interacting multiscale processes govern spray vaporization and combustion processes downstream of the near-injector atomization region in combustors [2]. The liquid fuel must be broken up into small droplets and exposed to hot ambient gas, promoting rapid evaporation and mixing. Hence, the combustion characteristics are dominated by the spray and mixing processes owing to their larger timescales. In turn, the combustion of fuel vapor exerts a significant influence on the atomization and mixing processes. The dynamics of spray and combustion determine the flame stability, efficient utilization of fuel, and formation and decomposition of pollutant emissions [33]. Therefore, to develop advanced combustion strategies, efforts should be made to understand the interacting processes in turbulent spray combustion. Because liquid fuel is injected into a high-temperature and high-pressure

environment, liquid droplets are formed, broken up, dispersed, collided, heated, and evaporated. The spray process with a high injection pressure promotes the spray–turbulence interaction. If the environment temperature is sufficiently high for the formation of a spray flame, turbulence–chemistry interaction will occur. In addition, because of the competing effects of cooling due to spray evaporation and flame propagation toward the injector, stable quasi-steady combustion may be established. The multi-injection strategy is a very effective way for reducing particulate emissions without a large increase in NO_x emissions [35, 36]. Such a multi-injection design will further complicate the spray–turbulence–chemistry interactions. A detailed discussion of this complicated process is provided below.

2.1 Turbulence-chemistry interaction

The turbulence–chemistry interaction poses a great challenge in understanding the complex engine processes because such an interaction occurs over a wide range of time and length scales. In general, turbulence enhances the macromixing and micromixing of reactants as well as the chemical reactions, leading to changes in the temperature and gas density, and affect the flow itself. Moreover, both turbulence and combustion are strongly nonlinear phenomena, where small fluctuations in conditions can trigger remarkable changes in combustion behaviors such as flame instability and quenching. Under diesel engine-like conditions, especially the relevant conditions for advanced combustion engines, unresolved small fluctuations in the turbulent flow or thermochemical state can affect the prediction of the combustion process [37]. The interaction between turbulence and chemistry is expected to dominate the ignition process [9], flame configuration with both temperature and composition inhomogeneity [38, 39], chemical pathway through a series of elementary reactions [40, 41] and formation of emissions [11], as illustrated in **Fig. 5,** which will be discussed later in detail.

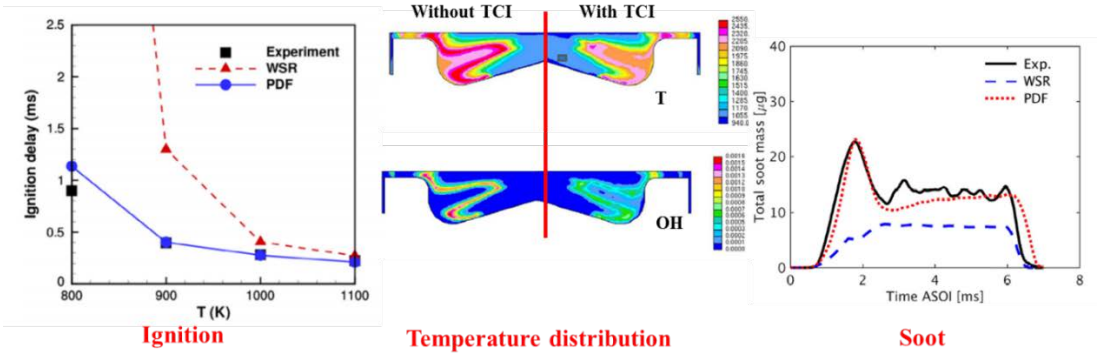

Fig. 5 Effects of turbulence–chemistry interaction on ignition delay time [9], temperature and OH distributions [37], and soot formation [11] under diesel engine-like conditions (the PDF method considers the TCI impact). Reprinted with permission of Elsevier.

2.1.1 Effect of turbulence on combustion

Turbulence affects the combustion process both directly and indirectly. Combustion depends on the mixing process between the fuel and oxygen at the molecular level. The eddy breakup forms smaller eddies, increasing strain and shear and therefore, steepening the concentration gradients of reactants, which in turn strengthens their molecular interdiffusion [42]. Turbulence can also wrinkle

and increase the flame surface and hence increase the global burning rate. Moreover, turbulence-enhanced heat losses can result in local flame quenching, and in the worst case, a premixed flame cannot survive under certain strong turbulence conditions [43]. Turbulence can induce a higher effective diffusion rate, leading to a thickened flame brush. Micro-mixing also depends on the local turbulent length scales. In a premixed flame, if the flame thickness (δ_L) is smaller than the minimum turbulence length scale (the Kolmogorov length scale, l_η), i.e., $\delta_L < l_\eta$, the entire reactive diffusive flame structure is embedded within the smallest eddies of the Kolmogorov scale, where the flow is quasi-laminar [42]. Turbulent fluctuations cannot perturb the flame; thus, its structure retains that of a laminar flamelet. When $l_\eta < \delta_L$, the flame thickness is larger than the Kolmogorov length scale such that the smallest scale of turbulence can stir the flame structure. Turbulent mixing at the smallest length scales is sufficiently energetic to disrupt the internal structure of the reaction zone [43]. This can only be true when the turbulence intensity is sufficiently high. Thus, a classical combustion regime diagram involving the laminar flame zone, thin reaction zone, corrugated reaction zone, wrinkled flamelets zone and broken reaction zone in terms of Da number and Karlovitz number (Ka) was proposed by Peters [42], which can describe the timescales of the flame–turbulence interaction. Turbulence with a fast timescale can homogenize the fuel–air mixture such that ignition is more prone to occur as spontaneous ignition [38]. However, fast mixing occurs only over a length scale smaller than the most energetic length scale of the temperature fluctuation. A high turbulence intensity results in the dissipation of heat and radicals during the first-stage ignition process, thereby retarding the ignition process [39].

The effect of turbulence on combustion differs significantly for different fuels. The combustion process of different fuels, including hydrogen, methane, and dodecane, was studied by varying the Karlovitz number (Ka), which is known as the ratio of the Kolmogorov timescale to the chemical timescale [44, 45]. A thickening factor was introduced to quantify the widening of the preheat zone in turbulent flames. The results showed an increase in the thickening factor for methane with a global Lewis number of unity, especially at low temperatures. For temperatures below approximately 760 K, the flame is at least 50% thicker, and the thickening factor increases up to 2.5 at a lower temperature. Even at a temperature of approximately 1220 K, some thickening can still be observed. For the premixed dodecane flame, the thickening effect of turbulence becomes more obvious at high Ka numbers. However, for a lean hydrogen flame with the global Lewis number of around 0.35, turbulence interacts with the premixed flame, creating regions of high positive curvature that can enhance the burning process. Compared to methane, fuel decomposition pyrolysis and oxidation occur in a relatively cool region. Although the basic oxidation pathways of species are largely unaffected by turbulent mixing, a large difference in the species distributions in the temperature space is observed between laminar and turbulent flames.

Turbulence can disturb the chemical pathways through a series of elementary reactions. Compared to those of a laminar flame, the temperature, species distribution, and heat release distributions can be considerably different in turbulent combustion, which directly affect the chemical pathways. The turbulent stirring process of small-scale eddies introduces spatially differentiated convective transport of species, thus altering the contributions of different reactions. At a low turbulence intensity or in a laminar flame, the transport of H radicals controlled by molecular diffusion is much slower than the local chemical timescale [46]. Owing to turbulent convection, the effective diffusion time is significantly shortened at a high turbulence level, which can be comparable to the local chemical timescale. The rapid transport of H radicals from regions of their formation enhances their concentration in the low-temperature region, thus significantly increasing the reaction rates of exothermic chain-terminating reactions, for example, $H + O_2 + M \rightarrow HO_2 + M$. Therefore, the low-temperature regions may exhibit enhanced heat release. A further study [47] showed that the locations with strong heat release appear at places away from regions of high fuel consumption through three reactions: $HO_2 + M \rightarrow HO_2 + M$, $HO_2 + H \rightarrow OH + OH$, and $HO_2 + OH \rightarrow H_2O + O_2$. No fuel molecule ($H_2$) is included in these reactions, which are responsible for much of the heat released at locations of negative curvature. Further studies to understand the global influence of turbulence on chemical pathways [40, 41] found that the contributions of several critical reactions to heat release can be influenced by turbulence. The dominant exothermic reaction $H + O_2 + M \rightarrow HO_2 + M$ changes by approximately 20%, and the importance of $H + OH + M \rightarrow H_2O + M$ reaction nearly doubles, which are a substantial effects.

Currently, the effects of turbulence are mostly studied in simple configurations, which neglects the high-speed injection process. In high-speed injection, the induced turbulence is greater than that in the ambient gas, and it is difficult to quantitatively study the effect of small-scale turbulence on combustion. Previous studies [48, 49] investigated the effects of macro-gas flow such as swirl on the spray flame. The swirl flow shortened the spray penetration and flame lengths. In addition, for the reacting case, strong liquid-gas interactions due to the anti-swirl flow could cause the local unburnt phenomenon.

2.1.2 Effect of combustion on turbulence

The combustion of fuel enhances the compositional gradients and alters the micromixing (or molecular mixing), which in turn has a significant influence on the reactions. Chemical reactions consume the fuel and oxidizer at the interface and steepen the scalar gradients in nonpremixed flames, thus enhancing the micromixing. The velocity statistics of turbulent flow are modified owing to the heat release and gas expansion [42, 50, 51]. The chemical heat release increases the gas temperature and thus the fluid viscosity, consequently dampening the turbulence. Experimental results reveal that combustion can modify turbulent flows and lead to the suppression of turbulence [52].

However, combustion can also generate turbulence, known as flame-generated turbulence, which plays a crucial role in the prediction of heat transfer, heat release, pollutant emissions, and instability in combustion devices [50, 53]. Flame-generated turbulence strongly depends on the level of heat release. A higher heat release results in a stronger flame turbulence effect [54]. Combustion also increases the turbulent kinetic energy (TKE) within the turbulent premixed flame brush because of the mean and fluctuating pressure terms [54]. Observations in experiments of freely propagating premixed flames reveal an increase in turbulence intensities across a flame, especially for the component normal to the flame brush, resulting in anisotropic turbulence after the flame passes [55]. Combustion can modify the turbulence intensity from different aspects. It can lead to a decrease in intensity due to dilatation and increased dissipation rates, which results from a rapid increase in viscosity. Combustion may also cause an increase in turbulence intensity owing to turbulent shear stresses, buoyancy, and interaction of density fluctuations with a small, self-induced pressure gradient [55]. The fundamental properties of turbulence can also be influenced by combustion. The increased dissipation dampens small-scale eddies, resulting in a lower frequency content and larger length scale. Volumetric expansion also increases the length scale [55]. In a direct numerical simulation (DNS) study of combustion effect on turbulence in a supersonic diffusion flame, the Reynolds stress budget was analyzed in detail [50]. It was found that, compared with the inert case, increasing the heat release leads to an intensification of the pressure–strain term in the reacting flow, which changes the flow anisotropy and the Reynolds stress components [50]. Moreover, the TKE budget via the pressure–strain contributes to combustion-generated turbulence [50, 51].

As for the effect of combustion on turbulence in a spray flame, a counter-clockwise vortex exists at the downstream position [56, 57]. The combustion-induced dilatation magnifies this vortex and even reverses the flow back towards the nozzle. The velocity component toward the nozzle can accelerate the transport of hot products upstream, which further influences the spray evaporation. A similar vortex structure was observed in the schlieren image [58]. In addition, in [59], by studying the interaction between local flow and flame structures, combustion could result in a 50–60% increase in local axial velocity owing to the density drop. Concurrent with the flow acceleration, the mixture transition from inert to reacting conditions led to radial expansion. Moreover, compared to the inert case, the simulation results showed that the entrainment of fresh air was reduced by approximately 25% for the reacting case, and the first drop in the entrainment rate appeared at the location of the flame LOL.

2.1.3 Prediction of spray flames based on TCI

Owing to the complex process of turbulent spray combustion, quantitative parameter studies using DNS [38, 39] are difficult to carry out in spray flames. An effective method for analyzing the effect of turbulence on spray flames is to compare the ignition and flame characteristics obtained from combustion models considering the TCI effect with those from the well-stirred reactor (WSR) model

[9, 60]. Unresolved turbulent fluctuations have been shown to affect the prediction accuracy of combustion and emissions of spray flames. In order to accurately predict turbulent spray flames, the TCI effects should be considered properly. Advanced combustion models that consider TCI effects show better accuracy in predicting the ID, flame LOL, distributions of temperature and intermediate products, such as CH_2O, H_2O_2, and soot precursor.

Neglecting the TCI effect may overpredict the local temperature distribution [61, 62]. With respect to the autoignition process, simulation results from those models considering TCI effects show better agreement with experiments, especially under low temperatures and/or low oxygen concentrations [9-11]. For example, for the case at a low initial gas temperature of 750 K, the WSR model fails to predict the ignition process, while the transport probability density function (PDF) model shows a reasonable agreement with experiments [11]. It was found that at higher temperatures, turbulent fluctuations play a less important role in global ignition behaviors than at low temperatures because the range of air/fuel ratio becomes wider and reactions can occur over a wider region in the mixture fraction space [11, 60]. As pointed out by Bhattacharjee and co-authors [9], detailed low-temperature chemistry at low reactivity conditions is required to sufficiently capture the autoignition process. In this case, the TCI effect becomes more pronounced by comparing the computed IDs and flame LOLs from the WSR and PDF methods at low- and high-temperatures conditions for both n-heptane and n-dodecane. As exhibited in **Fig. 6** , the difference in the ID introduced by considering TCI is $0.95\,\mathrm{ms}$ at f_{ign} for $T_{\mathrm{amb}} = 850\,\mathrm{K}$, compared to $0.27\,\mathrm{ms}$ for $T_{\mathrm{amb}} = 1000\,\mathrm{K}$, which indicates that TCI has a substantial effect at a low initial temperature of 850 K [60]. Shortly after the appearance of high-temperature kernels, spray flames reach the quasi-steady state, where the high-temperature region cannot move upstream and stabilize at a place. The inclusion of TCI effects by employing the transport PDF approach with two reduced mechanisms plays a much more important role in predicting the LOL than in modeling the ID [11, 63]. The LOL strongly reflects the quasi-steady state of a spray flame, which is also dependent on the fuel injection process and is relevant to the spray–combustion interaction discussed later.

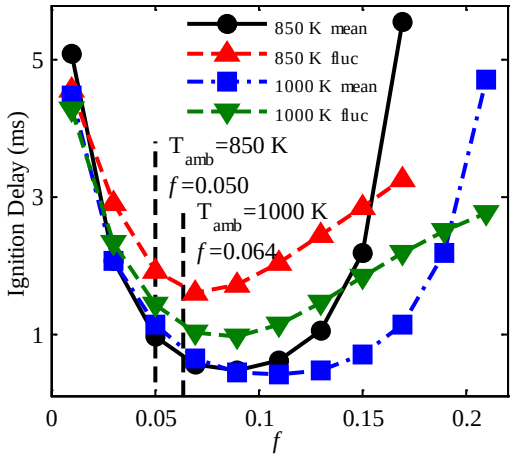

Fig. 6 The ignition delay as a function of the mixture fraction based on the TCI effect under n-heptane spray flame conditions at low and high initial temperatures of 850 K and 1000 K, respectively [60].

Furthermore, the TCI effect also plays a critical role in the distributions of the mixture concentration, temperature, and intermediate species, such as OH. Previous studies [9, 37, 61, 62] have shown that neglecting the TCI may lead to an overestimated heat release rate, which results in a higher local temperature and OH concentration. A broader turbulent flame brush was found when the TCI effects were considered [9, 62]. From the ϕ–T maps in **Fig. 7**, it can be seen that both the PDF and WSR methods can obtain similar diffusion flame structures. However, compared to the WSR method, the PDF method can resolve many more thermochemical state points, which indicates more inert mixing and consequently a substantial effect on emissions predictions. It should be noted that the "rich-premixed core" and "outer diffusion flame" labels in **Fig. 7** indicate the characteristics of standard quasi-steady diesel combustion.

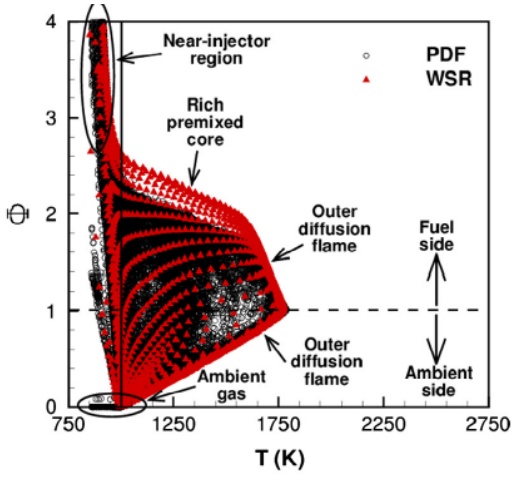

Fig. 7 Computed $\phi - T$ maps from WSR and PDF methods to analyze the effect of TCI on the flame structures for quasi-steady n-heptane spray flames at 8% oxygen concentration. Reprinted from Ref. [9] with permission of Elsevier.

Some other studies [10, 63] have focused on soot formation in turbulent spray flames considering the impact TCI. Soot formation is expected to be strongly dependent on air entrainment into the turbulent spray [64]. The current state of soot modeling is immature. TCI effects are expected to increase the soot oxidation rate, leading to considerably lower soot mass. In addition, TCI effects result in narrower soot distributions; and soot onset and peak are located at further downstream locations when the TCI is not considered [63]. As displayed in **Fig. 8**, the predicted flame structures show large differences between the WSR model and the transport PDF model in terms of the soot peak values and locations. Without considering the TCI, the WSR model overestimates the formation of soot and both the soot peak locations and flame heads move further downstream. Moreover, the WSR model overpredicts the flame LOL. Micromixing is completely ignored by the WSR model, leading to

a significant difference in the flame LOL. The macromixing prediction is also indirectly influenced by different combustion models. Large-scale gradients affecting macromixing are much lower in the transport PDF model than in the WSR model [63]. However, Mohan et al. [37] found the opposite conclusion in modeling soot production in a heavy diesel engine. They found that the PDF model considering the TCI effect resulted in more soot, which is closer to the experimental data than that from the WSR model. The main reason for this is that a wider range of thermochemical states is obtained by the PDF model, which is beneficial to soot prediction. It should also be noted that soot formation is a complicated process that is affected by both physical and chemical factors. Therefore, the effect of TCI under a wide range of conditions should be further studied to isolate its effect.

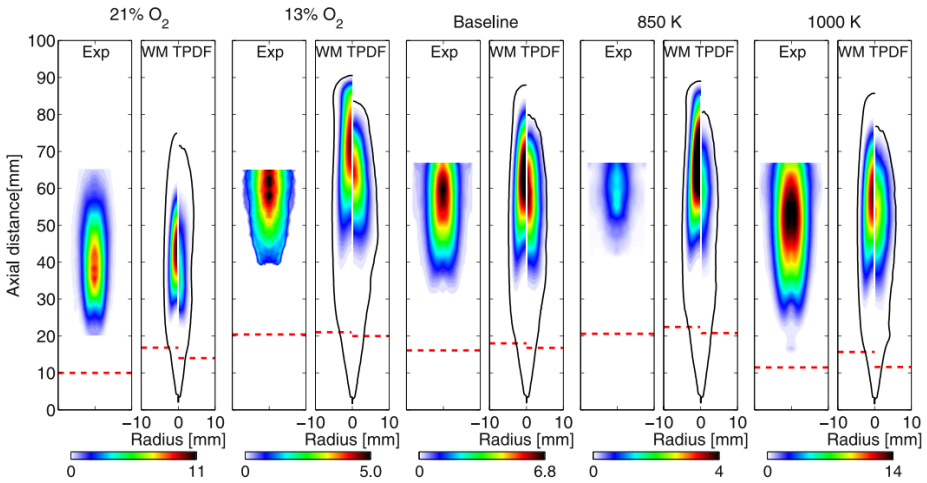

Fig. 8. Comparisons between flame structures from the WSR and transport PDF models [63]. The red dashed line represents the location of flame LOL. Reprinted with permission of Elsevier.

It is also noted that turbulent models in LES and RANS also influence the ignition and combustion. LES can obtain the transient spray flame structure involving the distributions of the mixture fraction, temperature, OH, and soot mass fraction, as well as accurate combustion characteristics of the ID and flame LOL at different initial temperatures [57]. More importantly, LES captures the multiple ignition spots in the mixing layer; in contrast, the RANS method can capture only one ignition spot.

2.1.4 Chemistry mechanism impact

In spray flame simulations, two essential aspects should be considered, i.e., the selection of the chemical kinetic mechanism and the TCI effect. As discussed above, the spray flame characteristics can be accurately captured by considering TCI based on the selection of an accurate chemical mechanism [65, 66]. More sophisticated chemical kinetic models with a very large number of species and radical reactions have been proposed for the main fuels of engines [67]. However, the application of detailed chemical kinetics in combustion simulations is very limited, and the major challenge is the computation-intensive nature of chemical kinetics integration for a large number of chemical species

and reactions over a wide range of chemical timescales involved. Therefore, a skeletal mechanism consisting of a selected subset of species and reactions derived from the detailed mechanism is usually applied to model the combustion process within certain accuracy, over a wide range (e.g., comparable to that of the detailed mechanism) of conditions, i.e., different pressures, temperatures, oxygen concentrations, and equivalence ratios. Over the past decade, great efforts have been made to develop sufficiently accurate skeletal or reduced mechanisms for n-heptane [68], iso-octane [69], dodecane [T. Yao, Y. Pei, B.-J. Zhong, S. Som, T. Lu and K. H. Luo, "A compact skeletal mechanism for n-dodecane with optimized semi-global low-temperature chemistry for diesel engine simulations," Fuel 191: 339-349 (2017)] and primary reference fuel [70] using different methods [67]. The reduced mechanisms were developed to cover engine-like temperature and pressure conditions. For instance, Frassoldati et al. [71] developed a reduced mechanism for n-dodecane, including 96 species and 993 reactions, from a detailed chemistry mechanism consisting of more than 450 species and 15,000 reactions [72]. The proposed reduced mechanism obtained a good qualitative agreement with the experimental data by comparing the IDs, species concentration profiles from flow reactors and JSRs, and laminar flame speeds over a wide range of conditions. It was concluded that the predictive capabilities were significantly affected by the low-temperature reactions including the early period for which the cool flame extends [65]. Therefore, a widely used kinetic mechanism should be able to accurately predict the first-stage ignition process (cool flame), especially under low-temperature and/or low oxygen concentration conditions, which are typical for LTC strategies.

Furthermore, the simulation accuracy of turbulent spray flames is also dependent on the boundary conditions including the injection conditions, ambient temperature and pressure, fuel properties, and numerical parameters [57, 73]. Related to this, uncertainty quantification analysis can be conducted to provide insights into the effect of boundary conditions on the spray flame characteristics. A global sensitivity analysis to understand the effect of boundary conditions on 17 variables was carried out by Pei et al. [73]. They found that the liquid penetration length is significantly affected by the uncertainty in the fuel temperature, whereas the vapor penetration length is very sensitive to the initial turbulence intensity and nozzle diameter. Furthermore, the ambient temperature has a strong effect on the ID and flame LOL at both a low temperature of 800 K and a high temperature of 1100 K, but its strong effect on soot emissions only happens at 800 K. Moreover, the nozzle diameter significantly influences the soot mass. A study of the influence of injection-to-injection variation with multiple realizations on the turbulent spray flame using the LES method was conducted [57]. Using the relevance index analysis, it was suggested that at least 5–6 realizations are required to capture a similar mixture fraction and temperature of approximately 99% compared to 16 realizations. However, the soot and OH mass fraction require more realizations of 8 and 14, respectively, because of the high fluctuations.

In summary, the validation of turbulent combustion models, chemical mechanisms and spray

models should be coupled in a real spray flame. Many studies have demonstrated that consideration of the TCI provides a better prediction over the WSR model in terms of flame LOL and ID [10, 63, 74]. The WSR model without considering the TCI can overpredict the ID, especially at low ambient temperatures and low oxygen concentrations [9, 75]. A thin flame structure with a considerably high local peak temperature and heat release rate was also observed when the TCI impact was not considered. Moreover, the TCI can also cause less soot emission but higher NO formation [76]. To accurately evaluate the TCI effect in turbulent spray flames, the spray models, boundary conditions, and chemical reaction mechanisms should be carefully considered first. In most studies, turbulence is induced by the spray process; however, the effect of ambient turbulent flow on combustion in turbulent spray flames under diesel engine-like conditions has not been well established. Furthermore, researchers have started to use LES with subgrid-scale models to consider small-scale fluctuations while resolving large-scale turbulent fluctuations [77, 78]. Such studies help to clarify the TCI effects at different scales and should be extended to more realistic conditions.

2.2 Spray–turbulence interaction

The spray–turbulence interaction that occurs immediately after injection is important for the subsequent ignition and combustion processes. In this section, the effects of turbulence on droplet motion and liquid injection as well as the effects of spray on turbulent flow are discussed.

2.2.1 Effect of spray on turbulence

In combustion engines, cold fuel is directly injected into a high-temperature and high-pressure environment with a large initial velocity, forming a dense spray near the injector nozzle. The injection pressure provides a high spray momentum, thus promoting turbulence [79]. The momentum exchange between the ambient hot gas and the cold dense spray produces droplets and then vapor with strong kinetic energy to move downstream. The high-velocity gradients between the droplets/vapor and the ambient gas promote the generation of shear layers, entrainment vortices, and turbulence, which in turn improve mixing between the fuel vapor and air [80], as illustrated in **Fig. 9**. The entrainment of hot gas accelerates the evaporation of droplets, leading to large gradients in the local temperature and mixture concentration. The liquid phase can only exist in a small region close to the injector nozzle. Further downstream, it breaks up into small droplets, which then vaporize and mix with hot gas, forming an ignitable mixture.

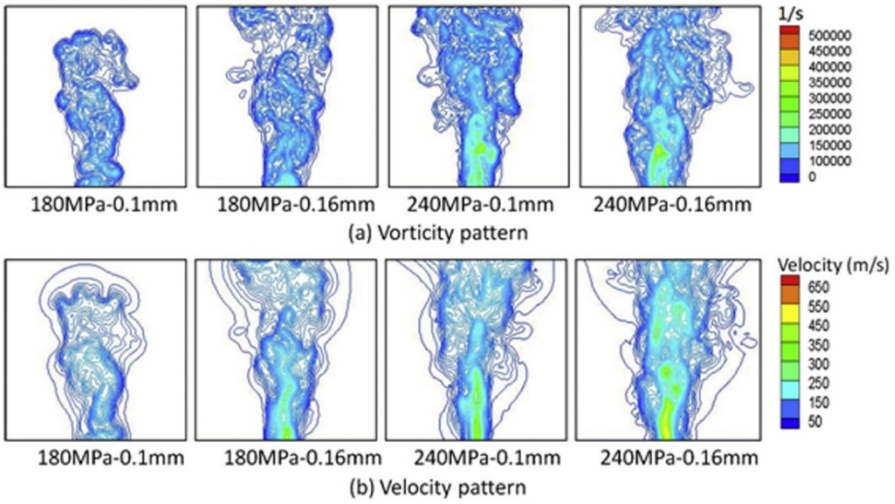

Fig. 9 Effects of spray injection pressure and injector diameter on the turbulent flow field. Reprinted from Ref. [80] with permission of Elsevier.

The length of the liquid phase, known as the liquid penetration length, is less dependent on the initial gas temperature [79]. Injection pressure and ambient density play important roles. An increase in gas density leads to shorter liquid penetration and faster breakup and mixing rates by (1) changing the droplet breakup rates and (2) increasing hot air entering the liquid spray [81]. However, the effect of turbulent fluctuations is negligible, as reported in [11]. The vapor phase shows strong instability and cycle-to-cycle variations in five different injection realizations [82]. As the vapor mixes with the hot ambient gas, the spray head becomes much wider and leaner. Meanwhile, attenuation in the spray axial velocity leads to slow movement of the vapor head. Simulation results also showed a rapid decrease in the scalar dissipation rate downstream of the spray, indicating that the flow timescale characterized by the reciprocal of the scalar dissipation rate becomes much longer.

Regarding the effect of spray on turbulence in multiple injections, it was found that the local turbulence intensity formed in the first injection is enhanced when the second injection moves into the first injection flow [83]. The effect of spray on turbulence also depends on the injection parameters, such as the dwell time (DT) and injection duration in split injections. The DT affects the interaction between the injections, the maximum penetration of the second injection, and the distribution of the TKE. The overlap region of two injections for the case with short DT has a high TKE, which can enhance mixing owing to the high local scalar dissipation [83]. However, the strong interaction limits the entrainment of the oxidizer ahead of the second injection, which is carried by the first injection toward the downstream locations.

2.2.2 Effect of turbulence on spray

Turbulent fluctuations in the fuel jet are the main sources of initial perturbations on the jet surface [84]. It is expected that the gas–phase turbulence affects the breakup process in the spray, but an in-depth understanding is lacking. Turbulent fluctuations induced by the liquid spray have a significant effect on liquid droplet evolution and considering the turbulent fluctuation effects in numerical

simulations can lead to a more accurate prediction of liquid penetration and distribution of fuel vapor [85, 86].

Turbulence effects on the breakup process

If a liquid is injected directly into the gas–phase ambient, the primary breakup length is expected to be strongly affected by the mean spray/gas velocity or gas–phase fluctuations and the turbulence intensity. Gas-phase turbulence affects the spray atomization process, which was first examined by Kolmogorov [87]. The results show that for gaseous flows with high Reynolds numbers, fragments of size D_B satisfy $D_B \gg l_\eta(\frac{v_l}{v_g})^{\frac{3}{4}}$ where l_η is the Kolmogorov scale, and turbulent 'resonant' atomization can be exhibited. Any droplet larger than l_η will exhibit turbulence-assisted atomization. If the relative velocity between the ambient gas and the liquid jet is sufficiently high, the liquid jet surface will show significant instabilities. An increase in the Reynolds number of the liquid jet can cause turbulent breakup [88]. For the effect of turbulence on droplet dispersion, it was shown that larger drop sizes have larger fluctuations of droplet concentration as a result of a similar timescale of droplet response compared to the Kolmogorov timescale [89]. Hence, random turbulence has a very important effect on the fluctuations in the droplet concentration of larger droplets.

Gas-phase fluctuations have a significant influence on the primary breakup morphology, and the deformation of droplets exhibits a clear dependence on the turbulent Weber number [88]. The occurrence of gas-phase velocity fluctuations is likely to randomize the break-up process. The concept of a turbulent Weber number was proposed by Kolmogorov and expanded by Hinze [90], as follows:

$$\mathrm{We}_t = \frac{\rho_g \overline{u_d^2} d}{\sigma} \qquad \text{Eq. 1}$$

where $\overline{u_d^2}$ represents the mean square of the velocity fluctuations between two points located at diametrically opposite positions on the surface of the droplet. ρ_g is the gas density, d indicates the droplet diameter, and σ is the coefficient of surface tension. To characterize the droplet shapes by considering the effect of gas-phase fluctuations, Kourmatzis and Masri [88] defined the turbulent Weber number We' by employing the mean droplet diameter $\langle d \rangle$ and the rms velocity u', as shown below:

$$\mathrm{We}' = \frac{\rho_g (u')^2 \langle d \rangle}{\sigma_1} \qquad \text{Eq. 2}$$

Based on the defined turbulent Weber number, they found that the aspect ratio of the droplet has a linear relationship with the turbulent Weber number and turbulent fluctuations can delay the evolution from deformed to more spherical droplets.

In the Lagrangian method, the effect of turbulence on the droplet motion is exerted by momentum exchange. In the high-velocity region, the spray-induced subgrid kinetic energy and droplet

turbulent dispersion can significantly alter the position and motion of the droplet [85, 86]. The Lagrangian operation for keeping track of the motion of these parcels is a series of ordinary differential equations, which govern the mass, momentum, and energy exchanges between the liquid spray and the gas. In the droplet Lagrangian equations, the drag force $F_{i,d}$ of the gas phase on a liquid drop is modeled as:

$$\frac{F_{i,d}}{m_d} = \frac{3}{8}\frac{\rho}{\rho_l}\frac{V_{rel}}{r_d}(\tilde{u}_i - v_{d,i})C_D \quad \text{Eq. 3}$$

where ρ_l is the density of the liquid droplet, and C_D is the drop drag coefficient. V_{rel} is the magnitude of the relative velocity between the liquid droplet and the gas, defined as $V_{rel} = |\tilde{u}_i + u'_{p,i} - v_{d,i}|$. Here $\tilde{u}_i$is the velocity of the surrounding gas, and $u'_{p,i}$ is turbulent dispersion velocity, which is randomly selected from a Gaussian distribution with a standard deviation of $\sqrt{2/3k}$, where k stands for the TKE. V_{rel} determines the momentum exchange and the gas-phase TKE affects the dispersion velocity. For the spray-induced kinetic energy, Bharadwaj et al.[86] developed a spray source model that considers the subgrid-scale energy exchange between the droplets and the gas phase with the correct scaling of *k*. The subgrid-scale energy eventually feeds back to both the spray droplets and the gas-phase turbulent mixing. The final spray source term can be defined as

$$\overline{\dot{W}^s} = -\frac{3}{8}\frac{C_D}{V_{cell}}\sum_d\left[\frac{m_d\rho V_{cell}}{r_d\rho_l}(\tilde{u}_i + u'_{p,i} - v_{d,i})(2\tilde{u}_i - 3\widetilde{\tilde{u}_i} + \widetilde{\widetilde{\tilde{u}_i}}\right] \quad \text{Eq. 4}$$

where $\approx$ represents two test filtering procedures. All filtered velocity fields can be obtained from the LES solution.

To further understand the effect of turbulence dispersion velocity on the spray process, Hindi et al. [91] conducted an LES study for a non-reacting n-dodecane spray with a stochastic turbulence dispersion model. A new criterion for determining mesh refinement was proposed based on the droplet Stokes number, which is defined as the ratio of the droplet response time to the turbulent eddy timescale. The adopted mesh should be sufficiently refined, and no turbulent dispersion modeling is required if the droplet Stokes number is above unity. The subgrid turbulence does not influence the droplets because the influence of turbulent dispersion on the droplets is already considered by the resolved scales.

Turbulence effects on atomization and evaporation

The turbulence formed inside the nozzle enhances the primary breakup and leads to a decrease in the droplet size and liquid penetration, and an increase in the radial dispersion of the spray [84, 92]. Huh and Gosman [93] proposed a phenomenological model that considers the effects of turbulent fluctuations in the jet on the breakup process. Later, Bianchi et al. [94] added the effects of turbulence to the Kelvin-Helmholtz (KH) model. They calculated the mean droplet size and production rate from the estimated mean turbulence properties of the nozzle flow. Then, Berg et al. [92] extended this idea by employing local nozzle flow and additional TKE from the cavitation bubble collapses to compute the local distribution of breakup rates in the orifice cross-section. As a result, based on the above

studies, Som and Aggarwal [84] developed a new primary breakup model (KH-ACT), which considers the effects of aerodynamic, cavitation, and turbulence. The results showed that the improved model can obtain good agreement with the X-ray experimental data for the liquid penetration length, spray cone angle, and liquid mass distribution, as well as the flame LOL and flame structure under a wide range of diesel engine conditions.

In internal combustion engines, entrainment is extremely important because enhanced entrainment helps promote soot oxidation, but overmixing leads to deteriorating unburned hydrocarbons (UHC) for LTC strategies [95]. Large-scale motions in turbulent jet engulf volumes of fluid in bulk, thus, promoting the entrainment of large packets of exterior fluid into the turbulent region [96]. Hence, the entrainment may be dominated by manipulating the boundary conditions. This conclusion can be confirmed by comparing the turbulent spray structures under different initial conditions, namely, gas temperature, oxygen concentration, and gas density [97]. A higher initial gas temperature, oxygen concentration, or gas density results in a thinner flame structure, inhibiting the contact area between the fuel droplet and the surrounding fresh gas. Hence, entrainment is very limited, leading to higher soot emissions [98]. Other researchers have argued that small-scale turbulent mixing at the highly sheared jet interface dominates the entrainment process [99]. Because of large-scale eddies, the ambient non-turbulent fluid can be ‘induced’ and ‘engulfed’ into the turbulent core, which is converted into turbulent motion by the action of small-scale eddies via ‘nibbling’. The spray tip region, regarded as the capturing section, provides more than 80% of the total gas mass flow [100]. High injection pressure enhances the TKE at the exit plane, promoting fuel atomization and mixing. However, only an ultrahigh injection pressure, such as 300 MPa, can enhance the mixing process; injection pressure ranging from 50 to 150 MPa has a weak influence on the liquid penetration and even the IDs [4, 101].

2.2.3 Momentum exchange between gas and liquid

In two-phase flow calculations, there are two methodologies for simulating liquid- and gas-phase flows, namely (1) the Eulerian method, where both liquid and gas phases are treated as continuum fluids in the entire flow domain, and (2) the Lagrangian method, where the liquid phase treated as clusters of droplets is tracked in the entire flow domain. When the Eulerian method is applied to treat a liquid phase, a liquid–gas flow structure with high fidelity can be obtained. However, this method is computationally expensive [21], and it can only be used for the near-nozzle region. The Lagrangian-Drop-Eulerian-Fluid (LDEF) method was then proposed and has been widely applied for gas–liquid flows [102] owing to its low cost. In this method, the liquid fuel is considered as a sequence of discrete particles tracked by the Lagrangian particle tracking method, and the ambient fluid (gas) is considered as a continuum fluid solved by the Eulerian method. The two-phase interaction is treated by introducing spray source terms into gas-phase conservation equations.

Although the Lagrangian particle tracking method can efficiently obtain the droplet motion trajectory, this method also has strong grid dependence [103, 104]. A previous study reported that this method cannot accurately capture the spray–turbulence interaction and causes incorrect momentum coupling between the gas and liquid phases, which consequently results in resolution-dependent results when the spatial distribution of droplets is highly nonuniform [105]. Araham [106] examined the grid dependency of spray models for vaporizing diesel sprays in a constant-volume chamber and showed that to accurately predict the spray structure, the nozzle region must be adequately resolved. Further studies demonstrated that the relative velocity between the liquid and gas phases is mesh-dependent and thus may cause a lower axial velocity, liquid and vapor penetration lengths for a vaporizing diesel spray when employing the LDEF method [104, 107].

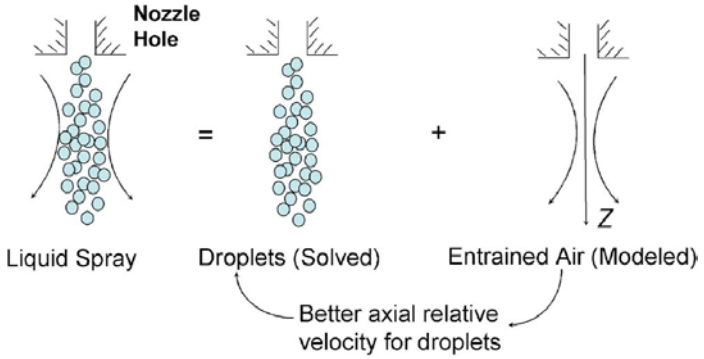

Fig. 10 Schematic of a spray model based on the gas jet theory considering the gas flow velocity induced by the spray process. Reprinted from Ref. [108] with permission of ASME.

Several studies have been conducted to address the above issue. Based on the momentum exchange between the gas flow and droplets, Abani et al. [108] and Beard et al. [104, 107] proposed improved spray models, which can obtain an accurate gas flow velocity induced by the spray process and consequently reduce grid dependency, as depicted in **Fig. 10**. In the new spray model, the spray flow has two components: the group of droplets, which comprises the liquid phase, and the air entrained, which represents the gas phase. For the gas jet theory, the improved spray model is briefly reviewed in the present work. In the equation for the magnitude of the relative velocity as shown above, $\tilde{u}_i$ is given as $\tilde{u}_i = (\tilde{u}_x, \tilde{u}_y, \tilde{u}_z)$, where $\tilde{u}_x$ and $\tilde{u}_y$ are respectively the x-direction and y-direction perpendicular components of the ambient gas-phase velocity solved by the original computational solution, while $\tilde{u}_z$ is the z-direction component derived from the entrained gas velocity model. The velocity $\tilde{u}_i$ is used to calculate the magnitude of the relative velocity between the liquid droplet and gas V_{rel}. At present, two equations including steady and unsteady equations are used to calculate the entrained gas velocity.

For the entrained gas velocity model according to the gas jet theory the velocity, $\tilde{u}_z$ is given by the Steady Equation Model [109] and the Unsteady Equation Model [110]. The Steady Equation Model is expressed as:

$$\tilde{u}_z = min\left[U_{inj}, \frac{3U_{inj}^2 d_{eq}^2}{32\upsilon_t z(1+\frac{3U_{inj}^2 d_{eq}^2 r^2}{256\upsilon_t^2 z^2})^2}\right] \quad \text{Eq. 5}$$

where U_{inj} is the injection velocity of the liquid jet, which is assumed to be the injection velocity of the gas jet; z stands for the axial distance between the droplet parcel and the nozzle; and *r* represents the radial distance of the droplet parcel from the spray axis. Based on this definition, the relative velocity between the ambient gas and fuel droplets in the near-nozzle region is assumed to be approximately zero. d_{eq} represents the equivalent diameter, which is defined as $d_{eq} = d_{noz}\sqrt{\frac{\rho_l}{\rho_g}}$, where d_{noz} stands for the effective nozzle diameter, and ρ_l and ρ_g are the densities of the liquid and gas phases, respectively. υ_t denotes the turbulent viscosity of the jet and is calculated as $\upsilon_t = C_t \pi^{0.5} U_{inj} d_{eq}/2$, where C_t is the entrainment constant, which is set to 0.00161.

Lee and Reitz further improved the spray model based on the gas jet theory and carefully studied the spray tip penetration of diesel sprays over a wide range of ambient gas density conditions [111, 112]. The results demonstrated that the new spray model can efficiently obtain the relative velocity of the droplets and gas based on accurate momentum exchange and entrainment rate predictions. Consequently, mesh independency over grid sizes with a maximum disparity of 16 times performed very well in terms of spray characteristics such as spray tip penetration, droplet size, and spray structure, as illustrated in **Fig. 11**.

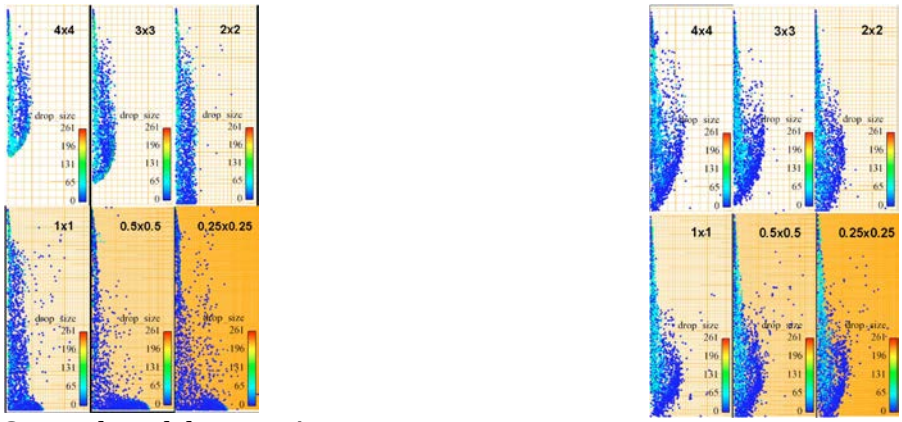

a) Original model in KIVA b) Improved model with gas-jet theory

Fig. 11 Predicted spray structure using the original and improved methods in KIVA. Reprinted from Ref. [108] with permission of ASME.

To summarize, this section discusses recent progress in the understanding and modeling of the spray–turbulence interaction. The mechanisms of spray effects on the turbulence as well as turbulence effects on the spray are discussed. The spray effect on turbulence strongly depends on the injection parameters. Actually, the core issue of the spray–turbulence interaction is the momentum exchange

between the ambient hot gas and cold dense spray, which enables the initial mixing process and subsequently determines the ignition and combustion processes. The gas jet theory [109, 113] thoroughly explains the importance of the momentum exchange between the gas flow and droplets. The spray–turbulence interaction is treated by introducing spray source terms to the gas-phase conservation equations to obtain an accurate gas flow velocity induced by the spray process, which reduces the grid dependency. On the other hand, a more accurate model considering spray–turbulence interaction is still required for very high injection pressures of more than 300 MPa.

2.3 Spray–chemistry interaction

The spray–chemistry interaction has obvious effects on the performance, stability, and reliability of internal combustion engines and gas turbine engines [114]. The evaporating fuel droplets feed the flame, and heat transfer from the high-temperature regions enhances the evaporation of fuel, thus, sustaining the fuel supply. Fuel evaporation occurs at small scales, and subsequently, the evaporated fuel mixes with air to form a combustible mixture. Large-scale turbulence promotes macromixing, whereas small-scale turbulence enhances micromixing. After mixing of the vapor fuel and air, ignition kernels appear at certain locations, which are controlled by the local mixture fraction state, the temperature and the level of scalar dissipation rate [30]. A strong coupling between the spray and combustion significantly increases the complexity because it occurs over a wide range of scales. The relative importance of the evaporation timescales versus the convective and molecular diffusion timescales in the surrounding gas determines the ignition modes. The presence of liquid droplets also alters the combustion dynamics. The local flow conditions, droplet distribution, scalar gradients, and mixture fraction distributions may determine the flame regimes [115]. It can be observed that at the inner side of the turbulent spray flames, where evaporation mainly occurs, the hot pilot transfers heat from the intense reaction regions to the spray mixture, thus enhancing the evaporation of fuel droplets. In turn, fuel evaporation provides fuel vapor to support the reactions for further expansion [12].

2.3.1 Effect of combustion on spray

Effect of combustion on species distribution and spray characteristics

Combustion is expected to greatly influence the evolution of the spray tip penetration and spray structure as a whole. Pieces of evidence have been collected both experimentally based on schlieren imaging [116] and numerically using a one-dimensional spray model [59]. The change in the spray tip penetration and flame structures depends on the initial temperature, pressure, density [117], and residence time [58]. In [117], the flame structures under different initial gas temperatures and densities were compared, showing that earlier ignition contributes to the acceleration of spray tip penetration at a higher gas temperature. In addition, low-temperature chemistry leads to a small decrease in density and accelerates evaporation. The hot gas expansion causes faster transport of fuel vapor in the radial direction [118]. García-Oliver [59] revealed that combustion-induced heat release downstream of the

flame LOL leads to a strong change in the flow pattern, whereas chemical activity upstream of the flame LOL exhibits very little influence on the spray flow. The initial operating conditions also affect the distribution of key species within the spray flames. For example, **Fig. 12** shows the axial flame structures during the low-temperature ignition (LTI) and HTI stages and under different oxygen concentrations [119]. At the early stage t_1, evaporation of cold fuel droplets results in a decrease in temperature in the near-injector region, where oxygen is insufficient, and low-temperature reactions are formed downstream of the spray after premixing. Hence, a cool flame represented by the CH_2O formation region exists in a wider zone along the axial direction in the spray under low oxygen conditions owing to the reduction in the mixture reactivity and the longer residence time. After the high-temperature kernels appear at the periphery of the spray where the gradients of the mixture fraction and temperature are not very steep [30], the LTC products are quickly consumed but still remain in a wide region. High-density and high-pressure environments compress the spray and prevent the flame from dilating outside. The compressing effect outweighs the gas expansion influence although the high-temperature reactions and radial expansion appear earlier at high densities [29].

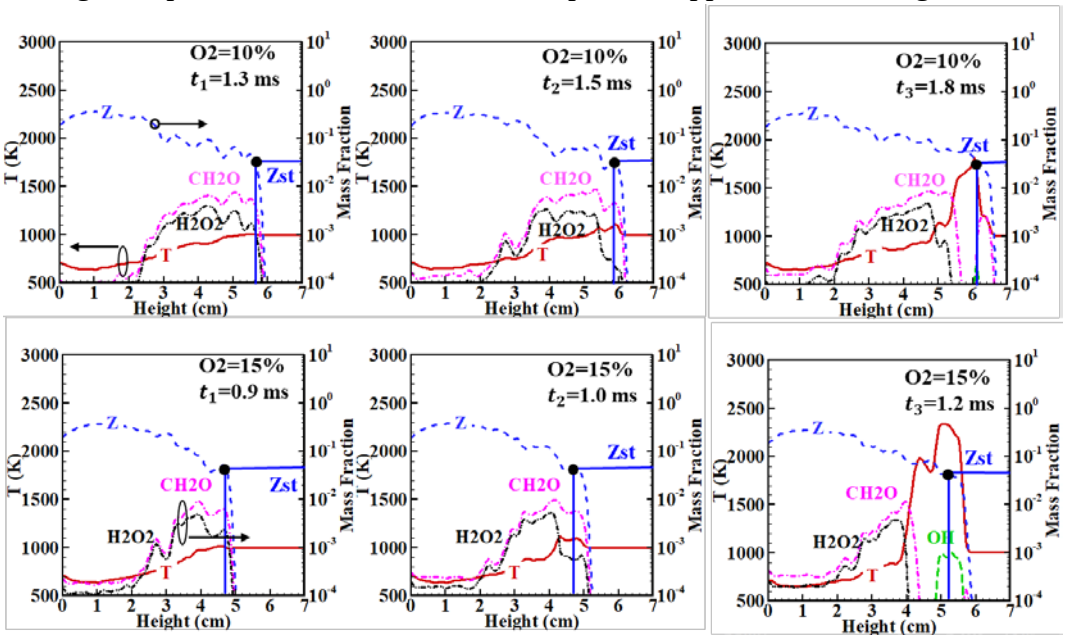

Fig. 12 Axial profiles of temperature, mixture fraction, and mass fraction of species for 10% (top) and 15% (bottom) oxygen concentration [119].

The effect of combustion on the spray structures can be determined by investigating the difference between the non-reacting and reacting conditions. During the early stage (approximately 0.2 ms after the start of injection), two sprays injected into environments with and without oxygen have similar structures [27]. In the reacting case (with oxygen in the ambient gas), a 'softening' effect is observed in the schlieren images near the head of the spray, indicating LTC, which is also confirmed by the formaldehyde distributions. The low-temperature reactions result in an increase in temperature, leading to reduced gradients in the local refractive index. Thus, prior to HTI, the tip penetration of the reacting spray is slightly longer as a result of the low-temperature reactions [116, 120]. Subsequently,

combustion significantly accelerates the movement downstream. The reacting spray becomes wider and longer than the nonreacting spray. Fuel type mainly affects the time when the reacting spray starts to separate from the inert one. The higher the fuel reactivity, the earlier the occurrence of autoignition. In addition, after approximately 2.0 ms, the ratio of the spray penetration lengths under the reacting (S_r) and inert (S_i) conditions becomes quasi-steady, indicating that the acceleration effect is negligible.

Effect of combustion on split injections

The combustion of split injections is much more complex because both the ignition and structure of the second spray are affected by the temperature increase and intermediate species in the previously injected spray. The effect of density decrease on spray was analyzed well in an LES study of split injections [117], where the second injection penetrated a hot environment with a low density as a result of the combustion of the previously injected spray. The resistance met by the second spray is much lower, thus accelerating the movement of spray head downstream. An increase in the axial velocity for the second spray was observed in the experiments by Skeen et al. [121]. It was found that the second injection enters a 'slipstream' produced by the first injection, promoting mixing for the second injection as displayed in **Fig. 13** [121]. Similar phenomena were also reported by Bolla et al. [122] using the transport PDF method. In addition, Moiz et al. [123] pointed out that the initial gas temperature also has a significant influence on the vapor penetration length. For the case with a low initial temperature, the evaporation rate is relatively low. Consequently, the effect of the slipstream becomes small. The DT between split injections also affects the mixing process, and a short DT is prone to increase the mixing rate at the head of the second injection [124]. Furthermore, earlier ignition of the second spray accelerates the movement of the second head owing to gas expansion [116]. As a result, the second injection moves downstream at a higher speed [117]. It should also be noted that in studies of the combustion effect on the spray, the radiative heat transfer plays a role in droplet evaporation, which will be quantitatively analyzed in later sections.

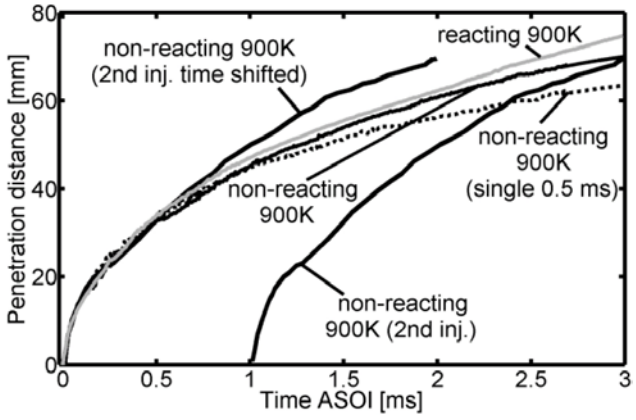

Fig. 13 Temporal evolution of vapor penetration after the start of injection for single and split injection strategies under inert and reacting conditions. Reprinted from Ref. [121] with permission of SAE International.

2.3.2 Effect of spray on combustion

The continuous and dispersed phases influence each other because of the momentum exchange at the droplet surface. The atomization and evaporation of cold fuel provide an ignitable mixture that may undergo a multistage ignition process. Split injection strategies involve a strong spray–combustion interaction, which affects the ignition [121, 125], flame structure [126], and soot formation [121, 127]. Once the injection is split into two injections, the ignition process and flame structures are strongly influenced by the first injection, and the already burnt flame shows intense interaction with the upcoming second injection with respect to the ignition process, flame structures, and pollutant emissions.

2.3.2.1 Effect of spray on ignition

The effect of spray on the ignition process is due to the fact that the continuous injection is split, which gives rise to different ignition processes depending on the design parameters, for example, the initial gas temperature. Scatters of the temperature and CH_2O mass fraction in the mixture fraction space at different ambient temperatures are illustrated in **Fig. 14**. The already formed intermediate species and hot environment can proceed with the formation of high-temperature kernels in the second injection, thus shortening the ID time. The temperature increase has the most significant influence, followed by the formation of species, i.e., CH_2O and H_2O_2 [128]. As pointed out in a previous study [123], high-temperature kernels are only formed after the end of the second injection by decreasing the initial temperature to 750 K, leading to an extremely long mixing time for the fuel and air. The injected fuel mass during the first injection is very small, approximately 1.18 mg. Thus, the fuel–air mixture becomes too lean to initiate high-temperature kernels. When the subsequent injection interacts with the already formed cool-flame products, high-temperature kernels appear in the second injection, which is confirmed by formaldehyde planar laser-induced fluorescence (PLIF) images. Thus, the interaction between the two injections promotes spray ignition. However, at higher ambient temperatures, i.e., 900 K and 800 K, high-temperature reactions appear twice for the split injections. The earlier ignition of the second injection heats the region close to the injector, thus promoting the evaporation of fuel droplets. Hence, the liquid penetration length is also reduced. After ignition, the high-temperature burning zone induced by the second injection moves slightly downstream of the liquid length, and before the combustion recession, the flame LOL of the second injection approached the injector.

Furthermore, injection parameters, such as the DT, can change the ignition mechanism for the second injection. For the case with a short DT, the already formed high-temperature region strongly influences the second injection, which can be more likely ignited by the hot flame. However, by extending the DT, the second injection requires more time to interact with the first one. Autoignition controls the combustion process again [129]. The interactions between two injections are very limited

if the DT is very long, and combustion of the second injection may initiate at a time when the combustion arising from the first injection is diminished or extinguished [126, 129]. As a result, the effects of the temperature increase and intermediate species due to the reactions in the first injection on the second spray are very limited. At the same time, the oxidizer in the surrounding gas supplies the consumption in the first injection, which promotes the ignition of the second injection, but its effect is insignificant. For the case with a short DT, once the second injection interacts with the high-temperature or cool-flame region because of the reactions in the first injection, the high-temperature kernels appear very quickly. By reducing the DT, the spray–combustion interaction between two injections becomes more intense, leading to high soot emissions due to the insufficient mixing time [126]. However, experimental results [125] showed that the variations in the ID of the second injection with different DTs are negligible. This may be attributed to the small variations in DTs for different cases. The time interval when the second injection catches up with the first one is very short owing to the acceleration effect of the first injection.

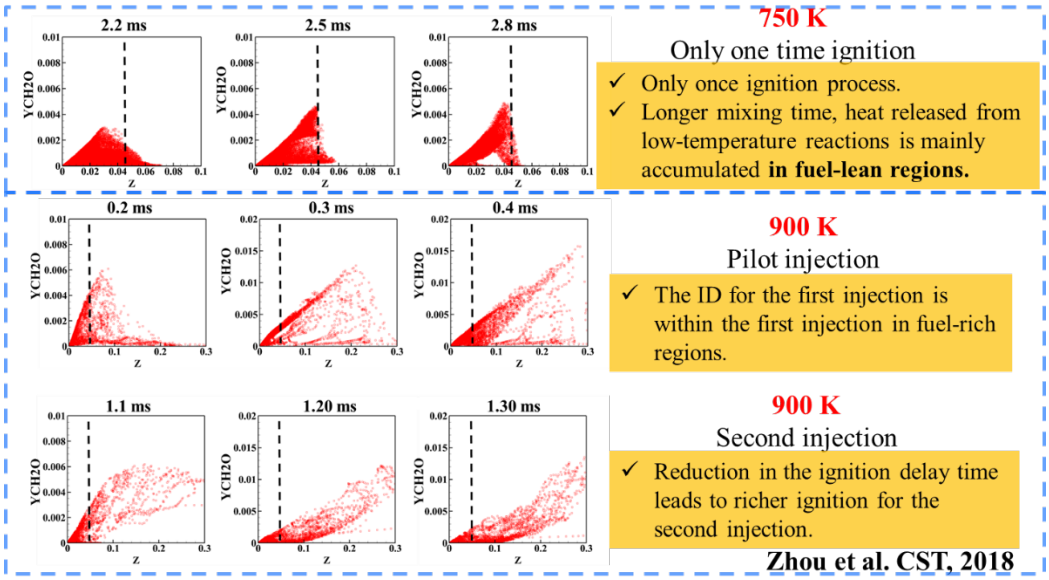

Fig. 14 Comparison of the CH_2O mass fraction in the mixture fraction space at 750 K and 900 K for single and double injection operations (the dashed line represents the position of the stoichiometric mixture fraction)

2.3.2.2 Effect of spray on flame structures

Effect of DT

When a single injection is split into two injections, the flame structure is significantly affected [130]. Cung et al. [126] reported that at a short DT, the flame has high-temperature regions in its middle section because of the location of the first flame which is bypassed by the high-momentum less-combusted flame from the second injection. After a long DT, the flame from the first injection cools down and the second flame is warmed up gradually by the hot products of the first injection.

Intensity axial time (IXT) [131] plots can be used to indicate the flame LOL location, flame

height, and even the internal flame structure by radially integrating planar fields of OH, CH_2O, and C_2H_2

$$I_{xt,i} = \int \tilde{Y}_i\,(x, y, t)dy \quad \text{with} \quad i = \text{OH, } CH_2O, C_2H_2 \qquad \text{Eq. 6}$$

The intensity I_{xt} is a function of the axial distance and time, as shown in **Fig. 15**. The CH_2O formation region represents the cool-flame region, and the main OH formation region shows the HTC region and flame height [126, 129]. After evaporation and fuel–air mixing, low-temperature reactions occur in the radial periphery of the spray jet, producing different intermediate species and radicals, such as RO_2, CH_2O, and H_2O_2 [16, 27]. As a result, the turbulent cool-flame wave propagates from the initiation location to both the upstream and downstream locations [132]. **Fig. 15** shows the CH_2O formation region moves toward the upstream location at 1.0 ms for the case with the shortest DT. The OH and C_2H_2 regions move upstream toward the injector nozzle; however, the upcoming cold fuel pushes the CH_2O formation downstream with a smaller maximum value for the IXT plots in the second spray. Owing to the limited mixing time and oxygen concentration ahead of the second spray, higher levels of C_2H_2 are observed especially for the case with the shortest DT. However, for a longer DT, fresh air enters into the low-density and already burnt regions, leading to an increase in the oxidizer concentration. Hence, the C_2H_2 concentration in the second spray is significantly reduced. In addition, **Fig. 15** clearly illustrates the strong spray–flame interactions can be affected by the DT. By enlarging the time interval between the two injections, the consumption of fuel in the first injection becomes more complete. Less CH_2O and OH formation regions overlapped in the two injections, indicating that the influence of the first spray on the ignition and combustion of the second one is reduced. The spray–flame interaction between the two injections is less intense when a longer DT is used. An increase in the entrainment rate causes less C_2H_2 formation.

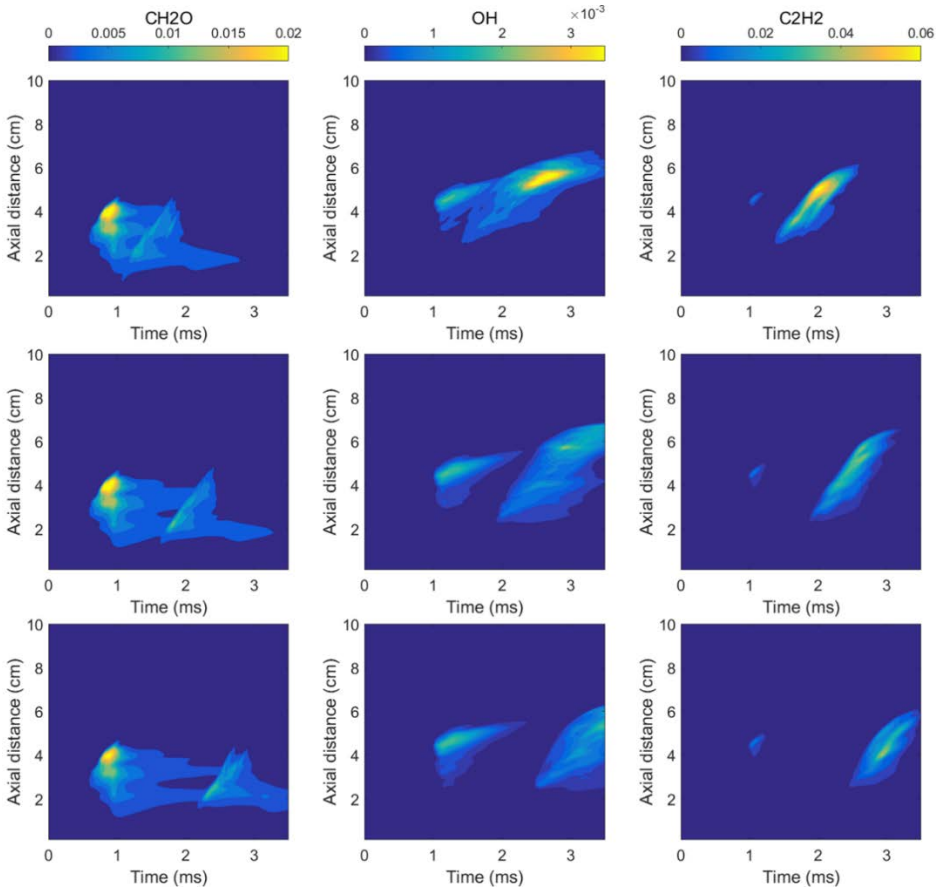

Fig. 15 Radially integrated intensity for OH, CH_2O, and C_2H_2 with different DTs to present strong spray–flame interactions (top: DT = 0.5 ms; middle: DT = 1.0 ms; bottom: DT = 1.5 ms [129])

Effect of injection duration

The injection duration affects the amount of injected fuel mass and concentration of the subsequently formed ignitable mixture. Desantes et al. [125] compared the combustion process for double injections with different durations of the first injection. They found that neither the ID nor flame LOL for the second injection was affected by the duration of the first injection because the near-nozzle flow was not modified. However, a longer duration of the first injection could contribute to the prolongation of the ID because the cold fuel vapor penetrated the pre-ignition region and pushed the hot pool with intermediate species downstream. As a result, the appearance of high-temperature kernels was inhibited.

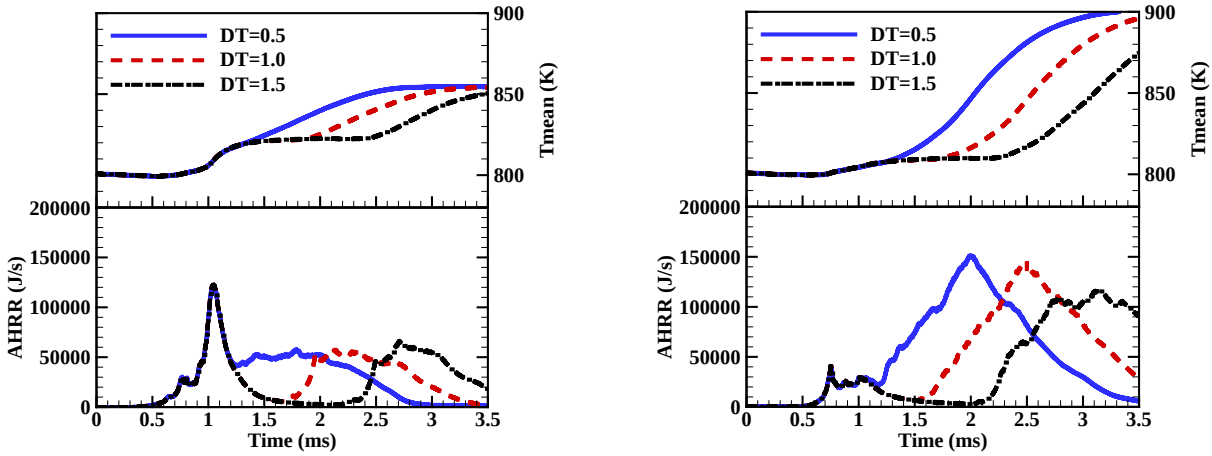

(a) FID=0.5 ms (b) FID= 0.3 ms

Fig. 16 Effect of injection strategy on the evolutions of AHRR and mean temperature [129]

To further understand the effects of the first injection duration (FID) on the mechanism of local spray–flame interaction, the temperature evolution, heat release rate and flame structures were obtained, as shown in **Fig. 16** [129]. For the split injection with FID = 0.5 ms, the injection durations for the first and second injections were set to 0.5 ms, consistent with the experiment [121]. For the pilot-main injection, the two injection durations were 0.3 ms and 1.2 ms, respectively, indicating that less fuel is injected into the computational domain during the first injection under the injection pressure of 150 MPa. These injection strategies significantly affected the heat release process. The first peak is formed because of the premixed combustion caused by the first injection, while the second one occurs because of the heat release in the second injection. The early ignition process is less dependent on the FID owing to its high reactivity. More fuel is injected into the combustion chamber after the first injection, which leads to a fuel-rich mixture and subsequently a higher peak value of the apparent heat release rate (AHRR) before 1.2 ms. However, for the pilot-main injection, the fuel–air mixture is very lean before the appearance of the HTI. As a result, the peak of the AHRR is lower than that of the split injection. It can be found that the second peak of the AHRR is relevant to the DT. By increasing the DT, the onset of the peak AHRR can be delayed. However, the increase in DT will lead to a more complete combustion of fuel in the first injection owing to the longer residence time.

Another interesting phenomenon is flame recession in the local spray–flame interaction. Both experimental and numerical studies [77, 121] have confirmed the combustion recession in split injections at a high initial temperature of 900 K. This means that the combustion region moves toward the upstream locations in the near-injector region after the end of the first injection. The combustion recession contributes to a significant decrease in the ID of the second injection owing to the high-temperature region, intermediate species, and radical pools. The prediction of the combustion recession also depends on the adopted numerical method, as reported in [77], where the RANS method failed to model the combustion recession, but the LES provided a good prediction.

2.3.2.3 Effect of spray on soot formation

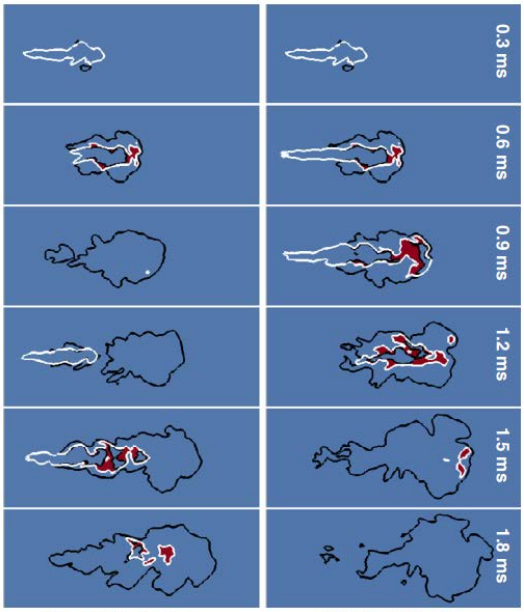

Fig. 17 Comparison of the soot formation zone in double and single injections (the white and black lines are the iso-contours of $\phi = 2$ and T=1600 K, respectively). Reprinted from Ref. [130] with permission of Elsevier.

To understand the effect of split injection on soot formation, **Fig. 17** compares snapshots of the soot zone for single and double injections. It is evident that the structures of the fuel-rich zone ($\phi > 2$) and high-temperature region (T > 1600 K) are completely different. At 0.6 ms, an increase in the local temperature is observed together with the appearance of soot formation. With the uninterrupted fuel injection for the single injection, soot is observed in a narrow region along the spray center at 0.9 ms. Moreover, nearly all soot is oxidized ahead of the upcoming second injection. The results at 1.2 ms reveal the influence of the air entrainment due to the injection pausing, which in turn promotes premixing and leads to a reduction in the soot zone [130]. In addition, an increase in the injection duration or fuel mass of the first injection leads to an increase in soot emission [125]. This may be because an increase in the injected fuel mass creates a fuel-rich region where soot formation is favored. An overlap between the injection and combustion also contributes to the limitation of air entrainment. For the case with a short duration, the limited mixing time before the ID is sufficient to form a fuel-lean mixture. Thus, nearly no soot is formed during the first injection. However, for the case with a longer DT of the first injection, a large amount of soot is formed, which also consumes the oxidizer. Thereafter, the second injection penetrates the rich region with hot combustion products formed in the first injection and starts to combust. The lack of oxygen and the high temperature in this region lead to an increase in soot production.

2.3.3 Conceptual summary with respect to spray–chemistry interaction

The underlying mechanism of the spray–chemistry interaction has been reviewed in detail in this

section. To provide a general understanding of this phenomenon, a conceptual model with respect to spray–chemistry interaction was constructed by Cung et al. [126] based on experimental images by varying the DT between two injections, as shown in **Fig. 18.** Compared with the single injection, spray flames for the multi-injection process are also associated with spray–spray interaction, which further increases the complexity. The second spray is injected into a completely different environment compared to the first injection, which forms different types of intermediate species. Experimental images also show that the IDs for all second injections are shortened compared to those of single injections because of the warm environment full of intermediate species, which has a significant influence on the combustion process [121, 133]. The shorter ID limits the mixing time for fuel and air, producing a richer mixture, which in turn affects the heat release process as well as the formation of emissions. The movement of the low- and high-temperature regions toward the nozzle before the start of the second injection plays a critical role in the ignition and stabilization processes [124]. According to the work by Cung et al. [126], the mechanism of spray–chemistry interaction can be summarized as follows:

1) For the first injection, the air entrainment is generated from the spray boundary. Subsequently, the fuel is vaporized and an ignitable mixture is formed. Under certain conditions, ignition will occur mostly in fuel-rich mixture regions, which will cause a lack of oxidizer and a high-temperature region for the second injection.
2) Consequently, the outer boundary region of the mixture in front of the second injection is favorable for ignition under a short DT compared to the frontal region.
3) For a medium DT, the second injection is pushed into a region of hot products, and the entire mixture in front of the second injection can be ignited.
4) With a further increase in the DT, the second injection will not affect the first spray flame, and the effect of the first injection is also gradually reduced.
5) NO_x and soot formation can be decreased by optimizing the split injection strategy.

Therefore, further research regarding the interaction between the local flow and chemistry timescale, which affects the ignition and emission formation under different split injection strategies and boundary conditions, is a very urgent task.

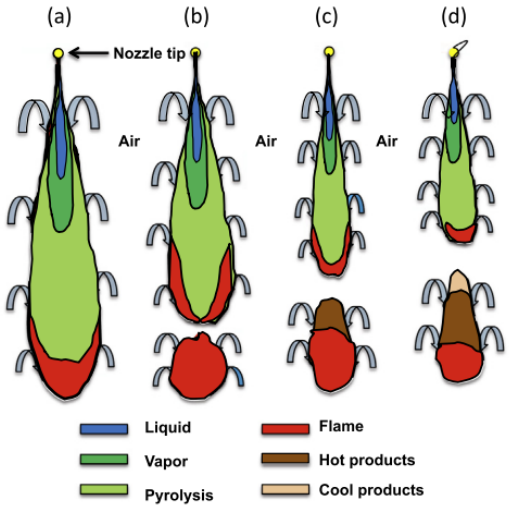

Fig. 18. A conceptual model of spray–combustion interaction using single and multiple injections with different DTs: (a) single injection; (b) double injection with short DT; (c) double injection with medium DT; (d) double injection with long DT. Reprinted from Ref. [126] with permission of Elsevier.

2.4 Characteristics of turbulent spray combustion

Spray–turbulence–chemistry interactions determine the behavior of ignition, combustion, and flame stabilization involving cool and high-temperature flames under diesel engine-like conditions. This section discusses two important aspects.

2.4.1 Two-stage ignition mechanism

Hydrocarbon fuels, especially n-heptane, are often involved in two-stage autoignition, including cool flames to HTI processes under diesel-like conditions [134]. A three-dimensional DNS study of an n-heptane/air jet flame shows that LTI precedes the formation of high-temperature kernels in fuel-rich mixtures and at low scalar dissipation rates, and consequently increases the mixture fraction gradient [134]. Once ignited, the kernels grow rapidly, coupled with the growth of the existing burning surface (developed by edge-flame propagation). In the DNS of the two-stage ignition process, the location of the low-temperature autoignition may first be initiated in the fuel-lean part of the dimethyl ether (DME)/air mixture [135], at the stoichiometric mixture [136] or on the fuel-rich side of the DME/methane/air mixture [137]. The subsequent steps are similar in the two mixtures, which consist of (a) formation of a cool flame, (b) propagation of the cool flame towards even richer mixture, (c) appearance of high-temperature autoignition kernels, (d) development of edge flames from ignition kernels, and (e) formation of high-temperature flames. Depending on the fuel mixtures and other parameters, either triple flames or tetrabranchiate flames coexist in the field, including cool flame, fuel-lean-/fuel-rich-premixed flames, and diffusion flame.

For turbulent spray flames in more realistic configurations, the interactions between the local flow, spray, and chemistry are even more complex [37, 61, 62], which have not been fully understood. Related to this, two main objectives should be addressed:

(1) to understand the two-stage ignition process of spray flames involving low- and high-temperature reactions, ignition location, and early flame evolution; and

(2) to understand how the initial conditions, including temperature, density, and pressure, influence the two-stage ignition characteristics and flame structures.

Some studies [27, 119] focused on understanding the mechanism of two-stage ignition to determine the temporal evolution of the early flame. During the early stage after evaporation, the cold fuel vapor mixes with the hot gas, forming an ignitable mixture. Consequently, it reacts with the oxidizer, accompanied by the onset of low-temperature chemistry. During the first-stage ignition process, the fuel molecules are decomposed into various intermediate species with considerable heat release. The LTC also results in a lighter region at the margin of the spray head, as confirmed by the experiments [27], implying a consequence of reduced gradients in the local refractive index due to the local temperature increase after LTI. Therefore, the intermediate species formed during the first-stage ignition process, such as H_2O_2, RO_2, and OH, can be used to study the evolution of the two-stage ignition process and determine the influence of the boundary conditions. HTI occurs first at a fuel-rich equivalence ratio of approximately 2, based on the temporal evolution in the composition-temperature space for the ambient conditions of 1000 K and 21% O_2 [9]. The two-stage ignition process of n-heptane spray flames based on the evolution of these key intermediate products was distinguished in [138]. CH_2O is considered as a precursor to the first stage of ignition [8, 139] and is generally utilized to distinguish the ‘cool flame’ in the spray flame under engine-like conditions [15]. It is mainly formed in the fuel-lean region at a low temperature of 850 K, which is followed by HTI in the fuel-rich region, as exhibited in **Fig. 19**. It is further indicated that the first-stage ignition occurs in the fuel-lean region first at a low initial temperature. Then, the second-stage ignition moves toward the fuel-rich region. The formation of H_2O_2 and the consumption of RO_2 imply the onset of the first-stage ignition between 1.3 ms and 1.4 ms. The rapid consumption of H_2O_2 and the formation of OH radical at the stoichiometric locations between 1.5 ms and 1.6 ms suggest the initialization of the second-stage ignition. Overall, different types or modes of ignition exist in turbulent spray combustion, depending on the timescales of evaporation, convection, diffusion, and chemical reactions. In most cases, autoignition first appears at locations with the “most reactive mixture fraction” (Z_{mr}) in nonpremixed mixtures and low scalar dissipation rates [28, 140]. In turbulent spray flames, the reactivity of the fuel–air mixture decreases owing to the fuel evaporation effects. Consequently, at a lower initial temperature, the fuel-lean mixture easily locates at the most reactive mixture fraction region to promote ignition occurrence [138].

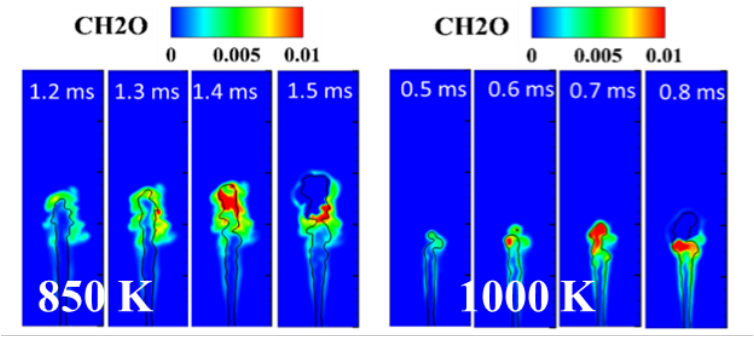

Fig. 19 Snapshots of CH_2O at different times after start of injection (ASOI) at 850 K and 1000 K (the black solid lines represent the stoichiometric mixture fraction (Z_{st}) [138])

Previous results indicate that the combustion of spray flames is a multistage and multimode process [5, 14, 15]. To distinguish the different combustion modes, i.e., LTC or HTC mode, an analysis based on some key intermediate species such as hydroxyl radical (OH) and CH_2O was performed by Krisman et al. [141]. Different combustion modes for multistage processes, namely, the LTC mode (M_{LTC}) associated with the first stage of ignition or cool flame, lean-premixed HTC mode ($M_{HTC-lean}$), rich-premixed HTC mode ($M_{HTC-rich}$), and nonpremixed combustion mode ($M_{HTC-dif}$) were distinguished. Their results also reveal that during the early stage, the first stage of ignition transitions to a cool flame with a slight increase in the heat release rate. After the appearance of low-temperature chemistry, it exists during the entire combustion process. The M_{LTC} mode is important because nearly a quarter of the heat is released during this stage. The bulk of the HTC heat release rate in the simulation was attributed to either $M_{HTC-rich}$ or $M_{HTC-dif}$. Thereafter, the method was also used to identify the key combustion features of n-dodecane flames using DNS [142, 143]. In this investigation, it needs a selection of threshold or critical value of key chemical species to identify the regions of different combustion modes. However, Krisman et al. [141] found that the regions of combustion modes were not very sensitive to the selection of critical value.

Recently, an LES study first adopted similar definitions to identify the LTC and HTC regions in turbulent spray flames [138]. Three combustion modes were distinguished based on the mass fractions of CH_2O and OH.

- M-LTC mode: $Y_{CH2O} > Y_{CH2O|CRIT}$. It represents the LTC region and it is associated with the appearance of cool flames.
- M-HTC mode: $Y_{CH2O} < Y_{CH2O|CRIT} \cap Y_{OH} < Y_{OH|CRIT}$. This is the HTC region with intense high-temperature reactions.
- M-HTC-dif: $Y_{OH} > Y_{OH|CRIT}$. It represents the HTC with a nonpremixed flame concentrated on Z_{st}.

The results indicate that the high-temperature diffusion region is located in the stoichiometric mixture region and is surrounded by the HTC regions with low Y_{CH2O} and Y_{OH}, as depicted in **Fig. 20**.

The LTC region with rich CH_2O is located in the upstream regions. After the formation of high-temperature kernels, the reaction progress of the fast-reacting mixture is mainly limited by the slow local transport, where non-premixed combustion plays a dominant role [119]. It was found that this method has the ability to distinguish the four combustion modes involving the LTC, lean-premixed HTC, rich-premixed HTC, and HTC-diffusion combustion for two-stage combustion processes, which is similar to the flame index method proposed by Briones et al. [144].

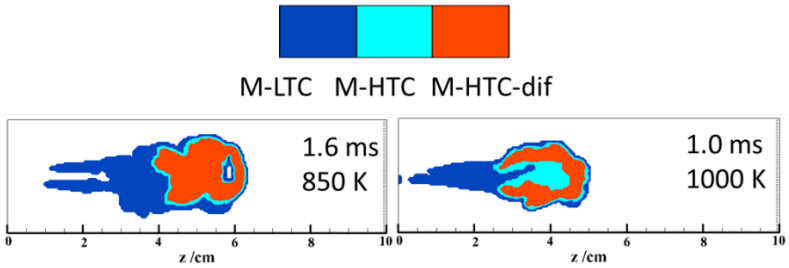

Fig. 20 Different combustion modes in spray flames at selected time instants of 850 K and 1000 K [138] based on key intermediate species analysis

2.4.2 Flame stabilization mechanism

Turbulent spray flames can be stabilized at the flame LOL position, which is defined as the farthest upstream location where HTC can exist along the spray axis. The high-temperature regions cannot move further upstream, and the upcoming cold fuel or products formed in the pre-oxidized reactions start to be consumed and penetrate the high-temperature regions. The detailed spray flame structure and emission characteristics are significantly affected by the flame LOL. Therefore, the combustion and pollutant emission characteristics in spray flames are strongly coupled with the flame lift-off behavior, as revealed by several previous studies [145, 146]. To reduce soot production, it is very helpful if the liquid phase does not penetrate the high-temperature reaction region by adopting an ultrahigh injection pressure and a small nozzle hole diameter [100], i.e., the flame LOL is much longer than the liquid penetration length, preventing the formation of soot emissions.

Different theories have been proposed to explain the stabilization mechanisms of turbulent spray flames. Broadwell et al. [147] pointed out that large-scale turbulent structures carrying hot combustion products to the edge of the jet can lead to upstream ignition. Otherwise, too rapid mixing between the re-entrained products and the unburnt gas leads to extinction. Therefore, the interaction of large-eddy structures with hot products and the unburnt upcoming gas may result in the ignition and extinction of turbulent spray flames. Recently, a conceptual model [146] revealed that the main stabilization mechanism for the spray flame depends on two types of autoignition, namely the isolated autoignition and autoignition assisted by the burnt mixture. In addition, triple flames were also found at the periphery of the spray flame, which had insufficient propagation velocity to contribute to flame stabilization.

Before the fuel–air mixture is consumed at downstream locations, it may undergo low-temperature reactions. The interaction between the turbulence and low-temperature products may contribute to the stabilization process. Recently, laser-induced plasma ignition was used to study the stabilization mechanism of turbulent spray flames both experimentally [145, 148] and numerically [149]. The presence of laser ignition leads to a sudden decrease in the flame LOL, which moves toward the upstream direction and becomes steady after a relatively long time (approximately 7 ms). The kernel induced by laser ignition propagates toward the main flame region in a premixed regime, which merges with the main flame very rapidly. Experiments also showed the importance of a cool flame in assisting flame stabilization [145]. If forced ignition by a laser occurs upstream of formaldehyde, the lift-off position moves rapidly before it reaches the formaldehyde region. Thereafter, it returns slowly towards its natural position.

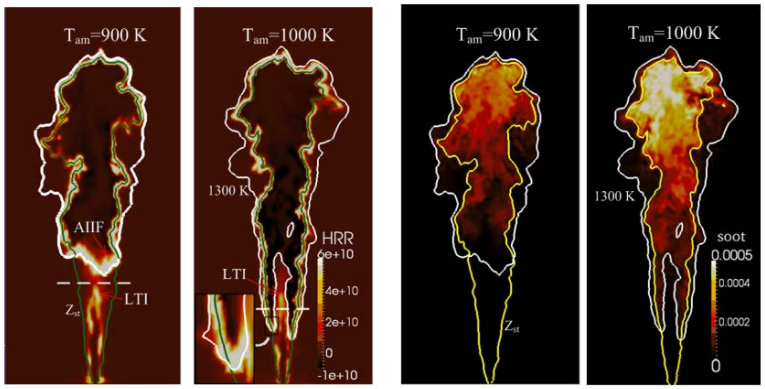

(a) heat-release rate (b) soot mass fraction

Fig. 21 Contours of (a) heat release rate and (b) soot mass fraction for n-dodecane spray flames at 900 K and 1000 K. Reprinted from Ref. [150] with permission of Elsevier.

The relative difference between the liquid penetration length and flame LOL may be derived from different stabilization mechanisms, as illustrated in **Fig. 21** [150]. It can be observed that at an initial temperature of 900 K, the heat release mainly originates from three locations: (1) LTI site, (2) autoignition induced flame front regions (AIIF, equal to the HTI regions), and (3) mixing-controlled diffusion flame region. The LTI products contribute to the stabilization process because they affect the location of the AIIF region. However, no AIIF can be found, and the two flame bases extend upstream toward the injector. The shorter flame LOL prevents the entrainment of fresh gas into the spray. Heat release from the LTI close to the flame LOL indicates that the flame propagation is significantly affected by the LTI ignition process.

Other theories have also been used to interpret the stabilization process of turbulent spray flames, such as local extinction owing to the high scalar dissipation rate [151], partially premixed flame propagation of triple flames [152] and autoignition [30, 60, 153]. The transport budget analysis proposed by Luo and Bray [50, 51] and Gordon et al. [154] is a widely used method for identifying the local characteristics of a flame based on the relative magnitudes of the reaction, diffusion, and

convection terms. A larger reaction term compared to the other two terms indicates that autoignition plays a dominant role in the stabilization process of turbulent spray flames [30, 60, 153].

The autoignition and premixed flame can be clearly distinguished using a preheat zone and a reaction zone. A balance between the reaction and diffusion indicates a diffusive–reactive flame structure. On the other hand, a dominant reaction term implies that combustion is controlled by autoignition [155]. As shown in **Eq. 7** of the steady modeled transport equation of the mean species mass fraction, the equation is balanced by the convection, diffusion, and chemical reaction terms.

$$0 = -\frac{\partial}{\partial x_i}\left(\langle\rho\rangle\tilde{u}_i\tilde{Y}_k\right) + \frac{\partial}{\partial x_i}\left(\frac{\mu_T}{Sc_T}\frac{\partial\tilde{Y}_k}{\partial x_i}\right) + \langle\rho\rangle\tilde{S}_k \qquad \text{Eq. 7}$$

where $\langle\rho\rangle$ is the mean density, $\tilde{u}_i$, $\tilde{Y}_k$, and $\tilde{S}_k$ are the Favre-averaged velocity, mass fraction and chemical source term, μ_T is the turbulent viscosity, and Sc_T is the turbulent Schmidt number. To understand the autoignition process and flame stabilization mechanism, several studies [30, 60, 153] have applied this method to investigate the stabilization mechanism in turbulent spray flames. All the studies obtained the same results and revealed that the reaction rates are much higher than the diffusion rates near the flame LOL positions regardless of the initial boundary conditions, indicating that the natural lifted flame is stabilized by autoignition. An increase in the initial oxygen concentration significantly increases the reaction rates, while the initial gas temperature plays a less important role, as shown in **Fig. 22**. The results also suggest that turbulent diffusion gradually increases with increasing temperature, which is attributed to radial diffusion [30]. Overall, it can be concluded from the budget analysis that the flame stabilization in turbulent spray flames is dominated by autoignition, and turbulent transport of heat also makes a contribution to flame stabilization.

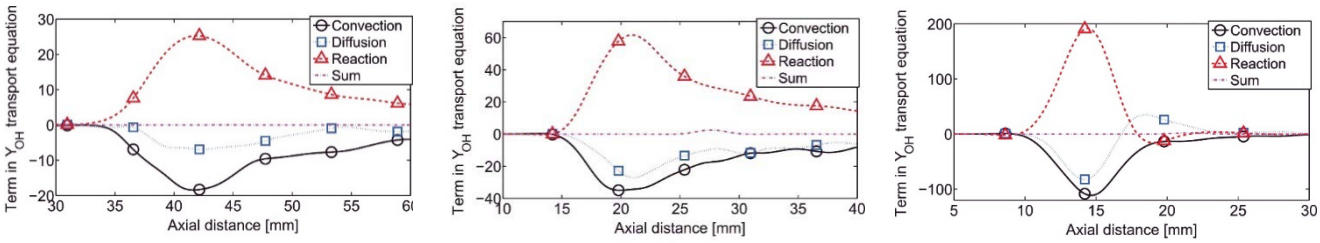

Fig. 22 Flame stabilization analysis by the transport budget method. Reprinted from Ref. [30] with permission of Elsevier.

The stabilization mechanism in turbulent n-heptane spray flames based on the analysis of the local chemical time scale and flow time scale was further analyzed [119, 156]. During the early stage of ignition in the spray flame, the reaction and mixing balanced with each other based on the analysis of the local flow and chemical timescales. The ratio of the integral timescale to the chemical timescale is defined as Da. Large Da values indicate that the chemical timescale is much smaller than the flow timescale and the flame is mixing-controlled. On the other hand, small values imply a large chemical timescale. Flame structures for n-heptane spray flames in terms of instantaneous temperature,

eigenvalue, and Da number contours are presented in **Fig. 23**. Here, Da is defined as $\mathrm{Da} = \tau_f \times |\lambda_e|$, where τ_f represents the integral time scale, which is calculated as $\tau_f = k/\varepsilon$. And the log scale of $Re(\lambda_e)$ is denoted as Λ_e where $\Lambda_e = sign(Re(\lambda_e)) \times log_{10}(\max(1, Re(\lambda_e)))$ and 'sign' is the sign function. A negative Λ_e indicates that the mixture has already burned. A positive Λ_e indicates that the ignition of the mixture is still underway [157]. It was demonstrated that multistage ignition processes are controlled by different mechanisms [119]. During the early stage of ignition, the low-temperature reactions in spray flames are initiated at the locations with Da in the order of unity, indicating that the spray flame is controlled by the balance between reaction and mixing. However, during the quasi-steady state, a significant increase in terms of the Da number is found, signifying that autoignition plays a dominant role.

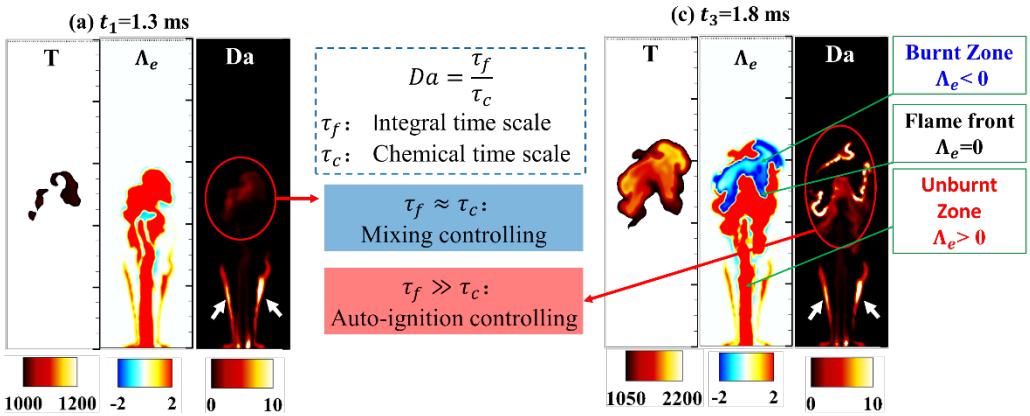

Fig. 23 Summary of ignition and spray flame characteristics for 10% oxygen concentrations at selected time instants according to the work [119] (contours of T, Λ_e, and the Da number)

In summary, significant progress has been made in the spray–chemistry–turbulence interaction. The above sections provide a comprehensive summary of the mechanism of spray–turbulence–chemistry interaction under engine-like conditions, which can be illustrated in **Fig. 24**. Different processes including fuel evaporation, mixing, autoignition, and HTC occur during the injection process. The fuel injection and subsequent evaporation enable the formation of an ignitable fuel–air mixture. The combustion of the fuel–air mixture, in turn, restricts the entrainment rate of fresh air into the spray, leading to fuel-rich ignition as shown in **Fig. 24.** Then, gas expansion as a result of combustion increases the turbulence intensity and causes acceleration of the spray head [119], leading to a longer reacting spray. The acceleration effect is more obvious with multi-injection because of the reduction in the resistance ahead of the subsequent injection [117].

The interactions are expected to influence the spray structure. Injection with a higher pressure leads to a longer vapor penetration length and stronger turbulence intensity, which can promote fuel–air mixing, thus shortening the ID [4]. Although earlier ignition leads to a longer spray structure, the structure is also affected by the ambient gas. A higher ambient density intensifies the resistance, which restricts the development of the spray tip, leading to a reduction in the vapor penetration. In summary,

a turbulent spray is formed owing to the breakup of cold fuel droplets, which are then dispersed, heated, and vaporized. A cool-flame structure is located between the liquid phase and the HTC region, characterized by a high concentration of CH_2O. The high turbulence due to high-speed injection enhances the heat losses and leads to a local balance between the flow and reaction during the early stage of ignition. However, autoignition dominates the stabilization process. The turbulent spray structure determines the entrainment rate and most of the fresh air enters the spray through the spray head, although a longer flame LOL can lead to better fuel/air mixing.

In addition, the interaction process between double injections also leads to a completely different ignition mechanism compared with the single injection, as identified by the chemical explosive mode analysis [129]. The combustion of the first injection is mainly controlled by autoignition, whereas that of the second injection is directly ignited by the high-temperature reacting spray with short dwell time. However, autoignition can play a critical role if a longer DT is used [129]. Under low reactivity conditions, for example, low temperature and/or low oxygen concentration, turbulence controls the ignition process because the already formed intermediate species and released heat are transported by turbulence. The combustion mode can be changed from LTC to cool-flame propagation mode [132] and diffusion-controlled mode. However, quantitative analysis of the effect of local spray characteristics in turbulent spray flames on ignition, especially cool-flame stage and combustion mode transition, should be further conducted. In addition, previous studies only focused on the ignition mechanism of a single-component fuel; however, a real engine fuel with multiple components in turbulent spray flames will result in more complicated ignition and flame stabilization mechanisms, which have not been studied well.

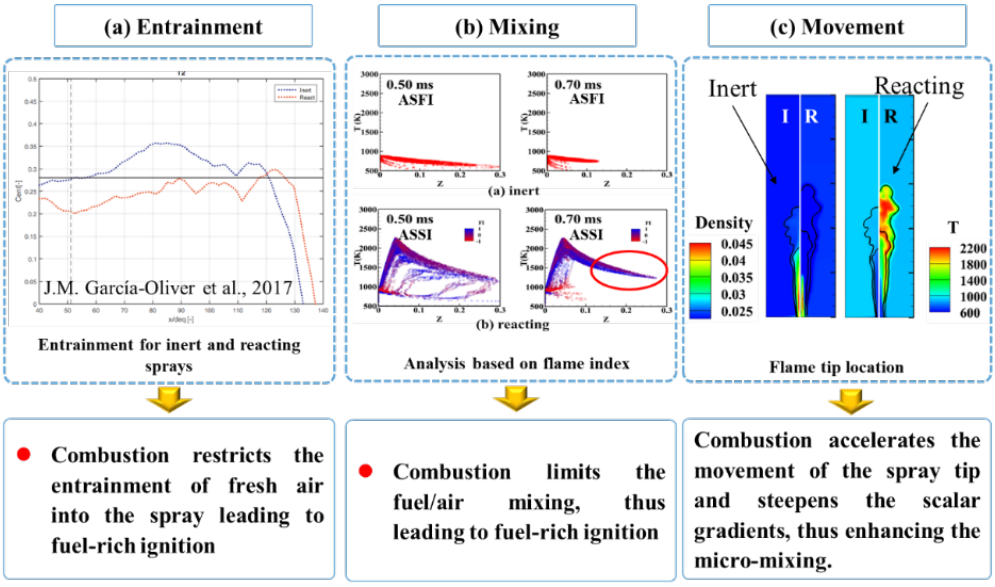

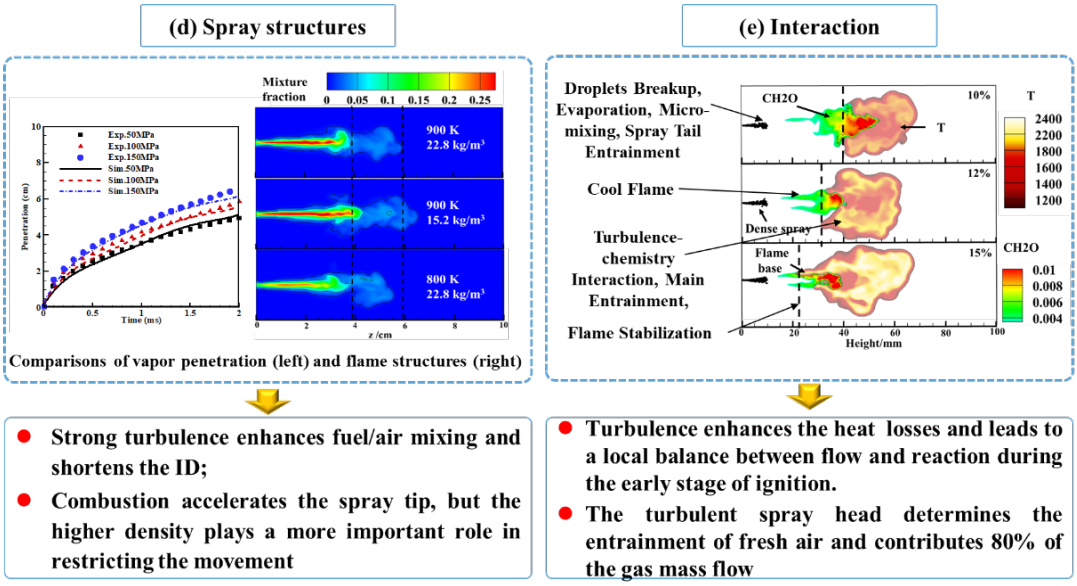

Fig. 24 Diagram for spray–chemistry–turbulence interactions. The image of the entrainment profile is reprinted from Ref. [59] with permission of Elsevier.

3. Other effects in realistic spray combustion systems

3.1 Turbulence–radiation interaction (TRI)

Radiative heat transfer plays a very critical role in energy balance and is known to have an effect on the wall heat loss in engines, particularly for large bore and heavy-duty diesel engines [158]. For turbulent nonpremixed flames, radiation can contribute substantially to the prediction of the temperature field and emission formation. In most conventional reacting flow simulations (i.e., RANS), radiation and turbulence are treated as independent processes, and the mean variables are used to calculate radiative intensities and properties, which makes it difficult to consider TRI [159]. Previous experimental and numerical studies [160-163] have demonstrated that TRI can substantially affect radiative heat loss [164, 165], and considering turbulent fluctuations in radiation calculation can elevate the radiative fluxes by up to 2–3 times. However, little attention has been paid to the effect of TRI on the combustion and emission characteristics of turbulent spray flames under engine-like conditions. Therefore, two important aspects should be considered. The first is to assess the importance of the TRI effects on heat transfer losses and emissions. The second is to distinguish the impact of molecular gas radiation and soot emission from the TRI effect.

Several studies [11, 76, 166, 167] regarding the effect of TRI on combustion and emission characteristics have been conducted by employing different radiative models with and without considering turbulent fluctuations. It can be concluded from the above studies that TRI effects are attributed to the periphery of the turbulent flame, particularly the region of the highly intermittent soot formation in terms of turbulent spray flames [11]. TRI can enhance radiative heat transfer and thus lead to a drop in the peak temperature by 10–20 K [76]. And a larger decrease in the peak temperature by 150 K (for a luminous, optically thicker flame) was also found [167]. Because NO emission is more

sensitive to the temperature than soot production, the reduction in temperature results in a decrease in NO mass by 5–10%, and the effect of radiation on soot formation is insignificant [76].

However, neglecting the unresolved turbulent fluctuations causes an increase in the NO mass by a factor of two. It can be found from the turbulent spray flame in a simple configuration that global TRI effects on heat losses and NO are relatively small compared to the TCI effect [76, 166]. However, radiative emission generated by soot approximately doubles when considering the TRI effect owing to the highly intermittent soot distribution. **Fig. 25** presents the temporal evolution of the NO mass obtained with (for the transported PDF model) and without (for the well-mixed model) the TRI effects using two different radiation models, i.e., the discrete ordinate method (DOM) and optically thin (OPT) models, as well as no radiation (No Rad). It can be observed that radiation causes a decrease in the total NO formation by approximately 5–10%, with the DOM model having a smaller effect than the OPT model. However, compared with the isolated TRI effects, including the TCI caused a larger decrease in the peak flame temperature and a much thicker reaction zone. Inclusion of the TCI effect using the transport PDF turbulent combustion model led to about 50% decrease in the predicted NO mass than using the well-mixed model without any TCI effect. Actually, the effect of TRI on the emitted radiation was found to be modest (10% at most) when using the transport PDF method. The results implied that the influence of radiation on NO emission is considerable but generally smaller than that of the selected combustion models. The above conclusion is further confirmed in a heavy-duty diesel engine [168], where both radiative emission and reabsorption are considered at part load and full load. In [168], to separate the TCI effect from the TRI effect, particle-level chemistry and radiation were employed. However, only the TCI effect was obtained by the particle-level chemistry and cell-level radiation. It was found that local instantaneous temperatures were changed by 50–100 K when employing a radiation model for various combustion models and radiation models. However, the global influence was relatively small (less than 10%) in terms of heat losses and engine-out emissions.

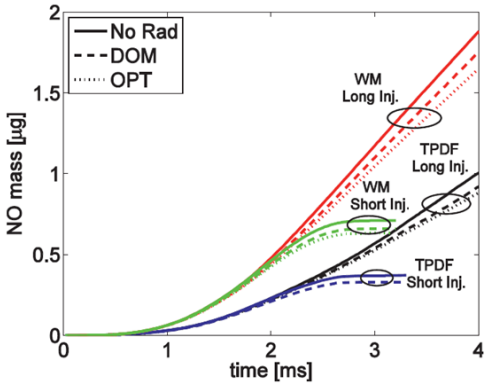

Fig. 25 Evolution of NO mass affected by TRI [76] with different radiative models and different combustion models with and without TCI effect (DOM: discrete ordinate method; OPT: optically thin model; WM: well-mixed model; TPDF: transported PDF). Reprinted with permission of Elsevier.

In addition, to evaluate the importance of molecular gas radiation (mostly CO_2 and H_2O) and soot radiation, the power spectra of radiation emitted over the full domain and of radiation reaching the walls were utilized [11]. The spectra and computed fields of radiative emission as well as the net radiative source terms were analyzed. It was confirmed that the total radiative emission and reabsorption are dominated by CO_2 because of its large optical thickness at the wavenumbers of the system, which is a plausible cause for the lower TRI effect compared to atmospheric turbulent nonluminous and luminous flames [76]. On the other hand, most CO_2 is reabsorbed before it reaches the wall, so H_2O radiation dominates the radiative energy flux to the walls. In addition, although most of the emitted soot radiation reaches the walls, a very small contribution of less than 10% to the soot radiation was observed. The conclusion is consistent with the work of Chishty et al. [166].

In summary, significant progress has been made in investigating the effects of turbulence–radiation–spray interactions on the combustion characteristics. The existing studies based on numerical simulations indicate that the TRI effect is smaller than the TCI effect. Quantitative measurements regarding the effect of TRI should be carried out. However, spray combustion is a complicated process, and the effects of turbulence–radiation–spray interactions under a wide range of engine-like conditions, such as the effect of radiation on droplet evaporation, require further in-depth studies.

3.2 Spray-flame–wall interactions

Spray-wall interaction (SWI) and flame-wall interaction (FWI) are among the most important considerations for the combustion chamber design of internal combustion engines [358, 359 (old reference numbers], gas turbines [360] and rocket engines [361]. These issues are especially relevant to downsize or light-duty engines. In diesel engines, the impinging spray flame has a substantial effect on the distribution of fuel, evaporation, fuel–air mixing, combustion, and even exhaust emissions. However, the complex interactions among the incident spray, flame, and wall are still far from being fully understood. An in-depth analysis of all the related processes is beyond the scope of this work, and here, we only briefly review the development of the spray–wall interaction mechanism. It should be noted that flame-wall interaction (FWI) is also one of the most important aspects of the design of the combustion chamber in internal combustion engines [169, 170], gas turbines [171], and rocket engines [172]. To achieve a higher combustion capacity and downsize the combustor, the effects of FWI should be considered. The important effects of FWI include increased heat loss, altered flame dynamics, local flame quenching, re-ignition due to hotspots on walls, and thermal stress. Here, we only focus on the spray–flame–wall interactions, including spray-wall impingement and spray FWI. A recent comprehensive review regarding the premixed FWI considering advanced laser diagnostics was presented by Dreizler and Böhm [173].

3.2.1 Spray–wall interaction

The phenomena of spray–wall interaction under real engine conditions is difficult to describe

owing to the complex in-cylinder flow, injection, and heat release processes. Thus, studies including single droplet impingement and spray/group droplet impingement were usually performed in simplified constant-volume combustion chambers to qualitatively investigate the key phenomenon. There are three typical conditions for single droplet impingement studies: dry surfaces, wetted surfaces, and hot walls. Droplet impingement on dry surfaces frequently occurs in nature and in a variety of industrial and agricultural applications [174]. The topic has been studied for over a century, but there is still disagreement even regarding the basic mechanisms involved [175, 176]. However, this review only focuses on the spray/group droplet impingement. **Fig. 26** presents the main features of spray impingement on the wall [20], including the primary liquid film formation, splash, secondary impingement of splashing droplets, and vortex–droplets interaction.

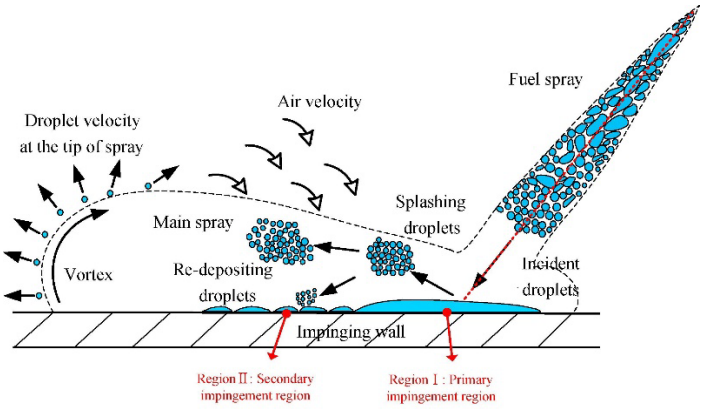

Fig. 26 Schematic of diesel fuel impingement on the wall. Reprinted from Ref. [20] with permission of Elsevier.

Many studies have been conducted to investigate spray–wall interaction. Most of the experimental studies have focused on the macroscopic features, such as spray morphology, spray penetration, Sauter mean diameter of droplets, and wall film characteristics [177, 178]. In the recent works by Xu et al. [177, 178], advanced optical methodologies were employed to investigate the liquid film formation mechanism near the impingement wall. It was concluded that the spray can substantially affect the wall film movement and further induce secondary breakup. They also proposed a spray impingement criterion to explain the cause of droplet gliding away without impinging the wall induced by the lift force of the boundary layer. In addition, Chen et al. [179] investigated the spray characteristics of a wall-impinging diesel fuel spray with various wall temperatures in a constant-volume combustion vessel. They found that by increasing the wall temperature, the vapor-rich field enters the near-wall region, and the area of high-vapor fluorescence intensity increases.

In numerical simulations, an established configuration to study the spray impingement is that of a single droplet impinging on a dry or wetted wall [180]. However, under certain conditions, such a configuration cannot accurately capture the characteristics of spray impingement [181, 182], which has been systematically summarized by Moreira et al. [183]. If droplet–droplet interaction in dense spray is neglected, the behavior of the spray–wall interaction will be altered. Consequently, there are

still many unresolved issues regarding the transition between deposition and splash, droplet–droplet interaction, and liquid fuel film formation under different conditions.

Considering the above issues, some studies were performed using simplified flow configurations [184-186]. Naber and Reitz [186] pioneered the modeling of spray–wall interaction by identifying three different regimes, namely stick, reflect, and jet, but the splash regime and the loss of energy and momentum of the impinged droplet are neglected. O'Rourke and Amsden [187] presented a spray–wall interaction model based on experimental data by considering the deposition and splash regimes, which have been successfully added into the KIVA code and other commercial software; however, the model cannot describe the realistic spray shape under engine-like conditions [188]. In the O'Rourke and Amsden model [187], a dimensionless splashing criterion is proposed with consideration of the effect of the film thickness and boundary layer thickness. For the secondary droplet, O'Rourke and Amsden [187] adopted two distribution functions to describe the normal and tangential velocities as follows:

$$f(w) = \frac{4}{\sqrt{\pi}} \frac{w^2}{w_{max}^3} \exp\left[-\left(\frac{w}{w_{max}}\right)^2\right] \quad \text{Eq. 8}$$

$$f(v) = \frac{1}{\sqrt{2\pi\delta^2}} \exp\left[-\frac{(v)^2}{2\delta^2}\right] \quad \text{Eq. 9}$$

where $w_{max} = 0.2w_0$ and $\delta = 0.1w_0$. Then, the total velocity of the secondary droplet can be expressed as:

$$V = wn + (0.12w_0 + v)\left(\cos\Psi e_t + \sin\Psi e_p\right) + 0.8v_0 e_t \quad \text{Eq. 10}$$

where n and e_t are the unit vectors normal and tangential to the wall, respectively, and e_p is the unit vector, which is normal to n and e_t simultaneously.

Further improvement in the spray–wall interaction model by considering the liquid saturation temperature, low-energy impingement, and high-energy impingement was established by Senda et al. [189, 190]. The secondary breakup induced by a splash for the low-energy impingement case and the deposition and splash processes for the high-energy impingement case were considered. Based on previous works, Zhang et al. [191] improved the spray–wall interaction model with special emphasis on the high-injection pressure condition and achieved reasonably accurate predictions for the penetration of the impinging sprays and the secondary droplet characteristics compared to experimental data. They further improved the model by considering the film separation criterion, mass ratio of the film separation, and film atomization model based on the Rayleigh-Taylor (RT) instability theory [192]. The results showed good agreement between the predicted size distribution of the detached droplets and the experimental data using the improved model, as shown in **Fig. 27**. The improved model demonstrated a better ability of capturing film separation characteristics. In the wall film separation model by Zhang et al. [192], a new separation criterion coupled with the film atomization model based on the RT instability theory is adopted:

$$f_R = \frac{\rho_l u_f^2 \sin\theta_c}{\sigma(1+\sin\theta_c) + L_b h_f \rho_l g \cos\theta_c} \quad \text{Eq. 11}$$

where f_R is the force ratio, σ is the liquid surface tension, and L_b is the film characteristic breakup length. In the film atomization model, the following dispersion equation is utilized:

$$\omega_f = -\left[\frac{\sigma - a_f\left(\frac{\rho_l - \rho_g}{\kappa^2}\right)}{2\mu_l h_f}\right]\left(\frac{\kappa h_f \sinh(\kappa h_f)\cosh(\kappa h_f) - \kappa^2 {h_f}^2}{\cosh^2(\kappa h_f) + \kappa^2 {h_f}^2}\right) \quad \text{Eq. 12}$$

where ω_f is the growth rate, κ is the wavenumber, and a_f is the film acceleration around the corner. By maximizing the above equation, the growth rate of the fastest-growing wave on the liquid film can be calculated. Furthermore, the wavelength of the fastest growing wave can be obtained based on the relationship between the growth rate and wavenumber. Cylindrical ligaments are assumed to be produced after film separation, and the diameter of the cylindrical ligaments can be determined based on mass conservation. Finally, the ligaments are supposed to further break into the detached droplets of various sizes, and the size distribution of the detached droplets is described by a Rosin–Rammler distribution function.

In summary, the development of the spray–wall interaction model should consider the following issues: 1) effect of turbulence on droplet/wall interaction; 2) wall conditions such as dry wall, wetted wall, inclined wall surface, and rough wall; 3) impingement regimes and transition criteria; 4) energy conservation; 5) effect of liquid film thickness and film separation criterion; 6) estimation of post-impingement characteristics including rebound velocity, fraction of the mass deposited on the wall, droplet size, and velocity distributions of the secondary droplets for the splash regime [188].

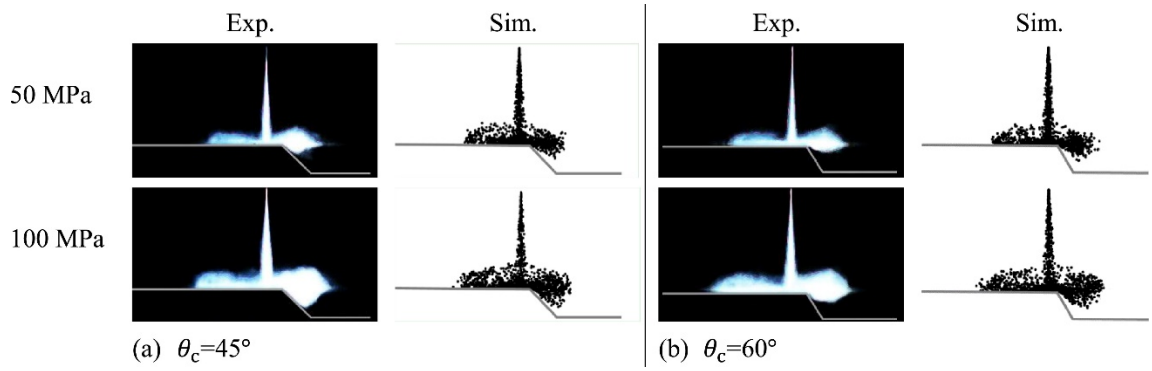

Fig. 27 Comparison of the predicted and measured impinging spray profiles at different injection pressures and expanding corner angles. Reprinted from Ref. [192] with permission of Elsevier.

3.2.2 Spray flame–wall interaction

Combustion characteristics such as flame structure and emissions are greatly affected by the spray flame-liquid film–turbulence–wall interactions. Significant progress has been made by measurements and numerical simulations in both engines and constant-volume combustion chambers to study the effect of spray flame-wall.

Flame morphology

Compared to the studies on the spray–wall interaction, those on the spray FWI is relatively scarce.

Generally, when a jet encounters a wall, the leading edge frequently deforms, flattening the diffusion flame along the wall surface [193]. Compared with a free spray flame, combustion can be strengthened by using an appropriate impinging distance (longer than the liquid-phase penetration) [194]. From previous studies, it can be concluded that the injection parameters and operation conditions, including the wall conditions [179], injection pressure [195, 196], impinging distance [194], nozzle hole diameter, and ambient pressure [179], mainly determine the combustion processes. The ultrahigh injection pressures and microhole size nozzle can affect the flame structure, including the flame area, flame length and flame height. It was found that a higher injection pressure resulted in a larger flame length and flame area; however, the flame height was independent of the injection pressure but dependent on the nozzle hole diameter [196]. A smaller hole diameter led to a lower flame height. Furthermore, the heat flux increased owing to the increased convection due to turbulence induced by the higher injection pressure and larger nozzle hole diameter. In addition, a larger impingement distance (50 mm) can lead to a smaller value of the average heat flux owing to the prolonged combustion duration and small flame contact area [195]. Recently, Chen et al. [179] identified the effects of different wall temperatures and ambient pressures on the flame characteristics, including ignition position, flame area, and height in a constant-volume combustion vessel, as shown in **Fig. 28**. They concluded that the flame area and height are more sensitive to the wall temperature at a lower ambient pressure. Increasing the wall temperature promotes the ignition process and decreases the flame area and height. Overall, only a limited number of experimental and computational studies have been devoted to the autoignition mechanism, including the two-stage ignition process near the wall for impinging turbulent spray flames.

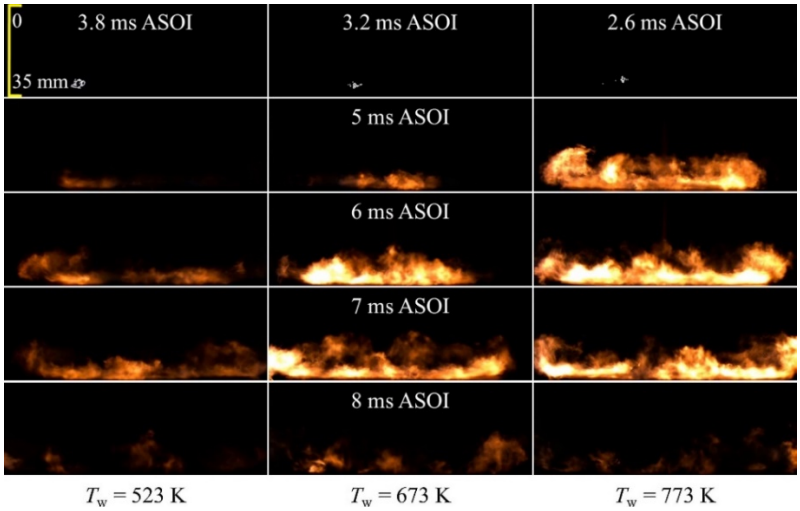

Fig. 28 Flame morphology at different wall temperatures (523, 673, and 773 K) and lower ambient pressure (2 MPa) compared to the ambient pressure of 4 MPa. Reprinted from Ref. [179] with permission of Elsevier.

Formation of pollutants

The flame development is affected by the wall heat loss corresponding to the heat transfer from the reacting flame to the relatively low-temperature liquid film or wall. This leads to the formation of

UHC and consequently the formation of pollutants, especially soot. Experimental studies on the effect of spray/wall impingement on emissions, particularly soot formation, were carried out in both engines [197] and constant-volume chambers [179, 198, 199]. Bruneaux [198] presented the flame structure of an impinging jet by simultaneously employing formaldehyde, polycyclic aromatic hydrocarbons (PAH), and OH laser-induced fluorescence techniques, as well as spectral analysis, which allows a comprehensive understanding of the flame structures and soot formation, as shown in **Fig. 29**. It can be observed that the jet impinging-wall flame is substantially influenced by the jet–wall vortex, which can generate a higher mixing rate. The higher mixing rate results in broader regions of OH in the tip region and reduces the formation of PAHs and soot in this region. In addition, near the wall region, spray impingement results in soot formation.

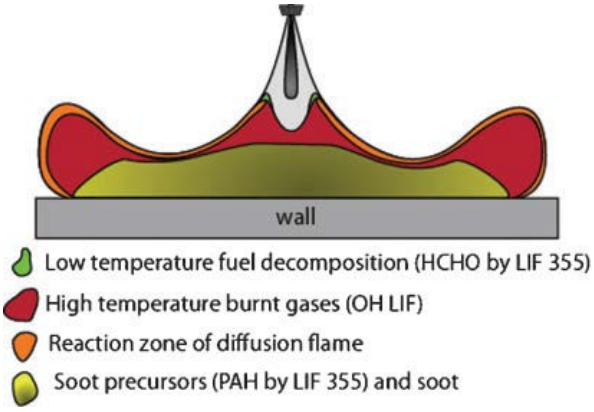

Fig. 29 A conceptual model of the jet FWI at low-temperature conditions. Reprinted from Ref. [198] with permission of SAGE publications.

Many studies [194, 196, 200-205] were carried out to reveal the mechanism of soot formation during the spray–wall interaction. Pickett and Lopez [204] investigated the soot formation in a diesel fuel jet impingement on a wall using the PLIF technology. They found that soot formation was smaller for a plane wall jet compared to a free jet under diesel engine-like conditions. Two possible explanations were given for this conclusion: (1) the wall impingement can promote the mixing of fuel vapor and ambient air [206], which reduces soot formation; (2) the jet–wall interaction leads to a decrease in temperature near the wall, which results in a slower rate of soot formation. However, according to the findings by Wang et al. [196] and Li et al. [194, 200], the jet–wall interaction worsens the combustion substantially compared with that in a free spray flame, which yields more unburnt fuel and soot based on different injection pressures and injector nozzles. They further found that an ultrahigh injection pressure can result in a relatively lower soot level, especially for the micro-hole size of 0.08 mm. Chen et al. [179] attributed this difference to different wall temperatures. They concluded that a higher wall temperature easily leads to the formation of more soot in the flame.

The mechanisms of the wall effect on the soot production can be summarised as follows:

1) Increased soot formation: The wall temperature has a substantial influence on the evaporation of the deposited liquid film on the wall. By increasing wall temperature, a richer fuel–air

mixture is formed in the area near the wall due to the evaporation of the liquid film, which becomes the source of soot formation [179].

2) Decreased soot formation: An increase in the fuel mixing with ambient air is achieved owing to the jet vortex effect [206], which finally reduces soot formation and enhances soot oxidation [204]. Pickett and Lopez [204] also pointed out that a small portion of soot deposits onto the wall. In fact, the mixing process also depends on the spray parameters such as the spray angle and injection pressure.

In summary, the wall conditions including wall temperature, dry/wetted wall, and rough or smooth wall can significantly affect the soot formation process. However, the spray FWI involving the multi-stage ignition process is rather complex and not fully understood; thus, further studies are necessary.

Spray flame/liquid film–turbulence–wall interactions

The wall heat flux also plays a vital role in the spray flame in an engine-like environment, which affects the ignition process and can quench the flame [173]. However, very limited studies on the spray FWI have considered the effect of the wall heat flux. The heat transfer process, especially in an internal combustion engine, is controlled by forced convection, which is substantially affected by the mean gas flow, turbulence, premixed flame propagation, and spray impingement on the combustion chamber walls. All these factors contribute to a transient heat flux, leading to a rapidly changing temporal and spatial temperature distributions at the surface of the combustion chamber walls [207, 208]. , **Fig. 30** presents a brief mechanism for the mutual interaction between spray, flame, wall, and turbulence based on several studies [173, 207-210]. The three key processes are:

1) The first process (spray–flame–wall): The heat flux characteristics change owing to the existence of the liquid film. The wall with a liquid film can quench the flame because of the heat loss corresponding to the heat transfer from the flame to the relatively low-temperature liquid film, which affects the pollutant formation, especially soot. In addition, the high-temperature burnt mixture with active radicals can react and promote liquid film evaporation. The wall also limits the flame wrinkling, and the liquid fuel can be burned on the wall, which affects the heat load of the wall and further causes the heat losses. However, different from the flame interaction with a dry wall, as the flame approaches the fuel film on the wall, the peak combustion temperature can increase because of the increased equivalence ratio due to film evaporation [210].
2) The second process: Turbulence dominates the liquid distribution and liquid film thickness, which further affects the mixture formation. Similarly, the wall changes the liquid droplet motion and further influences the mixture formation. Meanwhile, a cold liquid film or spray can change the turbulent velocity and temperature boundary layer.
3) The third process: The flame can affect turbulence due to the expansion of the flame front induced by combustion and the viscosity increase in the burnt gases. However, the effect is weakened by

the existence of a low-temperature liquid film. In addition, turbulence can wrinkle and strain the flame surface and promote the burning rate. In turn, turbulence also promotes heat transfer loss, which leads to flame extinction.

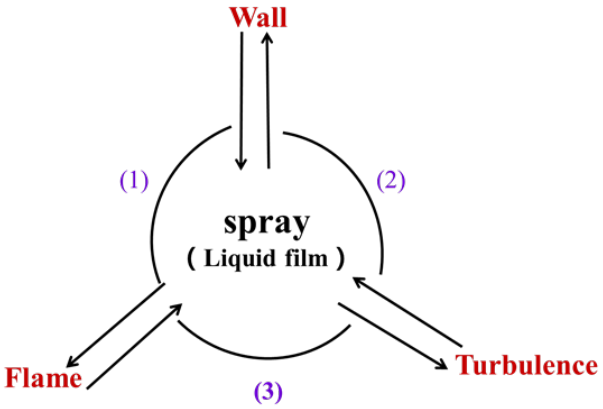

Fig. 30 Mechanism of the mutual interactions between the spray, flame, wall, and turbulence

In summary, it is important to understand the spray flame–wall–turbulence interactions for new insights and engine performance improvement. Even with the significant advances made over the past decades, major gaps in understanding the complex mechanism of the spray flame–wall–turbulence interactions still exist. These can be addressed through the following superordinate topics: 1) turbulent FWI on the dry wall and liquid film under real engine-like conditions with high-precision experiments and high-fidelity simulations; 2) the effect of different turbulent intensities on the droplet motion, flame propagation, heat transfer from the wall, and soot emissions in terms of spray FWIs.

4. Further challenges

Despite the significant progress made so far, several challenges and important problems remain in the turbulent spray flame field, such as the turbulence–spray–combustion interactions in a supercritical environment and in methane–air mixture, which generally occur in marine diesel engines and dual-fuel engines.

4.1 Supercritical spray flame

Currently, research on supercritical spray is becoming important because of the need for the development of high-pressure combustion devices [211, 212]. With new combustion technologies, the average pressure in diesel engines exceeds the critical pressure of most hydrocarbon fuels. For liquid-propellant rockets, the pressure under the working conditions is even higher. Fuel injection in such engines always occurs in supercritical regimes. Compared with subcritical situations, fluids under supercritical conditions exhibit different characteristics. Their surface tension and latent enthalpy values tend to approach zero, and the gas–liquid interface disappears, making the two-phase division in the traditional sense meaningless. Instead, fluids are described to be in the supercritical phase, where their density behaves similar to a liquid with its transport characteristics behaving like gas. When liquid fluids approach the supercritical phase, their thermodynamic and transport parameters such as specific

heat, viscosity, and thermal conductivity change remarkably. The solubility of gases in liquids also undergoes an abrupt change. Consequently, the structure of a supercritical spray is completely different from that of a subcritical spray. The supercritical spray process involves two key points: the evaporation rate and transition of the fuel–air mixing process from the two-phase breakup and evaporation processes to single-phase diffusion-controlled mixing [213-215]. Significant advances have been made in recent years in understanding supercritical spray flames from the microscale [213, 216] to the macro-spray process [214, 215]. However, many unsolved problems remain, and it is necessary to address future challenges of supercritical spray flames in the following areas:

1) Although theories on supercritical droplet behaviors have been developed, the existing studies regarding the high-pressure spray flame mechanisms are still limited [215, 217]. High-fidelity experiments and numerical simulations are required to explain the mechanisms of supercritical jet atomization and combustion processes.

2) Quantitative methods for calculating the gasification rate of supercritical droplets are insufficient, especially for multicomponent droplets. Experiments have been performed to obtain the droplet lifetime in different situations [218, 219], but an accurate theoretical formula for predicting the high-pressure fuel gasification rate is necessary. For static spray, Li et al. [220] proposed a constant rate evaporation model, which assumes that the gasification rate of a supercritical liquid is maintained at the value of the critical point. For droplets in a forced convection environment, Litchford and Jeng [221] proposed a stripping evaporation rate model based on the pneumatic stripping theory. However, the accuracy of both models needs to be evaluated further.

3) Reliable multiphase numerical simulation techniques are required under supercritical conditions with the disappearance of a distinct phase interface. Studies using liquid breakup and atomization models based on the subcritical KH-RT theory would introduce errors. Simeoni [211] and Banuti [212, 222] observed a diesel jet injected into a nitrogen environment under supercritical conditions. The supercritical interface was found to be a continuous turbulence-mixing layer and can be divided into three different areas: a liquid-like area in the jet core region near the nozzle, a supercritical gas-like area at the edge of the jet, and a transition area between the two areas. In the transition area, gas and liquid can be dissolved into each other, and a pseudo-boiling phenomenon occurs. Trans/supercritical effects need to be considered in spray models. Alternatively, simulating a spray with the Euler method viewing spray as a continuous phase can precisely predict the interface shape and eliminate errors [223]. Finally, simulating the interfacial process and the subsequent combustion by molecular dynamics is a feasible way [213, 216, Gong et al., 2021] for understanding the detailed mechanism of supercritical spray combustion. In particular, Gong et al. [14. Y. Gong, G. Xiao, X. Ma, K. H. Luo, S. Shuai and H. Xu, “Phase transitions of multi-component fuel droplets under sub- and supercritical conditions,” Fuel 287, Article No. 119516 (2021). DOI: 10.1016/j.fuel.2020.119516] studied the phase

transition of a three-component hydrocarbon fuel (5.3 wt% isooctane, 25.8 wt% n-dodecane and 68.9 wt% n-hexadecane) under subcritical and supercritical nitrogen environments using molecular dynamics. Under certain combinations of high temperature and pressure, the dominant mixing between the multicomponent fuel and the surrounding transitioned from evaporation to diffusion.

4) The influence of turbulence on supercritical spray needs to be clarified. Importantly, a systematic study is necessary to assess the capability of the current turbulence models for the supercritical spray process.

4.2 Turbulent spray flames in dual-fuel engines

Most studies on turbulent spray flames were performed under ambient air conditions. However, in dual-fuel engines, a pilot diesel igniter is generally used to trigger the ignition of the methane–air mixture. Several studies [224-227] have investigated fuel injection into a methane–air mixture ambient. In general, the addition of methane to the ambient mixture prolonged the autoignition of n-heptane spray [224], and both the pre-ignition and post-ignition processes were affected in a complex manner depending on the initial methane concentration and boundary conditions [228]. However, it is noteworthy that the pre-ignition oxidative reactions of the premixed methane–air mixture before the injection of n-heptane will induce an increase in ambient temperature and produce intermediate radicals, which finally promote n-heptane ignition [227]. Furthermore, the two-stage ignition process in turbulent spray flame under dual-fuel engine-like conditions, in which DME was injected into a methane–air mixture [136, 137], was investigated. In these studies, a reduced DME/CH_4 oxidization mechanism with 25 species and 147 elementary reactions was incorporated. Low-temperature autoignition is found to be initialized in the fuel-rich region, and then a cool flame was formed, propagating toward the even richer mixture through a balanced reaction–diffusion mechanism. The cool flame facilitated the formation of high-temperature kernels, which eventually triggered the premixed methane–air mixture. During the process, triple or tetrabranchial flames, including cool flame, fuel-rich-premixed flame, diffusion flame, and fuel-lean-premixed flame, coexist in the field. The effects of methane on the first- and second-stage ignition processes were also studied by Srna et al. [229] and Kahila et al. [14, 16, 230] both experimentally and numerically. Methane was found to delay both the first and second stage of ignition, and it mostly deferred the cool-flame reactivity. Many active intermediate species, such as OH and O, were consumed by CH_4, thus prolonging the early decomposition of n-dodecane. The first detection of CH_2O showed a small dependence on the methane concentration [229]. The deferring effect of LTI from methane plays the dominant role in prolonging the HTC of spray flames. Further work is required to establish the controlling mechanisms behind the highly complex multiscale multiphysics process to achieve optimal engine performance and reduce emissions. Finally, turbulence–spray–combustion interactions involving the effects of fuel-stratified methane–air as well as temperature and species inhomogeneity effects on the ignition process in dual-

fuel engine-like conditions should be further considered.

4.3 Turbulent spray flames in real diesel fuels

Advanced compression-ignition combustion strategies include higher pressures, lower temperatures, varying degrees of fuel–air premixing, high levels of EGR, and multiple fuel-injection events [9]. Most studies on diesel combustion typically adopted single-component fuels (n-heptane and dodecane) as surrogates to simulate the combustion process of using advanced combustion strategies, such as those aforementioned in this review. It is currently impossible for a single-component fuel to represent all aspects of fuel behaviors in diesel engines. However, there are some basic conclusions and methods that are independent of the fuels, such as the mechanisms of TCI and radiation effects on the key aspects, i.e., the autoignition process and flame LOL or diffusion flame stabilization in diesel spray combustion discussed in the review. In addition, numerical model validation requires well-defined experimental conditions with an open-access data repository for spray flames. Thus, the existing studies using single-component fuels can be used as references to understand the autoignition, flame development and flame stabilization mechanisms of real fuels under diesel-like conditions.

Currently, little is known about the spray combustion behaviors of real fuels over a wide range of thermophysical conditions. Studies on the combustion of real fuels with all the hydrocarbon species included are highly unrealistic considering the limitations of the present computational and experimental facilities [231]. Conventional engine fuels are complex hydrocarbon mixtures, including hundreds to thousands of chemical compounds, which have different thermophysical properties, such as vapor diffusivity, viscosity, density, vapor pressure, surface tension, and chemical kinetics [232-234]. Therefore, high-efficiency and high-fidelity surrogates of real diesel fuels simultaneously considering both physical and chemical aspects should be established to reproduce key real fuel characteristics. These are important particularly for the development of multicomponent vaporization models and chemical mechanisms of real engine fuels using advanced methods [234, 235], such as the physical surrogate group chemistry representation (PSGCR) method [231], decoupling physical-chemical surrogate (DPCS) model [232, 236] and the hybrid chemistry (HyChem) approach [233, 234].

In the PSGCR method, the components in the physical surrogate and chemical surrogate are essentially the same; thus, the physical and chemical submodels can be directly coupled. However, it is probably impossible to fully couple the physical properties with the chemical properties of actual fuels with complicated compositions at present [237]. The breakup and evaporation of the spray in diesel engines are critical to the subsequent combustion process. The DPCS model was proposed to investigate the spray and combustion characteristics of real fuels [232, 236], where the discrete multi-component model was introduced to describe the physical properties based on the major components of real fuels. The skeletal chemical mechanism of the chemical surrogate is employed to reproduce the

chemical behavior of real fuels. The DPCS model was applied to predict the spray penetration of soybean methyl ester (SME) as well as the combustion and emissions of a PCCI engine fueled with SME, in which methyl decanoate, methyl 5-decenoate, and n-decane ($C_{10}H_{22}$) were included in the chemical surrogate. The results showed that the DPCS model reproduces spray penetration, indicated specific fuel consumption and emissions better than single-component model.

Recently, a HyCHEM method has been developed for real jet fuels [233, 234]. This method combines experimental constraints, a lumped pyrolysis model for fuel decomposition and a detailed kinetic model for oxidative pyrolysis of the oxidation of the decomposition products to accurately describe the combustion process over a wide range of thermodynamic conditions. Based on the HyCHEM method, an LES study of turbulent spray combustion fueled with Jet-A considering the real fuel chemistry was carried out for an aeronautical combustion chamber. It was difficult to solve the real fuel mechanism directly, so an analytically reduced chemistry was introduced. Compared with the experimental data, the LES results could accurately reproduce the gas velocity, temperature and species mass fractions, especially for the NOx levels [238].

With detailed chemical kinetics of real fuel surrogates being used in turbulent spray combustion simulations, the computational cost will become excessive because of the large number of chemical species and reactions and the wide range of chemical timescales involved. Therefore, accelerating methods, such as dynamic adaptive chemistry (DAC) [239-242], dimension reduction [243], cell agglomeration methods [244, 245], and TDAC [246] should be suitably utilized to resolve this issue without compromising the prediction accuracy. However, similar to the most stand-alone accelerating methods, once these methods are employed, they will cover the entire simulation without considering the different combustion stages with different chemistry reaction features, such as LTC stage and autoignition process. This limits the computational efficiency of the accelerating methods. To address this limitation, recently proposed methods, such as the static adaptive chemistry acceleration approach [247, 248] and dynamic adaptive acceleration method (DAAM) [249], aim to achieve high-efficiency computation under complex thermodynamic conditions in engine combustion chambers. At a given reaction fractional step, the DAAM dynamically selects the optimal acceleration method for each computational cell based on the encountered composition inhomogeneity, which is quantified through reconstructing the histogram in a low-dimensional composition subspace determined by the principal component analysis [250].

Overall, an in-depth study of the turbulent spray flame of real fuels under diesel-like conditions is very rare currently. Thus, for future work, more well-designed experiments should be conducted and a high-fidelity real fuel surrogate model that simultaneously considers both physical and chemical aspects should be developed. In the spray process, the surrogate should closely match the actual distillation curve and fuel vapor mixture, and in the combustion process, the combustion behavior of

the real fuel should be matched over a wide range of thermodynamic conditions.

5. Conclusions and outlook

5.1 Concluding remarks

Fuel sprays play a critical role in liquid-fuel combustion and are very effective for controlling the combustion process and consequently the performance of engines. Therefore, studies on turbulent spray flames are comprehensively discussed in terms of the turbulence-chemistry, spray–turbulence, and spray–chemistry interactions under diesel engine-like conditions. Significant progress has been made in understanding the spray–chemistry–turbulence interaction over the last decade.

In the context of spray-turbulence interaction, the dynamics of high-speed spray promote turbulence generation in the flow field, which in turn affects the cavitation, primary and secondary spray breakup, droplet evaporation, and mixing via momentum exchange. Considering the turbulent fluctuation effects can lead to more accurate predictions of the liquid penetration and distribution of fuel vapor. For the ignition process, the relative timescales of droplet evaporation, convection, molecular diffusion gas, chemistry, and temperature determine the ignition modes. For the two-stage ignition process, a cool flame can occur in the fuel-lean region first at a low temperature owing to the evaporation of cold fuel; then, the second-stage ignition moves toward the fuel-rich region. The stabilization mechanism of the spray flame can be scrutinized through the budget analysis. Most studies have found that the reaction terms are larger than the diffusion terms near the flame LOL positions under various diesel engine-like conditions. This implies that the flame stabilization is dominated by autoignition, and the turbulent transport of heat also makes a contribution to the flame stabilization. Various phenomena occur, including LTC with cool flames, high-temperature flames, and diffusion flames, which interact with turbulence.

For turbulent spray combustion, incorporation of TCI effects yields improved predictions of ID, flame LOL, distributions of temperature, species, and soot production, especially at low temperatures and low oxygen concentrations. Neglecting the TCI can overpredict the ID and result in a thin flame structure with a considerably high local peak temperature and heat release rate. Furthermore, the TRI effect on the spray flame is found to be less than 10%, as predicted by the transport PDF approach coupled with three different radiative transfer solvers, which is smaller than the TCI effect. In addition to the TCI effect, fuel chemistry strongly influences the ignition process, and the predictive capabilities are significantly enhanced by the inclusion of low-temperature chemistry. Overall, the accuracy and usefulness of turbulent spray flame simulations under engine-like conditions are limited by availability of accurate and reliable chemical mechanisms for multicomponent fuels, radiation treatment, turbulence models, flow and physiochemical properties under supercrical conditions, and near-wall models. Comparable experimental data are badly needed for model development and validation. It is

also important to perform systematic uncertainty quantification analysis in order to use simulation results judicially.

5.2 Future research directions

Over the past decade, great progress has been made in understanding the underlying mechanisms of turbulent spray flames. However, there are still many unsolved issues that requires further investigation, as discussed below.

Turbulent spray flames: Efforts to understand the complex process of turbulent spray flames have been made both experimentally and numerically. However, there is a lack of quantitative optical diagnostics for turbulence–spray–combustion interactions. Future work should be focused on developing advanced optical diagnostics to detect intermediate species under low to medium temperature conditions to study ignition and combustion involving cool flames and ignition/extinction, among others. Regarding numerical simulations, a high priority should be given to the development of spray breakup models and atomization models of multicomponent fuels. In the spray process, the KH–RT breakup model is widely utilized to describe the primary and secondary breakup processes. However, the model requires further assessment and development for ultra-high injection pressures (> 300 MPa), which will affect the prediction of highly relevant velocity or shock waves on droplet breakup [251]. Meanwhile, accurate and reliable models are necessary to account for the effects of cavitation and turbulence on the breakup process in the dense spray regime.

Turbulent spray FWI: It is important to understand the spray flame–wall–turbulence interactions to improve engine performance. Further research should be focused on these superordinate topics: 1) effect of turbulence on the spray FWI, 2) mechanisms of liquid spray ignition by hot surface, and 3) effects of near-wall multiphase flow/turbulence/combustion models on the numerical prediction of spray flame structures.

Acknowledgment

This work was supported by the National Natural Science Foundation of China (Grant No. 91741119) and the National Science Fund for Distinguished Young Scholars (Grant No. 51825603). K.H. Luo gratefully acknowledges support from the UK Engineering and Physical Sciences Research Council (Grant Nos. EP/R029598/1 and EP/S012559/1).

Nomenclature

δ_L	Fame thickness	LTI	Low-temperature ignition
l_η	Kolmogorov length scale	LOL	Fame lift-off length
χ	Scalar dissipation rate	TCI	Turbulence-chemistry interaction
ϕ	Equivalence ratio	TKE	Turbulent kinetic energy
Z_{mr}	Most reactive mixture fraction	WSR	Well-stirred reactor model
Z_{st}	Stoichiometric mixture fraction	PDF	Probability density function

We	Weber number	LES	Large eddy simulation
C	Reaction progress variable	DNS	Direct numerical simulation
D_B	Fragments of size	RANS	Reynolds-averaged Navier-Stokes
τ_f	Integral time scale	IXT	Intensity axial time
$Re(\lambda_e)$	Real part of the largest nonzero eigenvalue	DT	Dwell time
		ID	Ignition delay
Λ_e	The logscale of $Re(\lambda_e)$	AHRR	Apparent heat release rate
V_{rel}	Magnitude of the relative velocity between the liquid droplet and the gas	TRI	Turbulence-radiation interactions
d_{eq}	Equivalent diameter	PLIF	Planar laser-induced fluorescence
Abbreviations		FWI	Flame-wall interaction
LTC	Low-temperature combustion	DAC	Dynamic adaptive chemistry
HCCI	Homogeneous charge compression ignition	UHC	Unburned hydrocarbons
HTC	High-temperature combustion	FID	First injection duration
HTI	High-temperature ignition	EGR	Exhaust gas recirculation
Ka	Karlovitz number		
Da	Damköhler number		

References

[1] P. Jenny, D. Roekaerts, N. Beishuizen, Modeling of turbulent dilute spray combustion, Prog. Energy Combust. Sci. 38 (2012) 846-887.

[2] A.L. Sánchez, J. Urzay, A. Liñán, The role of separation of scales in the description of spray combustion, Proc. Combust. Inst. 35 (2015) 1549-1577.

[3] S.-Y. No, A Review on Empirical Correlations for Jet/Spray Trajectory of Liquid Jet in Uniform Cross Flow, International Journal of Spray and Combustion Dynamics 7 (2015) 283-313.

[4] H. Kahila, A. Wehrfritz, O. Kaario, M. Ghaderi Masouleh, N. Maes, B. Somers, V. Vuorinen, Large-eddy simulation on the influence of injection pressure in reacting Spray A, Combust. Flame 191 (2018) 142-159.

[5] A. Irannejad, A. Banaeizadeh, F. Jaberi, Large eddy simulation of turbulent spray combustion, Combust. Flame 162 (2015) 431-450.

[6] Y. Minamoto, H. Kolla, R.W. Grout, A. Gruber, J.H. Chen, Effect of fuel composition and differential diffusion on flame stabilization in reacting syngas jets in turbulent cross-flow, Combust. Flame 162 (2015) 3569-3579.

[7] A.K. Agarwal, A.P. Singh, R.K. Maurya, Evolution, challenges and path forward for low temperature combustion engines, Prog. Energy Combust. Sci. 61 (2017) 1-56.

[8] M.P.B. Musculus, P.C. Miles, L.M. Pickett, Conceptual models for partially premixed low-temperature diesel combustion, Prog. Energy Combust. Sci. 39 (2013) 246-283.

[9] S. Bhattacharjee, D.C. Haworth, Simulations of transient n-heptane and n-dodecane spray flames under engine-relevant conditions using a transported PDF method, Combust. Flame 160 (2013) 2083-2102.

[10] M. Bolla, D. Farrace, Y.M. Wright, K. Boulouchos, E. Mastorakos, Influence of turbulence-chemistry interaction for n-heptane spray combustion under diesel engine conditions with emphasis on soot formation and oxidation, Combust. Theory Modell. 18 (2014) 330-360.

[11] S.F. Fernandez, C. Paul, A. Sircar, A. Imren, D.C. Haworth, S. Roy, M.F. Modest, Soot and spectral radiation modeling for high-pressure turbulent spray flames, Combust. Flame 190 (2018) 402-415.

[12] Y. Hu, R. Kurose, Nonpremixed and premixed flamelets LES of partially premixed spray flames using a two-phase transport equation of progress variable, Combust. Flame 188 (2018) 227-242.

[13] Y. Hu, H. Olguin, E. Gutheil, A spray flamelet/progress variable approach combined with a transported joint PDF model for turbulent spray flames, Combust. Theory Modell. 21 (2017) 575-602.

[14] H. Kahila, O. Kaario, Z. Ahmad, M. Ghaderi Masouleh, B. Tekgül, M. Larmi, V. Vuorinen, A large-eddy simulation study on the influence of diesel pilot spray quantity on methane-air flame initiation, Combust. Flame 206 (2019) 506-521.

[15] A. Wehrfritz, O. Kaario, V. Vuorinen, B. Somers, Large Eddy Simulation of n-dodecane spray flames using Flamelet Generated Manifolds, Combust. Flame 167 (2016) 113-131.

[16] H. Kahila, A. Wehrfritz, O. Kaario, V. Vuorinen, Large-eddy simulation of dual-fuel ignition: Diesel spray injection into a lean methane-air mixture, Combust. Flame 199 (2019) 131-151.
[17]
S. Hoyas, J.M. Pastor, D. Khuong-Anh, J.M. Mompó-Laborda, F. Ravet. Application and evaluation of the Eulerian-Lagrangian spray atomization (ELSA) model on CFD diesel spray simulations. In: editor^editors. 2011: SAE p.
[18] S. Hoyas, A. Gil, X. Margot, D. Khuong-Anh, F. Ravet, Evaluation of the Eulerian–Lagrangian Spray Atomization (ELSA) model in spray simulations: 2D cases, Math Comput Modell 57 (2013) 1686-1693.
[19] K. Luo, C. Shao, M. Chai, J. Fan, Level set method for atomization and evaporation simulations, Prog Energ Combust 73 (2019) 65-94.
[20] H. Luo, K. Nishida, S. Uchitomi, Y. Ogata, W. Zhang, T. Fujikawa, Effect of temperature on fuel adhesion under spray-wall impingement condition, Fuel 234 (2018) 56-65.
[21] J. Shinjo, A. Umemura, Simulation of liquid jet primary breakup: Dynamics of ligament and droplet formation, Int. J. Multiphase Flow 36 (2010) 513-532.
[22] W. Edelbauer, Numerical simulation of cavitating injector flow and liquid spray break-up by combination of Eulerian–Eulerian and Volume-of-Fluid methods, Computers & Fluids 144 (2017) 19-33.
[23] M.B. Luong, G.H. Yu, S.H. Chung, C.S. Yoo, Ignition of a lean PRF/air mixture under RCCI/SCCI conditions: Chemical aspects, Proc. Combust. Inst. 36 (2017) 3587-3596.
[24] P. Zhang, W. Ji, T. He, X. He, Z. Wang, B. Yang, C.K. Law, First-stage ignition delay in the negative temperature coefficient behavior: Experiment and simulation, Combust. Flame 167 (2016) 14-23.
[25] W. Ji, P. Zhao, T. He, X. He, A. Farooq, C.K. Law, On the controlling mechanism of the upper turnover states in the NTC regime, Combust. Flame 164 (2016) 294-302.
[26] H.H. Chiu, T.M. Liu, Group Combustion of Liquid Droplets, Combust. Sci. Technol. 17 (1977) 127-142.
[27] S.A. Skeen, J. Manin, L.M. Pickett, Simultaneous formaldehyde PLIF and high-speed schlieren imaging for ignition visualization in high-pressure spray flames, Proc. Combust. Inst. 35 (2015) 3167-3174.
[28] E. Mastorakos, Ignition of turbulent non-premixed flames, Prog. Energy Combust. Sci. 35 (2009) 57-97.
[29] W. Zhao, L. Zhou, W. Qin, H. Wei, Large Eddy Simulation of Multiple-Stage Ignition Process of n-Heptane Spray Flame, J. Eng. Gas Turbines Power 141 (2019).
[30] Y. Pei, E.R. Hawkes, M. Bolla, S. Kook, G.M. Goldin, Y. Yang, S.B. Pope, S. Som, An analysis of the structure of an n-dodecane spray flame using TPDF modelling, Combust. Flame 168 (2016) 420-435.
[31] R. Payri, F.J. Salvador, J. Gimeno, J.E. Peraza, Experimental study of the injection conditions influence over n-dodecane and diesel sprays with two ECN single-hole nozzles. Part II: Reactive atmosphere, Energy Convers. Manage. 126 (2016) 1157-1167.
[32] A.R. Masri, Turbulent Combustion of Sprays: From Dilute to Dense, Combust. Sci. Technol. 188 (2016) 1619-1639.
[33] X. Jiang, G.A. Siamas, K. Jagus, T.G. Karayiannis, Physical modelling and advanced simulations of gas–liquid two-phase jet flows in atomization and sprays, Prog. Energy Combust. Sci. 36 (2010) 131-167.
[34] J. Oefelein, R. Dahms, G. Lacaze, Detailed Modeling and Simulation of High-Pressure Fuel Injection Processes in Diesel Engines, SAE International Journal of Engines 5 (2012) 1410-1419.
[35] H.G. How, H.H. Masjuki, M.A. Kalam, Y.H. Teoh, Influence of injection timing and split injection strategies on performance, emissions, and combustion characteristics of diesel engine fueled with biodiesel blended fuels, Fuel 213 (2018) 106-114.
[36] X. Zhou, T. Li, Z. Lai, S. Huang, Similarity of split-injected fuel sprays for different size diesel engines, Int. J. Engine Res., doi:10.1177/1468087419849771(2019) 1468087419849771.
[37] V.R. Mohan, D.C. Haworth, Turbulence-chemistry interactions in a heavy-duty compression-ignition engine, Proc. Combust. Inst. 35 (2015) 3053-3060.
[38] C.S. Yoo, Z. Luo, T. Lu, H. Kim, J.H. Chen, A DNS study of ignition characteristics of a lean iso-octane/air mixture under HCCI and SACI conditions, Proc. Combust. Inst. 34 (2013) 2985-2993.
[39] M.B. Luong, G.H. Yu, S.H. Chung, C.S. Yoo, Ignition of a lean PRF/air mixture under RCCI/SCCI conditions: A comparative DNS study, Proc. Combust. Inst. 36 (2017) 3623-3631.
[40] D. Dasgupta, W. Sun, M. Day, T. Lieuwen, Effect of turbulence–chemistry interactions on chemical pathways for turbulent hydrogen–air premixed flames, Combust. Flame 176 (2017) 191-201.
[41] S.W. Dasgupta Debolina, Day Marc S, Lieuwen Tim C, Turbulence effects on the chemical pathways for premixed methane/air flames, 55th AIAA Aerospace Sciences Meeting 1782 (2017).
[42] N. Peters, Turbulent Combustion, Cambridge University Press2000.
[43] A.J. Aspden, M.S. Day, J.B. Bell, Turbulence–flame interactions in lean premixed hydrogen: transition to the distributed burning regime, Journal of Fluid Mechanics 680 (2011) 287-320.
[44] A.J. Aspden, M.S. Day, J.B. Bell, Three-dimensional direct numerical simulation of turbulent lean premixed methane combustion with detailed kinetics, Combust. Flame 166 (2016) 266-283.
[45] A.J. Aspden, J.B. Bell, M.S. Day, F.N. Egolfopoulos, Turbulence–flame interactions in lean premixed dodecane flames, Proc. Combust. Inst. 36 (2017) 2005-2016.
[46] H. Carlsson, R. Yu, X.-S. Bai, Direct numerical simulation of lean premixed CH4/air and H2/air flames at high Karlovitz numbers, Int. J. Hydrogen Energy 39 (2014) 20216-20232.
[47] A.J. Aspden, M.S. Day, J.B. Bell, Turbulence-chemistry interaction in lean premixed hydrogen combustion, Proc.

Combust. Inst. 35 (2015) 1321-1329.
[48] H. Wei, X. Chen, G. Wang, L. Zhou, S. An, G. Shu, Effect of swirl flow on spray and combustion characteristics with heavy fuel oil under two-stroke marine engine relevant conditions, Appl. Therm. Eng. 124 (2017) 302-314.
[49] L. Zhou, K.H. Luo, S.J. Shuai, M.Z. Xie, Large-eddy simulations of diesel spray with a fine grid in a constant-volume vessel, Proc. Inst. Mech. Eng. Pt. D: J. Automobile Eng. 229 (2015) 247-260.
[50] K.H. Luo, Combustion effects on turbulence in a partially premixed supersonic diffusion flame, Combust. Flame 119 (1999) 417-435.
[51] K.H. Luo, K.N.C. Bray, Combustion-induced pressure effects in supersonic diffusion flames, Symposium (International) on Combustion 27 (1998) 2165-2171.
[52] U. Burke, K.P. Somers, P. O'Toole, C.M. Zinner, N. Marquet, G. Bourque, E.L. Petersen, W.K. Metcalfe, Z. Serinyel, H.J. Curran, An ignition delay and kinetic modeling study of methane, dimethyl ether, and their mixtures at high pressures, Combust. Flame 162 (2015) 315-330.
[53] Y.-H. Im, K.Y. Huh, S. Nishiki, T. Hasegawa, Zone conditional assessment of flame-generated turbulence with DNS database of a turbulent premixed flame, Combust. Flame 137 (2004) 478-488.
[54] S. Zhang, C.J. Rutland, Premixed flame effects on turbulence and pressure-related terms, Combust. Flame 102 (1995) 447-461.
[55] B.D. Videto, D.A. Santavicca, Flame-Turbulence Interactions in a Freely-Propagating, Premixed Flame, Combust. Sci. Technol. 70 (1990) 47-73.
[56] Y. Pei, E.R. Hawkes, S. Kook, G.M. Goldin, T. Lu, Modelling n-dodecane spray and combustion with the transported probability density function method, Combust. Flame 162 (2015) 2006-2019.
[57] Y. Pei, S. Som, E. Pomraning, P.K. Senecal, S.A. Skeen, J. Manin, L.M. Pickett, Large eddy simulation of a reacting spray flame with multiple realizations under compression ignition engine conditions, Combust. Flame 162 (2015) 4442-4455.
[58] R. Payri, J.M. García-Oliver, T. Xuan, M. Bardi, A study on diesel spray tip penetration and radial expansion under reacting conditions, Appl. Therm. Eng. 90 (2015) 619-629.
[59] J.M. García-Oliver, L.-M. Malbec, H.B. Toda, G. Bruneaux, A study on the interaction between local flow and flame structure for mixing-controlled Diesel sprays, Combust. Flame 179 (2017) 157-171.
[60] L. Zhou, Z. Lu, Z. Ren, T. Lu, K. H. Luo, Numerical analysis of ignition and flame stabilization in an n-heptane spray flame, Int. J. Heat Mass Transfer 88 (2015) 565-571.
[61] T. Lackmann, A. Nygren, A. Karlsson, M. Oevermann, Investigation of turbulence–chemistry interactions in a heavy-duty diesel engine with a representative interactive linear eddy model, Int. J. Engine Res. 21 (2018) 1469-1479.
[62] Y. Pei, E.R. Hawkes, S. Kook, Transported probability density function modelling of the vapour phase of an n-heptane jet at diesel engine conditions, Proc. Combust. Inst. 34 (2013) 3039-3047.
[63] M.A. Chishty, M. Bolla, E.R. Hawkes, Y. Pei, S. Kook, Soot formation modelling for n-dodecane sprays using the transported PDF model, Combust. Flame 192 (2018) 101-119.
[64] D.R. Tree, K.I. Svensson, Soot processes in compression ignition engines, Prog. Energy Combust. Sci. 33 (2007) 272-309.
[65] F. Payri, J.M. García-Oliver, R. Novella, E.J. Pérez-Sánchez, Influence of the n-dodecane chemical mechanism on the CFD modelling of the diesel-like ECN Spray A flame structure at different ambient conditions, Combust. Flame 208 (2019) 198-218.
[66] L. Zhou, Z. Lu, Z. Ren, T. Lu, K. Luo, Numerical analysis of ignition and flame stabilization in an n-heptane spray flame, Int. J. Heat Mass Transfer 88 (2015) 656-571.
[67] T. Lu, C.K. Law, Toward accommodating realistic fuel chemistry in large-scale computations, Prog. Energy Combust. Sci. 35 (2009) 192-215.
[68] C.S. Yoo, T. Lu, J.H. Chen, C.K. Law, Direct numerical simulations of ignition of a lean n-heptane/air mixture with temperature inhomogeneities at constant volume: Parametric study, Combustion and Flame 158 (2011) 1727-1741.
[69] Y. Liu, M. Jia, M. Xie, B. Pang, Improvement on a skeletal chemical kinetic model of iso-octane for internal combustion engine by using a practical methodology, Fuel 103 (2013) 884-891.
[70] Y.-D. Liu, M. Jia, M.-Z. Xie, B. Pang, Enhancement on a Skeletal Kinetic Model for Primary Reference Fuel Oxidation by Using a Semidecoupling Methodology, Energ Fuel 26 (2012) 7069-7083.
[71] A. Frassoldati, G. D'Errico, T. Lucchini, A. Stagni, A. Cuoci, T. Faravelli, A. Onorati, E. Ranzi, Reduced kinetic mechanisms of diesel fuel surrogate for engine CFD simulations, Combust. Flame 162 (2015) 3991-4007.
[72] E. Ranzi, A. Frassoldati, S. Granata, T. Faravelli, Wide-Range Kinetic Modeling Study of the Pyrolysis, Partial Oxidation, and Combustion of Heavy n-Alkanes, Ind Eng Chem Res 44 (2005) 5170-5183.
[73] Y. Pei, M.J. Davis, L.M. Pickett, S. Som, Engine Combustion Network (ECN): Global sensitivity analysis of Spray A for different combustion vessels, Combust. Flame 162 (2015) 2337-2347.
[74] G. D'Errico, T. Lucchini, F. Contino, M. Jangi, X.S. Bai, Comparison of well-mixed and multiple representative interactive flamelet approaches for diesel spray combustion modelling, Combust. Theory Modell. 18 (2014) 65-88.
[75] P. Kundu, M.M. Ameen, S. Som, Importance of turbulence-chemistry interactions at low temperature engine conditions, Combust. Flame 183 (2017) 283-298.
[76] M. Bolla, M.A. Chishty, E.R. Hawkes, Q.N. Chan, S. Kook, Influence of turbulent fluctuations on radiation heat transfer, NO and soot formation under ECN Spray A conditions, Proc. Combust. Inst. 36 (2017) 3551-3558.

[77] C.K. Blomberg, L. Zeugin, S.S. Pandurangi, M. Bolla, K. Boulouchos, Y.M. Wright, Modeling Split Injections of ECN "Spray A" Using a Conditional Moment Closure Combustion Model with RANS and LES, SAE Int. J. Engines 9 (2016) 2107-2119.
[78] F. Salehi, M.J. Cleary, A.R. Masri, Y. Ge, A.Y. Klimenko, Sparse-Lagrangian MMC simulations of an n-dodecane jet at engine-relevant conditions, Proc. Combust. Inst. 36 (2017) 3577-3585.
[79] J. Gimeno, G. Bracho, P. Martí-Aldaraví, J.E. Peraza, Experimental study of the injection conditions influence over n-dodecane and diesel sprays with two ECN single-hole nozzles. Part I: Inert atmosphere, Energy Convers. Manage. 126 (2016) 1146-1156.
[80] S. Yu, B. Yin, H. Jia, J. Yu, Numerical research on micro diesel spray characteristics under ultra-high injection pressure by Large Eddy Simulation (LES), International Journal of Heat and Fluid Flow 64 (2017) 129-136.
[81] C. Espey, J.E. Dec, The Effect of TDC Temperature and Density on the Liquid-Phase Fuel Penetration in a D.I. Diesel Engine, SAE Transactions 104 (1995) 1400-1416.
[82] Q. Xue, S. Som, P.K. Senecal, E. Pomraning, LARGE EDDY SIMULATION OF FUEL-SPRAY UNDER NON-REACTING IC ENGINE CONDITIONS, Atomization and Sprays 23 (2013) 925-955.
[83] A. Hadadpour, M. Jangi, X.S. Bai, Jet-jet interaction in multiple injections: A large-eddy simulation study, Fuel 234 (2018) 286-295.
[84] S. Som, S.K. Aggarwal, Effects of primary breakup modeling on spray and combustion characteristics of compression ignition engines, Combust. Flame 157 (2010) 1179-1193.
[85] L. Zhou, M. Xie, M. Jia, Q. Zhou, C. Xu, Influences of subgrid turbulent kinetic energy and turbulent dispersion on the characteristics of fuel spray, SAE International, 2011.
[86] N. Bharadwaj, C.J. Rutland, S. Chang, Large eddy simulation modelling of spray-induced turbulence effects, Int. J. Engine Res. 10 (2009) 97-119.
[87] A.N. Kolmogorov, On the disintegration of drops in a turbulent flow, Dokl. Akad. Nauk SSSR 66 (1949) 825-828.
[88] A. Kourmatzis, A.R. Masri, The influence of gas phase velocity fluctuations on primary atomization and droplet deformation, Experiments in Fluids 55 (2014) 1659.
[89] S. Sahu, Y. Hardalupas, A.M.K.P. Taylor, Droplet–turbulence interaction in a confined polydispersed spray: effect of turbulence on droplet dispersion, Journal of Fluid Mechanics 794 (2016) 267-309.
[90] J.O. Hinze, Fundamentals of the hydrodynamic mechanism of splitting in dispersion processes, Aiche J 1 (1955) 289-295.
[91] G. Hindi, E.E. Paladino, A.A.M.d. Oliviera, Effect of mesh refinement and model parameters on LES simulation of diesel sprays, International Journal of Heat and Fluid Flow 71 (2018) 246-259.
[92] E. von Berg, W. Edelbauer, A. Alajbegovic, R. Tatschl, M. Volmajer, B. Kegl, L.C. Ganippa, Coupled Simulations of Nozzle Flow, Primary Fuel Jet Breakup, and Spray Formation, J. Eng. Gas Turbines Power 127 (2004) 897-908.
[93] K.Y. Huh, and Gosman, A. D., Phenomenological Model of Diesel Spray Atomisation, Proceedings of the International Conference on Multiphase Flows, Tsukuba,Japan, 1991.
[94] G.M. Bianchi , P. Pelloni, F.E. Corcione , L. Allocca, F. Luppino, Modeling Atomization of High-Pressure Diesel Sprays, Journal of Engineering for Gas Turbines and Power 123 (2000) 419-427.
[95] M.P.B. Musculus, T. Lachaux, L.M. Pickett, C.A. Idicheria, End-of-Injection Over-Mixing and Unburned Hydrocarbon Emissions in Low-Temperature-Combustion Diesel Engines, SAE International, 2007.
[96] B. Hu, M.P.B. Musculus, J.C. Oefelein, The influence of large-scale structures on entrainment in a decelerating transient turbulent jet revealed by large eddy simulation, Physics of Fluids 24 (2012) 045106.
[97] H. Wei, W. Zhao, L. Zhou, G. Shu, Numerical investigation of diesel spray flame structures under diesel engine-relevant conditions using large eddy simulation, Combust. Sci. Technol. 190 (2018) 909-932.
[98] H. Wang, Y. Ra, M. Jia, R.D. Reitz, Development of a reduced n-dodecane-PAH mechanism and its application for n-dodecane soot predictions, Fuel 136 (2014) 25-36.
[99] J. Westerweel, C. Fukushima, J.M. Pedersen, J.C.R. Hunt, Momentum and scalar transport at the turbulent/non-turbulent interface of a jet, Journal of Fluid Mechanics 631 (2009) 199-230.
[100] K. Nishida, J. Zhu, X. Leng, Z. He, Effects of micro-hole nozzle and ultra-high injection pressure on air entrainment, liquid penetration, flame lift-off and soot formation of diesel spray flame, Int. J. Engine Res. 18 (2017) 51-65.
[101] P. Kundu, T. Echekki, Y. Pei, S. Som, An equivalent dissipation rate model for capturing history effects in non-premixed flames, Combust. Flame 176 (2017) 202-212.
[102] X. Jiang, G.A. Siamas, K. Jagus, T.G. Karayiannis, Physical modelling and advanced simulations of gas–liquid two-phase jet flows in atomization and sprays, Prog Energ Combust 36 (2010) 131-167.
[103] D.P. Schmidt, C. Rutland, A new droplet collision algorithm, J Comput Phys 164 (2000) 62-80.
[104] P. Beard, J.-M. Duclos, C. Habchi, G. Bruneaux, K. Mokaddem, T. Baritaud, Extension of Lagrangian-Eulerian spray modeling: application to high-pressure evaporating diesel sprays, SAE transactions 109 (2000) 1417-1434.
[105] S. Post, V. IVER, J. Abraham, A study of near-field entrainment in gas jets and sprays under diesel conditions, J. Fluids Eng. 122 (2000) 385-395.
[106] J. Abraham, What is adequate resolution in the numerical computations of transient jets, SAE transactions 106 (1997) 141-155.
[107] P. Beard, O. Colin, M. Miche, Improved modelling of DI diesel engines using sub-grid descriptions of spray and combustion, SAE transactions 112 (2003) 73-86.

[108] N. Abani, A. Munnannur, R.D. Reitz, Reduction of numerical parameter dependencies in diesel spray models, Transactions-ASME Journal of engineering for gas turbines and power 130 (2008) 032809.
[109] J. Abraham, Entrapment Characteristics of Transient Gas Jets, Numerical Heat Transfer, Part A Applications 30 (1996) 347-364.
[110] N. Abani, R.D. Reitz, Unsteady turbulent round jets and vortex motion, Physics of Fluids (1994-present) 19 (2007) 125102.
[111] C.H. Lee, Y. Wang, R.D. Reitz, CFD simulation of diesel sprays over a wide range of ambient gas densities using an improved gas jet spray model, Atomization Sprays 21 (2011) 591-609.
[112] C.H. Lee, R.D. Reitz, CFD simulations of diesel spray tip penetration with multiple injections and with engine compression ratios up to 100: 1, Fuel 111 (2013) 289-297.
[113] S.L. Kokjohn, R.D. Reitz, Investigation of the roles of flame propagation, turbulent mixing, and volumetric heat release in conventional and low temperature diesel combustion, Journal of Engineering for Gas Turbines and Power 133 (2011) 1-10.
[114] C. Heye, V. Raman, A.R. Masri, Influence of spray/combustion interactions on auto-ignition of methanol spray flames, Proc. Combust. Inst. 35 (2015) 1639-1648.
[115] C. Heye, V. Raman, A.R. Masri, LES/probability density function approach for the simulation of an ethanol spray flame, Proc. Combust. Inst. 34 (2013) 1633-1641.
[116] J.M. Desantes, J.V. Pastor, J.M. García-Oliver, F.J. Briceño, An experimental analysis on the evolution of the transient tip penetration in reacting Diesel sprays, Combust. Flame 161 (2014) 2137-2150.
[117] L. Zhou, W. Zhao, H. Wei, Large Eddy Simulation on the Flame Structure for Split Injections of n-dodecane at Different Temperatures and Densities, Combust. Sci. Technol. 190 (2018) 2224-2244.
[118] C. Gong, M. Jangi, T. Lucchini, G. D'Errico, X.-S. Bai, Large Eddy Simulation of Air Entrainment and Mixing in Reacting and Non-Reacting Diesel Sprays, Flow, Turbul. Combust. 93 (2014) 385-404.
[119] H. Wei, W. Zhao, Z. Lu, L. Zhou, Effects of oxygen concentrations on the ignition and quasi-steady processes of n-heptane spray flames using large eddy simulation, Fuel 241 (2019) 786-801.
[120] J.M. Desantes, J.M. García-Oliver, T. Xuan, W. Vera-Tudela, A study on tip penetration velocity and radial expansion of reacting diesel sprays with different fuels, Fuel 207 (2017) 323-335.
[121] S. Skeen, J. Manin, L.M. Pickett, Visualization of Ignition Processes in High-Pressure Sprays with Multiple Injections of n-Dodecane, SAE Int. J. Engines 8 (2015) 696-715.
[122] M. Bolla, M.A. Chishty, E.R. Hawkes, S. Kook, Modeling combustion under engine combustion network Spray A conditions with multiple injections using the transported probability density function method, Int. J. Engine Res. 18 (2017) 6-14.
[123] A.A. Moiz, K.D. Cung, S.-Y. Lee, Simultaneous Schlieren–PLIF Studies for Ignition and Soot Luminosity Visualization With Close-Coupled High-Pressure Double Injections of n-Dodecane, J. Energy Resour. Technol. 139 (2017) 012207-012207-012212.
[124] G. Bruneaux, D. Maligne, Study of the Mixing and Combustion Processes of Consecutive Short Double Diesel Injections, SAE Int. J. Engines 2 (2009) 1151-1169.
[125] J.M. Desantes, J.M. García-Oliver, A. García, T. Xuan, Optical study on characteristics of non-reacting and reacting diesel spray with different strategies of split injection, Int. J. Engine Res. 20 (2018) 606-623.
[126] K. Cung, A. Moiz, J. Johnson, S.-Y. Lee, C.-B. Kweon, A. Montanaro, Spray–combustion interaction mechanism of multiple-injection under diesel engine conditions, Proc. Combust. Inst. 35 (2015) 3061-3068.
[127] T.I. Farouk, D. Dietrich, F.E. Alam, F.L. Dryer, Isolated n-decane droplet combustion – Dual stage and single stage transition to "Cool Flame" droplet burning, Proc. Combust. Inst. 36 (2017) 2523-2530.
[128] W. Zhao, L. Zhou, J. Qi, H. Wei, The influence of intermediate species on the combustion process of n-dodecane flame, Proceedings of the Institution of Mechanical Engineers, Part D: Journal of Automobile Engineering 234 (2019) 334-348.
[129] W. Zhao, H. Wei, M. Jia, Z. Lu, K.H. Luo, R. Chen, L. Zhou, Flame–spray interaction and combustion features in split-injection spray flames under diesel engine-like conditions, Combust. Flame 210 (2019) 204-221.
[130] A. Hadadpour, M. Jangi, K.M. Pang, X. Song Bai, The role of a split injection strategy in the mixture formation and combustion of diesel spray: A large-eddy simulation, Proc. Combust. Inst. 37 (2019) 4709-4716.
[131] N. Maes, M. Meijer, N. Dam, B. Somers, H. Baya Toda, G. Bruneaux, S.A. Skeen, L.M. Pickett, J. Manin, Characterization of Spray A flame structure for parametric variations in ECN constant-volume vessels using chemiluminescence and laser-induced fluorescence, Combust. Flame 174 (2016) 138-151.
[132] R.N. Dahms, G.A. Paczko, S.A. Skeen, L.M. Pickett, Understanding the ignition mechanism of high-pressure spray flames, Proc. Combust. Inst. 36 (2017) 2615-2623.
[133] D.M. Manias, E.A. Tingas, C.E. Frouzakis, K. Boulouchos, D.A. Goussis, The mechanism by which CH2O and H2O2 additives affect the autoignition of CH4/air mixtures, Combust. Flame 164 (2016) 111-125.
[134] A. Krisman, E.R. Hawkes, J.H. Chen, Two-stage autoignition and edge flames in a high pressure turbulent jet, J. Fluid Mech. 824 (2017) 5-41.
[135] T. Jin, X. Wang, K.H. Luo, K. Luo, J. Fan, Structure of tetrabrachial flames in non-premixed autoigniting dimethyl ether/air mixtures, Fuel 232 (2018) 90-98.
[136] T. Jin, K.H. Luo, X. Wang, K. Luo, J. Fan, Dynamics of triple-flames in ignition of turbulent dual fuel mixture: A

direct numerical simulation study, Proc Combust Inst 37 (2019) 4625-4633.
[137] T. Jin, Y. Wu, X. Wang, K.H. Luo, T. Lu, K. Luo, J. Fan, Ignition dynamics of DME/methane-air reactive mixing layer under reactivity controlled compression ignition conditions: Effects of cool flames, Appl Energ 249 (2019) 343-354.
[138] H. Wei, W. Zhao, L. Zhou, C. Chen, G. Shu, Large eddy simulation of the low temperature ignition and combustion processes on spray flame with the linear eddy model, Combust. Theory Modell. 22 (2018) 237-263.
[139] G. Borghesi, E. Mastorakos, Spontaneous ignition of isolated n-heptane droplets at low, intermediate, and high ambient temperatures from a mixture-fraction perspective, Combust. Flame 162 (2015) 2544-2560.
[140] E. Mastorakos, T. Baritaud, T. Poinsot, Numerical simulations of autoignition in turbulent mixing flows, Combust. Flame 109 (1997) 198-223.
[141] A. Krisman, E.R. Hawkes, M. Talei, A. Bhagatwala, J.H. Chen, Characterisation of two-stage ignition in diesel engine-relevant thermochemical conditions using direct numerical simulation, Combust. Flame 172 (2016) 326-341.
[142] D.K. Dalakoti, A. Krisman, B. Savard, A. Wehrfritz, H. Wang, M.S. Day, J.B. Bell, E.R. Hawkes, Structure and propagation of two-dimensional, partially premixed, laminar flames in diesel engine conditions, Proc. Combust. Inst. 37 (2019) 1961-1969.
[143] A. Krisman, E.R. Hawkes, J.H. Chen, A parametric study of ignition dynamics at ECN Spray A thermochemical conditions using 2D DNS, Proc. Combust. Inst. 37 (2019) 4787-4795.
[144] A.M. Briones, S.K. Aggarwal, V.R. Katta, A numerical investigation of flame liftoff, stabilization, and blowout, Phys Fluids 18 (2006) 043603.
[145] F. Tagliante, L.-M. Malbec, G. Bruneaux, L.M. Pickett, C. Angelberger, Experimental study of the stabilization mechanism of a lifted Diesel-type flame using combined optical diagnostics and laser-induced plasma ignition, Combust. Flame 197 (2018) 215-226.
[146] F. Tagliante, T. Poinsot, L.M. Pickett, P. Pepiot, L.-M. Malbec, G. Bruneaux, C. Angelberger, A conceptual model of the flame stabilization mechanisms for a lifted Diesel-type flame based on direct numerical simulation and experiments, Combust. Flame 201 (2019) 65-77.
[147] J.E. Broadwell, W.J.A. Dahm, M.G. Mungal, Blowout of turbulent diffusion flames, Symposium (International) on Combustion 20 (1985) 303-310.
[148] L.M. Pickett, S. Kook, H. Persson, Ö. Andersson, Diesel fuel jet lift-off stabilization in the presence of laser-induced plasma ignition, Proc. Combust. Inst. 32 (2009) 2793-2800.
[149] C. Gong, M. Jangi, X.-S. Bai, Diesel flame lift-off stabilization in the presence of laser-ignition: a numerical study, Combust. Theory Modell. 19 (2015) 696-713.
[150] C. Gong, M. Jangi, X.-S. Bai, Large eddy simulation of n-Dodecane spray combustion in a high pressure combustion vessel, Appl. Energy 136 (2014) 373-381.
[151] U. Azimov, K.-S. Kim, C. Bae, Modeling of flame lift-off length in diesel low-temperature combustion with multi-dimensional CFD based on the flame surface density and extinction concept, Combust. Theory Modell. 14 (2010) 155-175.
[152] J. Buckmaster, Edge-flames, Prog. Energy Combust. Sci. 28 (2002) 435-475.
[153] K.M. Pang, M. Jangi, X.-S. Bai, J. Schramm, J.H. Walther, Modelling of diesel spray flames under engine-like conditions using an accelerated Eulerian Stochastic Field method, Combust. Flame 193 (2018) 363-383.
[154] R.L. Gordon, A.R. Masri, S.B. Pope, G.M. Goldin, A numerical study of auto-ignition in turbulent lifted flames issuing into a vitiated co-flow, Combust. Theory Modell. 11 (2007) 351-376.
[155] H. Wei, J. Yu, L. Zhou, W. Zhao, C. Chen, The LES and LEM Study of End-Gas Auto-Ignition Mechanism in a Downsized Spark Ignition Engine: Effect of Turbulence, Combust. Sci. Technol. 191 (2019) 1917-1941.
[156] Y. Zhang, S. Xu, S. Zhong, X.-S. Bai, H. Wang, M. Yao, Large eddy simulation of spray combustion using flamelet generated manifolds combined with artificial neural networks, Energy and AI 2 (2020) 100021.
[157] M.B. Luong, G.H. Yu, T. Lu, S.H. Chung, C.S. Yoo, Direct numerical simulations of ignition of a lean n-heptane/air mixture with temperature and composition inhomogeneities relevant to HCCI and SCCI combustion, Combust. Flame 162 (2015) 4566-4585.
[158] G. Borman, K. Nishiwaki, Internal-combustion engine heat transfer, Prog Energ Combust 13 (1987) 1-46.
[159] R. Viskanta, M.P. Mengüç, Radiation heat transfer in combustion systems, Prog Energ Combust 13 (1987) 97-160.
[160] G. Li, M.F. Modest, Application of composition PDF methods in the investigation of turbulence–radiation interactions, JQSRT 73 (2002) 461-472.
[161] R.S. Mehta †, M.F. Modest ‡, D.C. Haworth, Radiation characteristics and turbulence–radiation interactions in sooting turbulent jet flames, Combust Theor Model 14 (2010) 105-124.
[162] A. Gupta, D.C. Haworth, M.F. Modest, Turbulence-radiation interactions in large-eddy simulations of luminous and nonluminous nonpremixed flames, Proc Combust Inst 34 (2013) 1281-1288.
[163] S.M. Jeng, M.C. Lai, G.M. Faeth, Nonluminous Radiation in Turbulent Buoyant Axisymmetric Flames, Combust. Sci. Technol. 40 (1984) 41-53.
[164] P.J. Coelho, Numerical simulation of the interaction between turbulence and radiation in reactive flows, Prog Energ Combust 33 (2007) 311-383.
[165] P.J. Coelho, Turbulence–Radiation Interaction: From Theory to Application in Numerical Simulations, J. Heat Transfer 134 (2012) 031001-031001-031013.
[166] M.A. Chishty, M. Bolla, E. Hawkes, Y. Pei, S. Kook, Assessing the Importance of Radiative Heat Transfer for ECN Spray A Using the Transported PDF Method, SAE International, 2016.

[167] G. Pal, A. Gupta, M.F. Modest, D.C. Haworth, Comparison of accuracy and computational expense of radiation models in simulation of non-premixed turbulent jet flames, Combust. Flame 162 (2015) 2487-2495.
[168] C. Paul, D.C. Haworth, M.F. Modest, A simplified CFD model for spectral radiative heat transfer in high-pressure hydrocarbon–air combustion systems, Proc. Combust. Inst. 37 (2019) 4617-4624.
[169] W.A. Daniel, Flame quenching at the walls of an internal combustion engine, Symposium (International) on Combustion 6 (1957) 886-894.
[170] M.C. Drake, D.C. Haworth, Advanced gasoline engine development using optical diagnostics and numerical modeling, Proc Combust Inst 31 (2007) 99-124.
[171] A.H. Epstein, Aircraft engines' needs from combustion science and engineering, Combust. Flame 159 (2012) 1791-1792.
[172] C. Maeding, D. Wiedmann, K. Quering, O. Knab, Improved heat transfer prediction engineering capabilities for rocket thrust chamber layout, EUCASS Proceedings Series – Advances in AeroSpace Sciences 2 (2011) 239-250.
[173] A. Dreizler, B. Böhm, Advanced laser diagnostics for an improved understanding of premixed flame-wall interactions, Proc. Combust. Inst. 35 (2015) 37-64.
[174] J. Hao, J. Lu, L. Lee, Z. Wu, G. Hu, J.M. Floryan, Droplet Splashing on an Inclined Surface, Phys Rev Lett 122 (2019) 054501.
[175] C. Josserand, S.T. Thoroddsen, Drop Impact on a Solid Surface, Annu Rev Fluid Mech 48 (2016) 365-391.
[176] A.L. Yarin, DROP IMPACT DYNAMICS: Splashing, Spreading, Receding, Bouncing…, Annu Rev Fluid Mech 38 (2006) 159-192.
[177] H. Pan, D. Xiao, D. Hung, M. Xu, X. Li, Experimental investigations of wall jet droplet impact on spray impingement fuel film formation, Fuel 241 (2019) 33-41.
[178] X. Li, H. Pan, X. Dong, D. Hung, M. Xu, Spray impingement wall film breakup by wave entrainment, Proc Combust Inst 37 (2019) 3287-3294.
[179] B. Chen, L. Feng, Y. Wang, T. Ma, H. Liu, C. Geng, M. Yao, Spray and flame characteristics of wall-impinging diesel fuel spray at different wall temperatures and ambient pressures in a constant volume combustion vessel, Fuel 235 (2019) 416-425.
[180] Q. Li, K.H. Luo, Achieving tunable surface tension in the pseudopotential lattice Boltzmann modeling of multiphase flows, Phys Rev E 88 (2013) 053307.
[181] I.V. Roisman, B. Prunet-Foch, C. Tropea, M. Vignes-Adler, Multiple Drop Impact onto a Dry Solid Substrate, JCIS 256 (2002) 396-410.
[182] I.V. Roisman, K. Horvat, C. Tropea, Spray impact: Rim transverse instability initiating fingering and splash, and description of a secondary spray, Phys Fluids 18 (2006) 102104.
[183] A.L.N. Moreira, A.S. Moita, M.R. Panão, Advances and challenges in explaining fuel spray impingement: How much of single droplet impact research is useful?, Prog Energ Combust 36 (2010) 554-580.
[184] N. Katsura, M. Saito, J. Senda, H. Fujimoto, Characteristics of a Diesel Spray Impinging on a Flat Wall, SAE International, 1989.
[185] F. Maroteaux, D. Llory, J.F. Le Coz, C. Habchi, Liquid Film Atomization on Wall Edges—Separation Criterion and Droplets Formation Model, J. Fluids Eng. 124 (2002) 565-575.
[186] J.D. Naber, R.D. Reitz, Modeling Engine Spray/Wall Impingement, SAE International, 1988.
[187] P.J. O'Rourke, A.A. Amsden, A Spray/Wall Interaction Submodel for the KIVA-3 Wall Film Model, SAE International, 2000.
[188] L. Allocca, L. Andreassi, S. Ubertini, Evaluation of Splash Models with High-Pressure Diesel Spray, SAE International, 2006.
[189] J. Senda, T. Kanda, M. Al-Roub, P.V. Farrell, T. Fukami, H. Fujimoto, Modeling Spray Impingement Considering Fuel Film Formation on the Wall, SAE International, 1997.
[190] J. Senda, T. Higaki, Y. Sagane, H. Fujimoto, Y. Takagi, M. Adachi, Modeling and Measurement on Evaporation Process of Multicomponent Fuels, SAE International, 2000.
[191] Y. Zhang, M. Jia, H. Liu, M. Xie, T. Wang, L. Zhou, DEVELOPMENT OF A NEW SPRAY/WALL INTERACTION MODEL FOR DIESEL SPRAY UNDER PCCI-ENGINE RELEVANT CONDITIONS, 24 (2014) 41-80.
[192] Y. Zhang, M. Jia, H. Duan, P. Wang, J. Wang, H. Liu, M. Xie, Numerical and experimental study of spray impingement and liquid film separation during the spray/wall interaction at expanding corners, Int. J. Multiphase Flow 107 (2018) 67-81.
[193] J.E. Dec, D.R. Tree, Diffusion-Flame / Wall Interactions in a Heavy-Duty DI Diesel Engine, SAE International, 2001.
[194] K. Li, K. Nishida, Y. Ogata, B. Shi, Effect of flat-wall impingement on diesel spray combustion, Proc. Inst. Mech. Eng. Pt. D: J. Automobile Eng. 229 (2015) 535-549.
[195] R. Mahmud, T. Kurisu, K. Nishida, Y. Ogata, J. Kanzaki, T. Tadokoro, Experimental study on flat-wall impinging spray flame and its heat flux on wall under diesel engine–like condition: First report—effect of impingement distance, Proc. Inst. Mech. Eng. Pt. D: J. Automobile Eng. 233 (2019) 2187-2202.
[196] X. Wang, Z. Huang, W. Zhang, O.A. Kuti, K. Nishida, Effects of ultra-high injection pressure and micro-hole nozzle on flame structure and soot formation of impinging diesel spray, Appl Energ 88 (2011) 1620-1628.
[197] K. Kim, D. Kim, Y. Jung, C. Bae, Spray and combustion characteristics of gasoline and diesel in a direct injection compression ignition engine, Fuel 109 (2013) 616-626.

[198] G. Bruneaux, Combustion structure of free and wall-impinging diesel jets by simultaneous laser-induced fluorescence of formaldehyde, poly-aromatic hydrocarbons, and hydroxides, Int. J. Engine Res 9 (2008) 249-265.
[199] J. Gao, S. Moon, Y. Zhang, K. Nishida, Y. Matsumoto, Flame structure of wall-impinging diesel fuel sprays injected by group-hole nozzles, Combust. Flame 156 (2009) 1263-1277.
[200] K. Li, M. Ido, Y. Ogata, K. Nishida, B. Shi, D. Shimo, Effect of Spray/Wall Interaction on Diesel Combustion and Soot Formation in Two-Dimensional Piston Cavity, Society of Automotive Engineers of Japan, 2013.
[201] K. Li, P. Dong, T. Matsuo, B. Shi, Y. Ogata, K. Nishida, Characteristics of Diesel Spray Flame under Flat Wall Impinging Condition --LAS, OH* Chemiluminescence and Two Color Pyrometry Results, SAE International, 2014.
[202] Z. Zhang, F. Liu, Y. An, H. Gao, W. Du, Y. Gao, J. Lou, Effect of wall surface temperature on ignition and combustion characteristics of diesel fuel spray impingement, Appl. Therm. Eng. 137 (2018) 47-53.
[203] H. Yu, X. Liang, G. Shu, Y. Wang, H. Zhang, Experimental investigation on spray-wall impingement characteristics of n-butanol/diesel blended fuels, Fuel 182 (2016) 248-258.
[204] L.M. Pickett, J.J. López, Jet-Wall Interaction Effects on Diesel Combustion and Soot Formation, SAE International, 2005.
[205] H. Liu, M. Huo, Y. Liu, X. Wang, H. Wang, M. Yao, C.-f.F. Lee, Time-resolved spray, flame, soot quantitative measurement fueling n-butanol and soybean biodiesel in a constant volume chamber under various ambient temperatures, Fuel 133 (2014) 317-325.
[206] G. Bruneaux, Mixing Process in High Pressure Diesel Jets by Normalized Laser Induced Exciplex Fluorescence Part II: Wall Impinging Versus Free Jet, SAE International, 2005.
[207] O. Laget, L. Muller, K. Truffin, J. Kashdan, R. Kumar, J. Sotton, B. Boust, M. Bellenoue, Experiments and Modeling of Flame/Wall Interaction in Spark-Ignition (SI) Engine Conditions, SAE International, 2013.
[208] D. Mayer, A. Seelig, T. Kunz, F. Kopple, M. Mansbart, M. Bargende, Experimental Investigation of Flame-Wall-Impingement and Near-Wall Combustion on the Piston Temperature of a Diesel Engine Using Instantaneous Surface Temperature Measurements, SAE International, 2018.
[209] G. Bruneaux, T. Poinsot, J.H. Ferziger, Premixed flame–wall interaction in a turbulent channel flow: budget for the flame surface density evolution equation and modelling, J. Fluid Mech. 349 (1997) 191-219.
[210] G. Desoutter, B. Cuenot, C. Habchi, T. Poinsot, Interaction of a premixed flame with a liquid fuel film on a wall, Proc Combust Inst 30 (2005) 259-266.
[211] G.G. Simeoni, T. Bryk, F.A. Gorelli, M. Krisch, G. Ruocco, M. Santoro, T. Scopigno, The Widom line as the crossover between liquid-like and gas-like behaviour in supercritical fluids, Nature Physics 6 (2010) 503-507.
[212] D. Banuti, M. Raju, P.C. Ma, M. Ihme, J.-P. Hickey, Seven questions about supercritical fluids - towards a new fluid state diagram, 55th AIAA Aerospace Sciences Meeting, American Institute of Aeronautics and Astronautics2017.
[213] G. Mo, L. Qiao, A molecular dynamics investigation of n-alkanes vaporizing into nitrogen: transition from subcritical to supercritical, Combust. Flame 176 (2017) 60-71.
[214] J. Manin, M. Bardi, L.M. Pickett, R.N. Dahms, J.C. Oefelein, Microscopic investigation of the atomization and mixing processes of diesel sprays injected into high pressure and temperature environments, Fuel 134 (2014) 531-543.
[215] R.N. Dahms, J.C. Oefelein, Liquid jet breakup regimes at supercritical pressures, Combust. Flame 162 (2015) 3648-3657.
[216] G. Xiao, K.H. Luo, X. Ma, S. Shuai, A molecular dynamics study of fuel droplet evaporation in sub- and supercritical conditions, Proc Combust Inst 37 (2019) 3219-3227.
[217] L.C. Selle, N.A. Okong'O, J. Bellan, K.G. Harstad, Modelling of subgrid-scale phenomena in supercritical transitional mixing layers: an a priori study, J. Fluid Mech. 593 (2007) 57-91.
[218] H. Nomura, Y. Ujiie, H.J. Rath, J.i. Sato, M. Kono, Experimental study on high-pressure droplet evaporation using microgravity conditions, Symposium (International) on Combustion 26 (1996) 1267-1273.
[219] H. Jia, G. Gogos, High pressure droplet vaporization; effects of liquid-phase gas solubility, Int. J. Heat Mass Transfer 36 (1993) 4419-4431.
[220] P. Li, F. Lei, K. Wang, L. Zhou, Evaporation characteristics of kerosene droplet under high-pressure conditions, 2018.
[221] R. Litchford, S. Jeng, LOX vaporization in high-pressure, hydrogen-rich gas, (1990).
[222] D.T. Banuti, K. Hannemann, The absence of a dense potential core in supercritical injection: A thermal break-up mechanism, Physics of Fluids 28 (2016) 035103.
[223] O. Desjardins, V. Moureau, H. Pitsch, An accurate conservative level set/ghost fluid method for simulating turbulent atomization, J Comput Phys 227 (2008) 8395-8416.
[224] S. Schlatter, B. Schneider, Y.M. Wright, K. Boulouchos, N-heptane micro pilot assisted methane combustion in a Rapid Compression Expansion Machine, Fuel 179 (2016) 339-352.
[225] P. Zhang, J. Ran, C. Qin, X. Du, J. Niu, L. Yang, Effects of Methane Addition on Exhaust Gas Emissions and Combustion Efficiency of the Premixed n-Heptane/Air Combustion, Energy Fuels 32 (2018) 3900-3907.
[226] A.E. Daca, Ö.L. Gülder, Soot formation characteristics of diffusion flames of methane doped with toluene and n-heptane at elevated pressures, Proc. Combust. Inst. 36 (2017) 737-744.
[227] H. Wei, W. Zhao, J. Qi, Z. Liu, L. Zhou, Effect of injection timing on the ignition process of n-heptane spray flame in a methane/air environment, Fuel 245 (2019) 345-359.
[228] R.G. Papagiannakis, D.T. Hountalas, Combustion and exhaust emission characteristics of a dual fuel compression ignition engine operated with pilot Diesel fuel and natural gas, Energy Convers. Manage. 45 (2004) 2971-2987.

[229] A. Srna, M. Bolla, Y.M. Wright, K. Herrmann, R. Bombach, S.S. Pandurangi, K. Boulouchos, G. Bruneaux, Effect of methane on pilot-fuel auto-ignition in dual-fuel engines, Proc. Combust. Inst. 37 (2019) 4741-4749.
[230] B. Tekgül, H. Kahila, O. Kaario, V. Vuorinen, Large-eddy simulation of dual-fuel spray ignition at different ambient temperatures, Combust. Flame 215 (2020) 51-65.
[231] Y. Ra, R.D. Reitz, A combustion model for multi-component fuels using a physical surrogate group chemistry representation (PSGCR), Combust. Flame 162 (2015) 3456-3481.
[232] P. Wang, M. Jia, Y. Zhang, G. Xu, Y. Chang, Z. Xu, Development of a decoupling physical-chemical surrogate (DPCS) model for simulation of the spray and combustion of multi-component biodiesel fuels, Fuel 240 (2019) 16-30.
[233] H. Wang, R. Xu, K. Wang, C.T. Bowman, R.K. Hanson, D.F. Davidson, K. Brezinsky, F.N. Egolfopoulos, A physics-based approach to modeling real-fuel combustion chemistry - I. Evidence from experiments, and thermodynamic, chemical kinetic and statistical considerations, Combust. Flame 193 (2018) 502-519.
[234] R. Xu, K. Wang, S. Banerjee, J. Shao, T. Parise, Y. Zhu, S. Wang, A. Movaghar, D.J. Lee, R. Zhao, X. Han, Y. Gao, T. Lu, K. Brezinsky, F.N. Egolfopoulos, D.F. Davidson, R.K. Hanson, C.T. Bowman, H. Wang, A physics-based approach to modeling real-fuel combustion chemistry – II. Reaction kinetic models of jet and rocket fuels, Combust. Flame 193 (2018) 520-537.
[235] Y. Chang, M. Jia, B. Niu, Z. Xu, Z. Liu, Y. Li, M. Xie, Construction of a skeletal oxidation mechanism of n-pentanol by integrating decoupling methodology, genetic algorithm, and uncertainty quantification, Combust. Flame 194 (2018) 15-27.
[236] Y. Zhang, M. Jia, P. Wang, Y. Chang, P. Yi, H. Liu, Z. He, Construction of a decoupling physical–chemical surrogate (DPCS) for practical diesel fuel, Appl. Therm. Eng. 149 (2019) 536-547.
[237] S.M. Sarathy, A. Farooq, G.T. Kalghatgi, Recent progress in gasoline surrogate fuels, Prog Energ Combust 65 (2018) 67-108.
[238] A. Felden, L. Esclapez, E. Riber, B. Cuenot, H. Wang, Including real fuel chemistry in LES of turbulent spray combustion, Combust. Flame 193 (2018) 397-416.
[239] Y. Shi, L. Liang, H.-W. Ge, R.D. Reitz, Acceleration of the chemistry solver for modeling DI engine combustion using dynamic adaptive chemistry (DAC) schemes, Combustion Theory and Modelling 14 (2010) 69-89.
[240] F. Contino, F. Foucher, P. Dagaut, T. Lucchini, G. D'Errico, C. Mounaïm-Rousselle, Experimental and numerical analysis of nitric oxide effect on the ignition of iso-octane in a single cylinder HCCI engine, Combust. Flame 160 (2013) 1476-1483.
[241] H. Yang, Z. Ren, T. Lu, G.M. Goldin, Dynamic adaptive chemistry for turbulent flame simulations, Combust Theor Model 17 (2013) 167-183.
[242] L. Liang, J.G. Stevens, S. Raman, J.T. Farrell, The use of dynamic adaptive chemistry in combustion simulation of gasoline surrogate fuels, Combust. Flame 156 (2009) 1493-1502.
[243] Z. Ren, G.M. Goldin, V. Hiremath, S.B. Pope, Reduced description of reactive flows with tabulation of chemistry, Combust Theor Model 15 (2011) 827-848.
[244] G.M. Goldin, Z. Ren, S. Zahirovic, A cell agglomeration algorithm for accelerating detailed chemistry in CFD, Combustion Theory and Modelling 13 (2009) 721-739.
[245] L. Liang, J.G. Stevens, J.T. Farrell, A dynamic multi-zone partitioning scheme for solving detailed chemical kinetics in reactive flow computations, Combust. Sci. Technol. 181 (2009) 1345-1371.
[246] F. Contino, H. Jeanmart, T. Lucchini, G. D'Errico, Coupling of in situ adaptive tabulation and dynamic adaptive chemistry: An effective method for solving combustion in engine simulations, Proc Combust Inst 33 (2011) 3057-3064.
[247] H. Wei, L. Zhou, H. Zhou, Z. Lu, Z. Ren, G.M. Goldin, Toward Efficient Chemistry Calculations in Engine Simulations Through Static Adaptive Acceleration, Combust. Sci. Technol. 189 (2017) 623-642.
[248] L. Zhou, W. Zhao, H. Wei, Effect of improved accelerating method on efficient chemistry calculations in diesel engine, Int. J. Engine Res 19 (2018) 839-853.
[249] W. Xie, Z. Lu, Z. Ren, G.M. Goldin, Dynamic adaptive acceleration of chemical kinetics with consistent error control, Combust. Flame 197 (2018) 389-399.
[250] H. Abdi, L.J. Williams, Principal component analysis, Wiley Interdisciplinary Reviews: Computational Statistics 2 (2010) 433-459.
[251] E. Song, Y. Li, Q. Dong, L. Fan, C. Yao, L. Yang, Experimental research on the effect of shock wave on the evolution of high-pressure diesel spray, Exp. Therm Fluid Sci. 93 (2018) 235-241.